

Photo-dissociation of self-assembled (anthracene-2-carbonyl)amino acid hydrogels

Phillip R. A. Chivers,^{a, b} Rebecca S. Dookie,^c Julie E. Gough^d and Simon J. Webb^{a, b}

^a Department of Chemistry, University of Manchester, Oxford Road, Manchester, M13 9PL, UK

^b Manchester Institute of Biotechnology, University of Manchester, 131 Princess St, Manchester, M1 7DN, UK

^c Manchester Collaborative Centre for Inflammation Research, University of Manchester, 2 Grafton Street, Manchester, M13 9NT, UK

^d Department of Materials, University of Manchester, MSS Tower, Manchester, M13 9PL, UK

Supplementary Information

Contents

S1.	Materials and instrumentation	3
S2.	Synthetic procedures.....	4
S2.1.	Synthesis of (anthracene-2-carbonyl)phenylalanine methyl ester (1).....	4
S2.2.	Synthesis of (anthracene-2-carbonyl)phenylalanine (2)	6
S2.3.	Synthesis of (anthracene-2-carbonyl)tyrosine methyl ester (3)	8
S2.4.	Synthesis of (anthracene-2-carbonyl)tyrosine (4).....	11
S2.5.	Synthesis of (anthracene-2-carbonyl)alanine methyl ester (5).....	13
S2.6.	Synthesis of (anthracene-2-carbonyl)alanine (6)	15
S2.7.	Synthesis of (anthracene-2-carbonyl)tryptophan methyl ester (7)	18
S2.8.	Synthesis of (anthracene-2-carbonyl)tryptophan (8).....	20
S2.9.	General procedure for synthesis of (anthracene-9-carbonyl)amino acids	23
S2.10.	Synthesis of (anthracene-9-carbonyl)phenylalanine.....	24
S2.11.	Synthesis of (anthracene-9-carbonyl)glycine	24
S2.12.	Synthesis of (anthracene-9-carbonyl)alanine.....	25
S2.13.	Synthesis of (anthracene-9-carbonyl)valine.....	25
S3.	Hydrogelation procedures.....	26
S3.1.	Using glucono- δ -lactone (GdL) to trigger hydrogelation	26
S3.2.	Using salts to trigger hydrogelation	27
S3.3.	Using media to trigger hydrogelation	27
S3.4.	Using heating/cooling to trigger hydrogelation	27
S4.	NMR spectroscopy studies of (Anth)Phe-OH gelation	31
S5.	T_{gel} experiments.....	33
S6.	Gel ageing study	35
S7.	Photo-dimerisation reactions.....	39
S7.1.	Photo-dimerisation in the solution-phase	40

S7.2.	Gel-phase reactions.....	52
S7.3.	Data for dimerisation of (Anth)Phe-OH weak gels formed by addition of GlyNH ₂ ·HCl.....	61
S8.	Scanning electron microscopy.....	62
S8.1.	Sample preparation.....	62
S8.2.	Further SEM images	62
S9.	Rheological data	65
S9.1.	Sample preparation.....	65
S9.2.	Further rheological data for (Anth)Phe-OH 2 hydrogels/gel-like materials.....	65
S10.	Fluorescence spectroscopy	68
S10.1.	Preparation of hydrogels/gel-like materials in cuvettes	68
S10.2.	Fluorescence parameters	68
S8.	Cell culture studies	71
S11.1	Cell culture procedure	71
S11.2	Preparation of gels in cell culture inserts.....	71
S11.3	Cell seeding.....	71
S11.4	Recovery of cells for analysis by flow cytometry	72
S11.5	Confocal microscopy	73
S11.6	Flow cytometry.....	75
S9.	References.....	78

S1. Materials and instrumentation

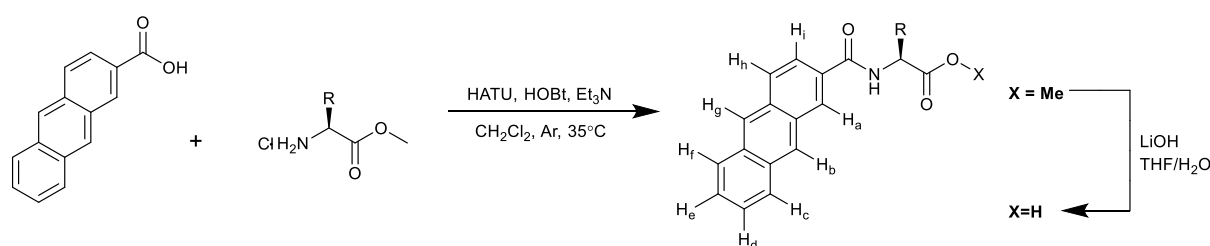
Anthracene-2-carboxylic acid, L-phenylalanine methyl ester hydrochloride and L-tyrosine methyl ester hydrochloride were purchased from Fluorochem, Derbyshire. All other synthetic reagents were purchased from Sigma Aldrich. Dulbecco's Modified Eagle's Medium (DMEM) was purchased from Sigma. All reagents were used without further purification.

^1H and ^{13}C nuclear magnetic resonance (NMR) spectra were obtained using a Bruker AVANCE 400 spectrometer (^1H 400 MHz, ^{13}C 101 MHz), with the exception of the spectra shown in Figure S38 (^1H 800 MHz, using a 800 MHz Bruker AVANCE III four-channel liquid-state spectrometer). Chemical shifts are quoted in parts per million (ppm) and coupling constants (J) in Hz to the nearest 0.5 Hz. ^1H and ^{13}C NMR shifts were referenced to the relevant solvent resonances. Low- and high- resolution mass spectra were recorded by staff at the University of Manchester. Electrospray (ES) spectra were recorded on a Waters Platform II. High-resolution mass spectra (HRMS) were recorded on a Thermo Finnigan MAT95XP and are accurate to ± 0.001 Da.

Infra-red (IR) spectra were recorded on an ATi Perkin Elmer Spectrum RX1 FT-IR. Absorption maxima are reported in wavenumbers (cm^{-1}). UV-visible absorption spectra were recorded on a Cary 400 Scan UV spectrophotometer and fluorescence spectra on a Varian Cary Eclipse fluorimeter, using a 10 mm cell at the stated concentration. Scanning electron microscopy (SEM) was performed on a TESCAN FIB-SEM. Rheological measurements were made using a stress-controlled TA Instruments Discovery HR2 rheometer equipped with 20 mm parallel plates. Irradiation experiments were performed using equipment provided by Thorlabs (Newton, NJ). Light emitting diodes (LEDs) emitted at a λ_{max} of 365 nm (part no. M365L2) and were powered by a DC4100 LED Driver.

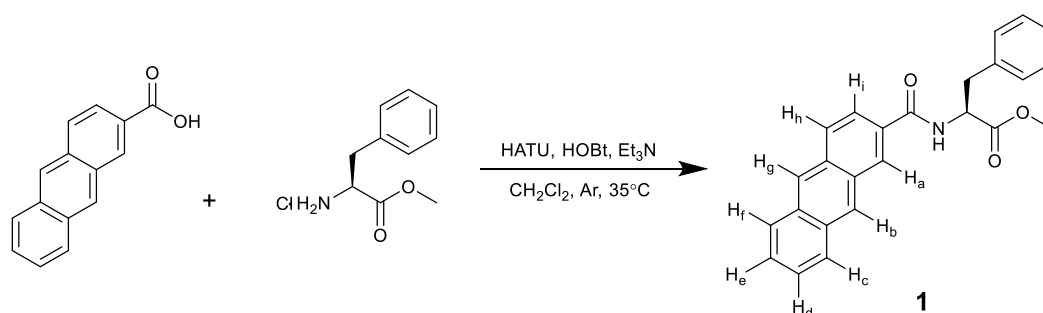
Light microscopy images were collected using a Zeiss upright microscope fitted with 4 \times objective lens under 10 \times magnification. Confocal microscopy was performed on a Leica TCS SP8 AOBS inverted microscope using a 20 \times objective. Flow cytometry measurements were recorded on a Fortessa (BD Systems, UK).

S2. Synthetic procedures



Scheme S1: General gelator synthetic scheme

S2.1. Synthesis of (anthracene-2-carbonyl)phenylalanine methyl ester (**1**)



Anthracene-2-carboxylic acid (222 mg, 1 mmol), 1-[bis(dimethylamino)methylene]-1*H*-1,2,3-triazolo[4,5-*b*]pyridinium 3-oxide hexafluorophosphate (HATU, 380 mg, 1 mmol) and 1-hydroxybenzotriazole (HOBT, 63 mg, 0.5 mmol) were charged into a dry flask and stirred in dry dichloromethane (5 mL) at 0°C under nitrogen gas. Triethylamine (0.5 mL, 3.6 mmol) was added *via* syringe and the solution stirred for a further 15 min at 0°C.

Separately, phenylalanine methyl ester hydrochloride (216 mg, 1 mmol) was stirred in dry dichloromethane (5 mL) in an oven-dried flask under nitrogen gas. Triethylamine (0.5 mL, 3.6 mmol) was added *via* syringe and the solution stirred at room temperature for 30 min. The clear, colourless solution was then transferred *via* syringe to the reaction mixture and stirred for 1 h at 0°C before heating to 35°C and stirring for a further 16 h. During this time the formation of a yellow precipitate was evident.

Upon reaction completion, the solvent was removed *in vacuo*. The resulting crude solid was resuspended in a separating funnel with ethyl acetate (*ca.* 20 mL) and washed sequentially with aqueous HCl (0.1 M, 3 × 10 mL) and saturated NaCl solution (3 × 10 mL). The solid was filtered and washed with further portions of ethyl acetate (3 × 20 mL) before drying *in vacuo* to yield a pale yellow, dusty solid (274 mg, 72%).

¹H NMR (400 MHz, CDCl₃): δ 8.51 (s, 1H, *H_g*), 8.45 (s, 1H, *H_b*), 8.42 (d, *J* = 1.5 Hz, 1H, *H_a*), 8.07-8.00 (m, 3H, *H_d*, *H_f*, *H_h*), 7.75 (dd, *J* = 9, 2 Hz, 1H, *H_i*), 7.56 – 7.48 (m, 2H, *H_c*, *H_e*), 7.36-7.27 (m, 3H, Phe-*H ortho* +

para), 7.21 – 7.17 (m, 2H, Phe-*H meta*), 6.77 (d, $J = 7.5$ Hz, 1H, *NH*), 5.18 (ddd, $J = 7.5, 6, 5.5$ Hz, 1H, CH), 3.81 (s, 3H, OCH_3) 3.26 (dd, $J = 14, 6$ Hz, 1H, CHH'), 3.15 (dd, $J = 14, 5.5$ Hz, 1H CHH'). ^{13}C NMR (101 MHz, CDCl_3): δ 172.3 (COOH), 167.0 (CONH), 136.0 (Ar-C), 132.9 (Anth-C), 132.3 (Anth-C), 132.2 (Anth-C), 130.6 (Anth-C), 130.5 (Anth-C), 129.5 (Ar-CH), 129.1 (Anth-CH), 128.8 (Ar-CH), 128.6 (Anth-CH), 128.5 (Anth-CH), 128.3 (Anth-CH), 128.3 (Anth-CH), 127.4 (Ar-CH), 126.5 (Anth-CH), 126.4 (Anth-CH), 126.0 (Anth-CH), 122.8 (Anth-CH), 53.8 (CH), 52.6 (CH_3), 38.1 (CH_2). ν_{max} (cm^{-1}): 3391w, 2980w, 2949w, 1745s, 1646m, 1500m. HRMS: $[(\text{C}_{25}\text{H}_{21}\text{NO}_3) - \text{H}^+]^-$ expected 382.1449, found 382.1449. Anal: Calcd for $\text{C}_{25}\text{H}_{21}\text{NO}_3 \cdot 1.5\text{H}_2\text{O}$: C, 73.15; H, 5.89; N, 3.41; O, 17.54. Found C 73.87, H 5.52, N 3.51.

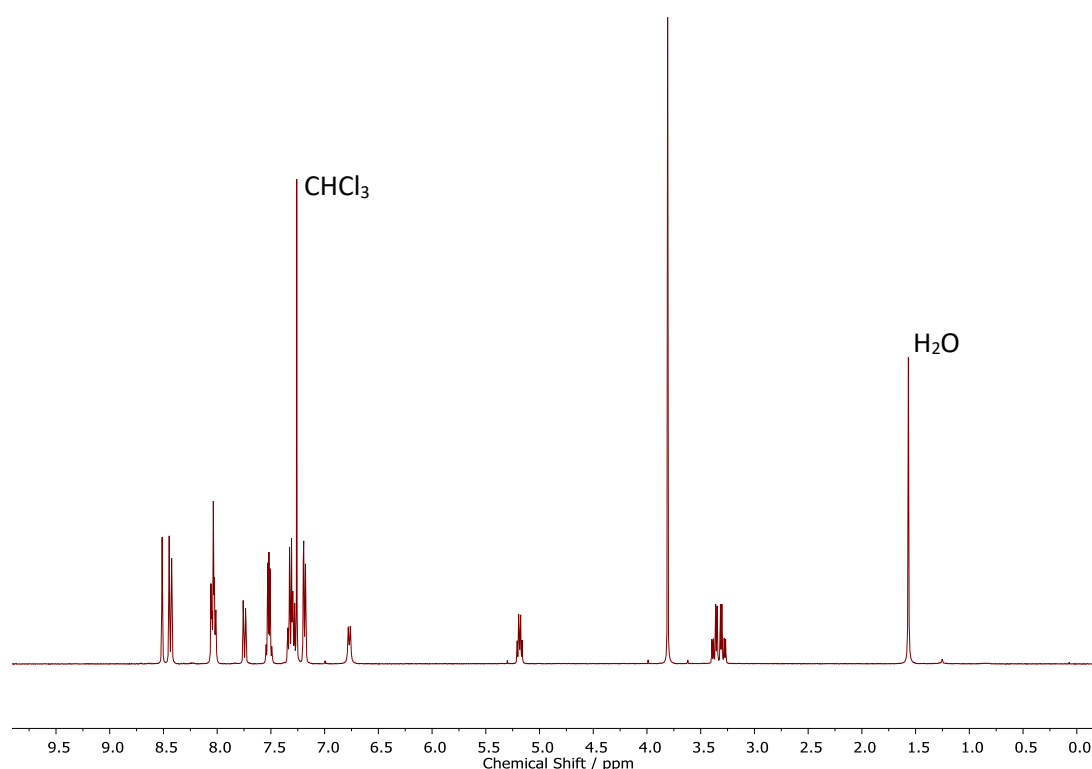


Fig. S1: ^1H NMR spectrum (400 MHz) of (Anth)Phe-OMe in CDCl_3

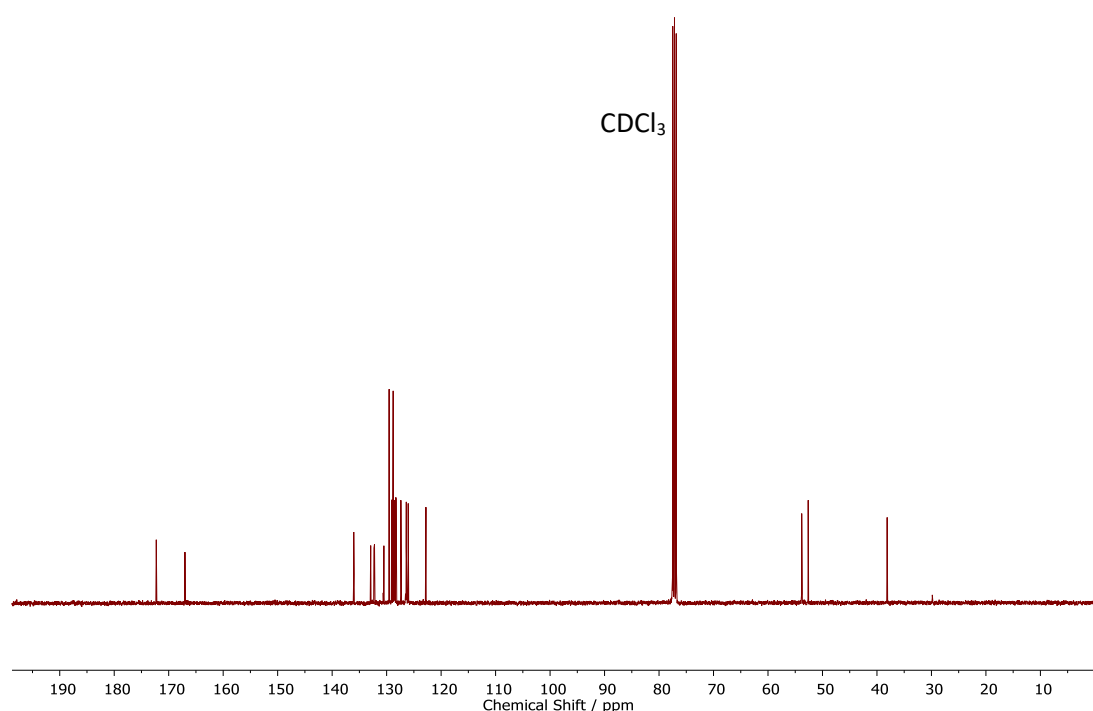
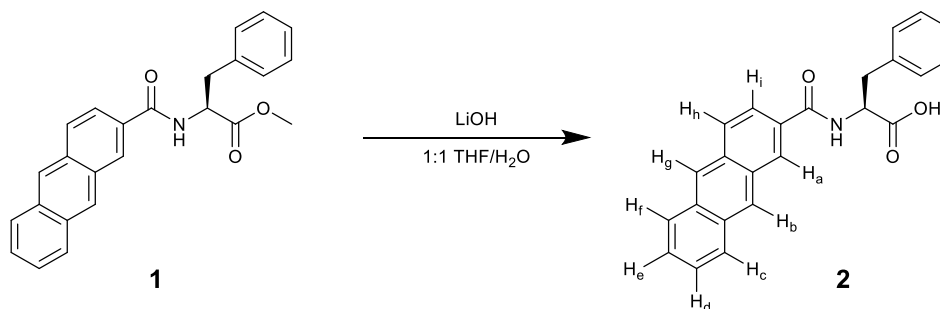


Fig. S2: ^{13}C NMR spectrum (101 MHz) of (Anth)Phe-OMe in CDCl_3

S2.2. Synthesis of (anthracene-2-carbonyl)phenylalanine (**2**)



(Anthracene-2-carbonyl)phenylalanine methyl ester (**1**, 200 mg, 0.5 mmol) was stirred in a 1:1 tetrahydrofuran/deionised water mixture. Lithium hydroxide (24 mg, 1 mmol) was added and the reaction stirred at room temperature for 16 h. The tetrahydrofuran was removed on a rotary evaporator, upon which a clear, yellow gel formed in the round-bottomed flask. The gel was diluted with further deionised H_2O (*ca.* 20 mL) and shaken to break down the gel. The resulting solution was washed thoroughly with diethyl ether. The aqueous layer was carefully acidified to *ca.* pH 4 with 0.1 M HCl, resulting in the precipitation of an off-white solid. This solid was extracted into ethyl acetate and dried *in vacuo* to yield small, pale yellow crystals of **2** (170 mg, 85%).

^1H NMR (400 MHz, $\text{DMSO}-d_6$): δ 12.81 (br s, COOH), 8.94 (d, $J = 8$ Hz, 1H, NH), 8.71 (s, 1H, H_g), 8.63 (s, 1H, H_b), 8.60 (d, $J = 1.5$ Hz, 1H, H_a), 8.20 – 8.09 (m, 3H, H_d , H_f , H_h), 7.85 (dd, $J = 9, 1.5$ Hz, 1H, H_i), 7.62 –

7.54 (m, 2H, H_c , H_e), 7.40-7.35 (m, 2H, Phe-*H meta*), 7.30 (dd, $J = 7.5$, 7.5 Hz, 2H, Phe-*H ortho*), 7.20 (tt, $J = 7.5$, 1.5 Hz, 1H Phe-*H para*), 4.72 (ddd, $J = 10.5$, 8, 4.5 Hz, 1H, CH), 3.26 (dd, $J = 14$, 4.5 Hz, 1H, CHH'), 3.15 (dd, $J = 14$, 10.5 Hz, 1H, CHH'). ^{13}C NMR (101 MHz, $\text{DMSO}-d_6$): δ 173.2 (COOH), 166.4 (CONH), 138.2 (Ar-C), 132.2 (Anth-C), 131.6 (Anth-C), 131.6 (Anth-C), 130.7 (Anth-C), 130.0 (Anth-C), 129.1 (Ar-CH), 128.4 (Anth-CH), 128.3 (Ar-CH), 128.2 (Anth-CH), 128.2 (Anth-CH), 128.1 (Anth-CH), 127.9 (Anth-CH), 126.4 (Ar-CH), 126.4 (Anth-CH), 126.0 (Anth-CH), 126.0 (Anth-CH), 123.5 (Anth-CH), 54.4 (CH), 36.4 (CH_2). HRMS: $[(\text{C}_{24}\text{H}_{19}\text{NO}_3) - \text{H}^+]^-$ expected 368.1292, found 368.1294. ν_{max} (cm^{-1}): 3304w, 3030w, 1714s, 1640s, 1521s. Anal: Calcd for $\text{C}_{24}\text{H}_{19}\text{NO}_3 \cdot \frac{1}{2}\text{H}_2\text{O}$ with 0.043 eq. EtOAc C, 75.96; H, 5.37; N, 3.66. Found: C 75.24, H 5.23, N 4.12.

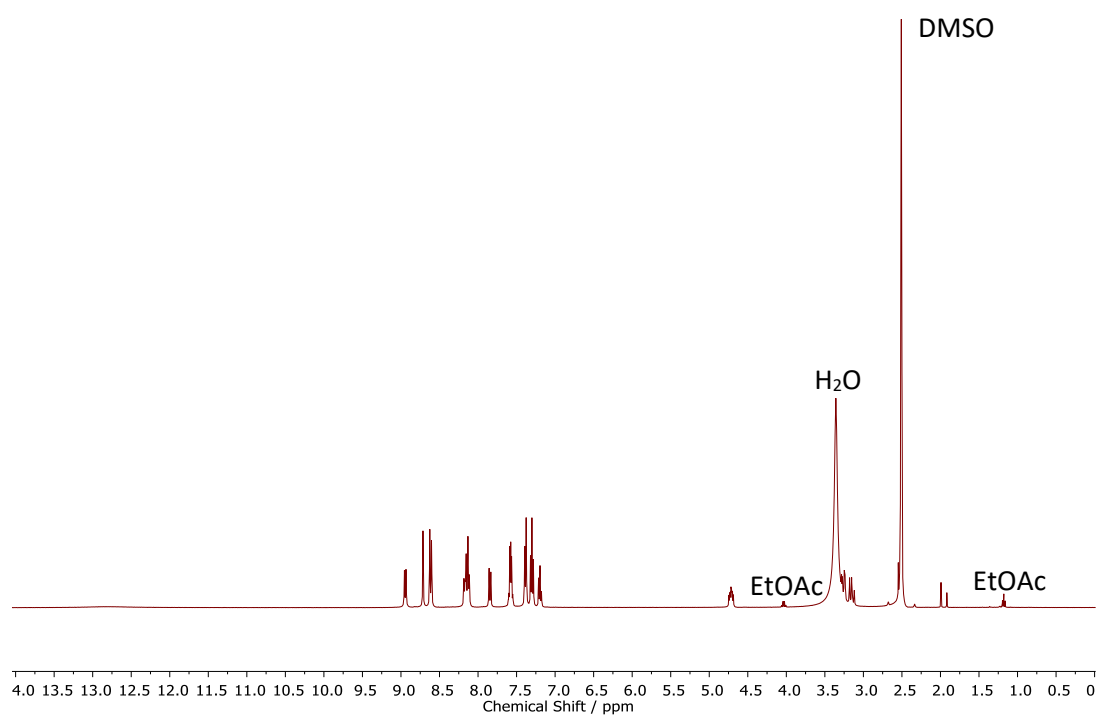


Fig. S3: ^1H NMR spectrum (400 MHz) of (Anth)Phe-OH in $\text{DMSO}-d_6$. Sample contains ca. 4.3% EtOAc

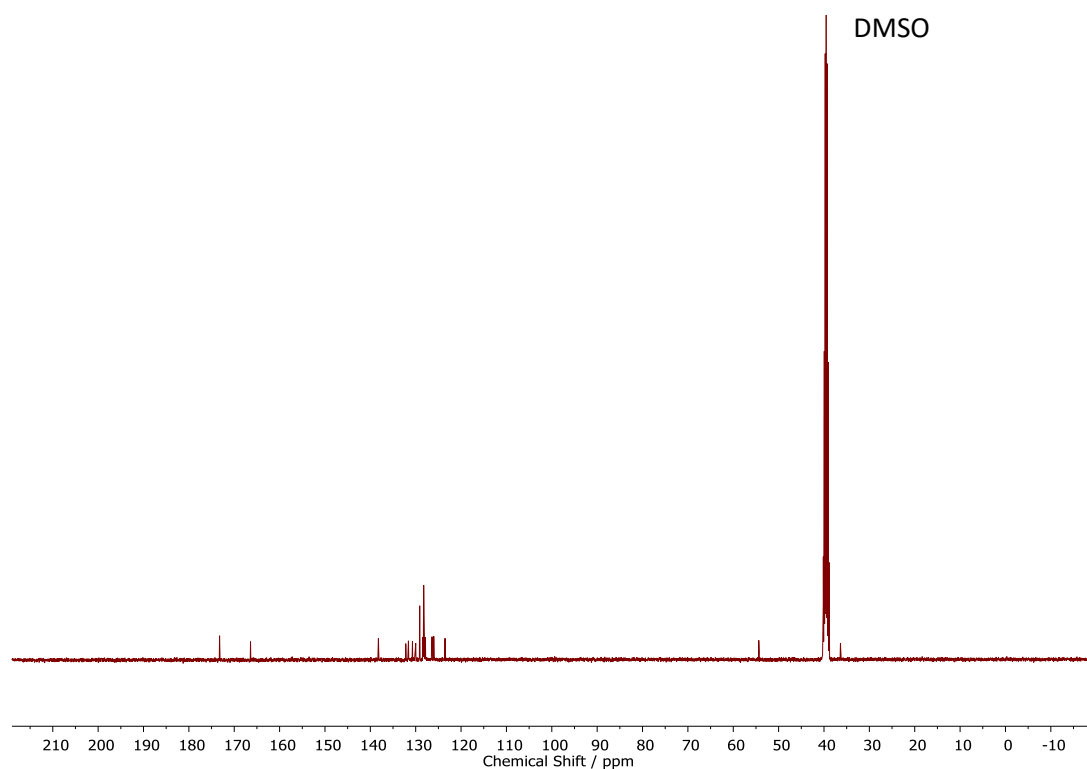
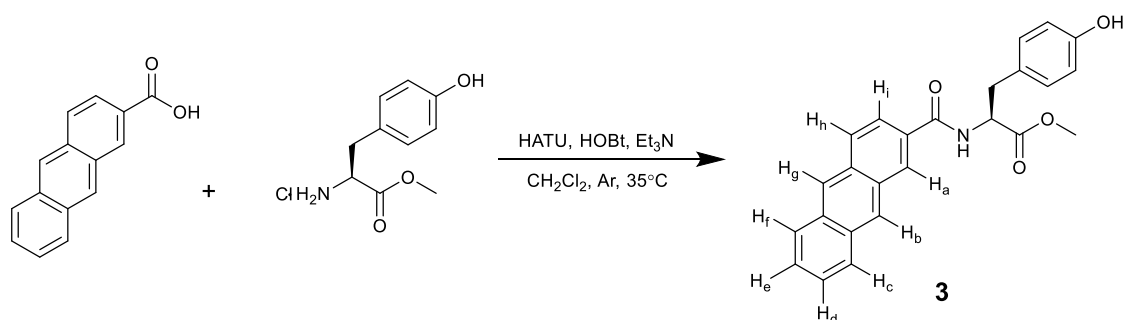


Fig. S4: ^{13}C NMR spectrum (101 MHz) of (Anth)Phe-OH in $\text{DMSO}-d_6$

S2.3. Synthesis of (anthracene-2-carbonyl)tyrosine methyl ester (**3**)



Anthracene-2-carboxylic acid (222 mg, 1 mmol), 1-[bis(dimethylamino)methylene]-1H-1,2,3-triazolo[4,5-b]pyridinium 3-oxide hexafluorophosphate (HATU, 380 mg, 1 mmol) and 1-hydroxybenzotriazole (HOBT, 63 mg, 0.5 mmol) were charged into a dry flask and stirred in dry dichloromethane (5 mL) at 0°C under nitrogen gas. Triethylamine (0.5 mL, 3.6 mmol) was added *via* syringe and the solution stirred for a further 15 min at 0°C.

Separately, tyrosine methyl ester hydrochloride (232 mg, 1 mmol) was stirred in dry dichloromethane (5 mL) in an oven-dried flask under nitrogen gas. Triethylamine (0.5 mL, 3.6 mmol) was added *via* syringe and the solution stirred at room temperature for 30 min. The clear, colourless solution was

then transferred *via* syringe to the reaction mixture and stirred for 1 h at 0°C before heating to 35°C and stirring for a further 16 h. During this time the formation of a yellow precipitate was evident.

Upon reaction completion, the solvent was removed *in vacuo*. The resulting crude solid was resuspended in a separating funnel with ethyl acetate (*ca.* 20 mL) and washed sequentially with aqueous HCl (0.1 M, 3 × 10 mL) and saturated NaCl solution (3 × 10 mL). The solid was filtered and washed with further portions of ethyl acetate (3 × 20 mL) before drying *in vacuo* to yield a yellow, dusty solid (202 mg, 51%).

^1H NMR (400 MHz, $\text{DMSO-}d_6$): δ 9.23 (s, 1H, OH), 9.04 (d, $J = 7.5$ Hz, 1H, NH), 8.73 (s, 1H, H_g), 8.64 (s, 1H, H_b), 8.62 (d, $J = 1.5$ Hz, 1H, H_a), 8.21-8.11 (m, 3H, H_d , H_f , H_h), 7.85 (dd, $J = 9, 1.5$ Hz, 1H, H_i), 7.62 – 7.54 (m, 2H, H_c , H_e), 7.14 (d, $J = 8.5$ Hz, 2H, Phe- H), 6.68 (d, $J = 8.5$ Hz, 2H, Phe- H), 5.18 (ddd, $J = 9.5, 7.5, 5.5$ Hz, 1H, CH), 3.66 (s, 3H, OCH_3) 3.10 (dd, $J = 14, 5.5$ Hz, 1H, CHH'), 3.03 (dd, $J = 14, 9.5$ Hz, 1H, CHH'). ^{13}C NMR (101 MHz, $\text{DMSO-}d_6$): δ 172.8 (C=O, ester), 167.0 (C=O, amide), 156.5 (Ar-C), 156.1 (Ar-C), 132.3 (Anth-C), 131.7 (Anth-C), 131.0 (Anth-C), 130.5 (Ar-CH), 129.0 (Anth-CH), 128.8 (Anth-CH), 128.8 (Anth-CH), 128.6 (Anth-CH), 128.4 (Anth-CH), 126.7 (Anth-CH), 126.5 (Anth-CH), 123.9 (Anth-CH), 115.5 (Ar-CH), 55.3 (CH), 52.4 (CH_3), 36.0 (CH_2). Some peaks were not observed in ^{13}C NMR spectra due to poor solubility of **3** in all available d-solvents; they were located in 2D NMR spectra. ν_{max} (cm^{-1}): 3486 br , 3384 w , 1738 s , 1644 s , 1509 s , 1241 s . HRMS: $[(\text{C}_{25}\text{H}_{22}\text{NO}_4) + \text{H}^+]^-$ expected 400.1543, found 400.1539.

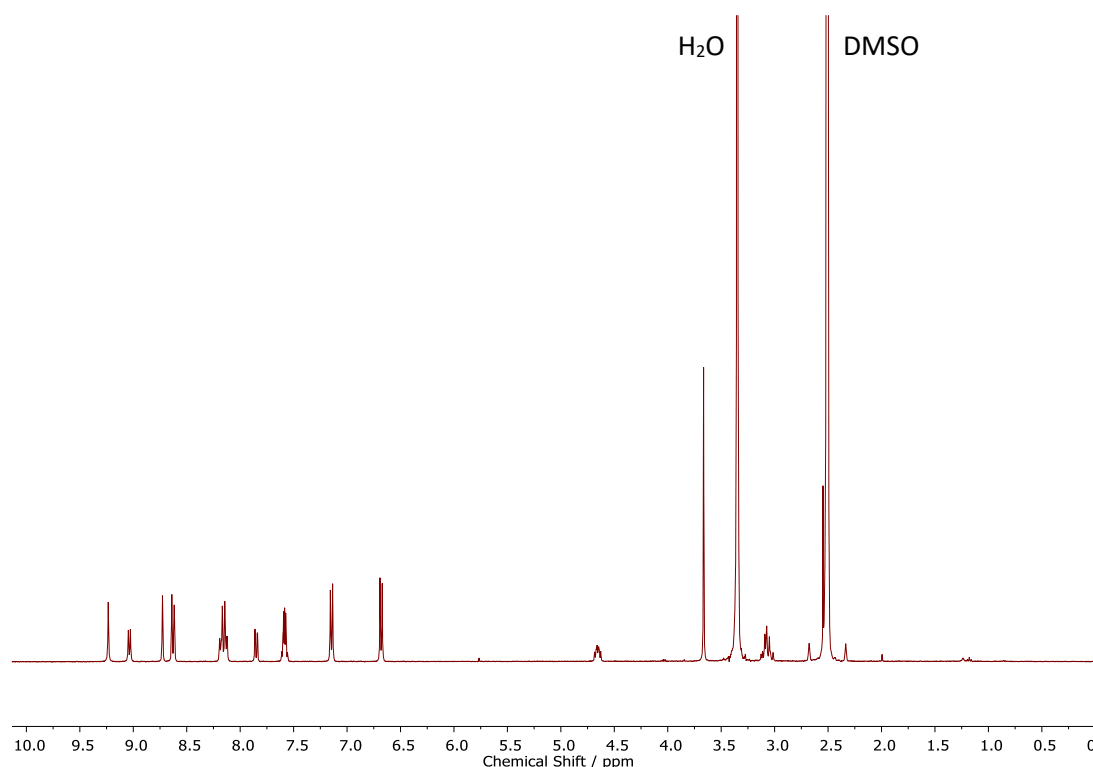


Fig. S5: ^1H NMR spectrum (400 MHz) of (Anth)Tyr-OMe in $\text{DMSO-}d_6$

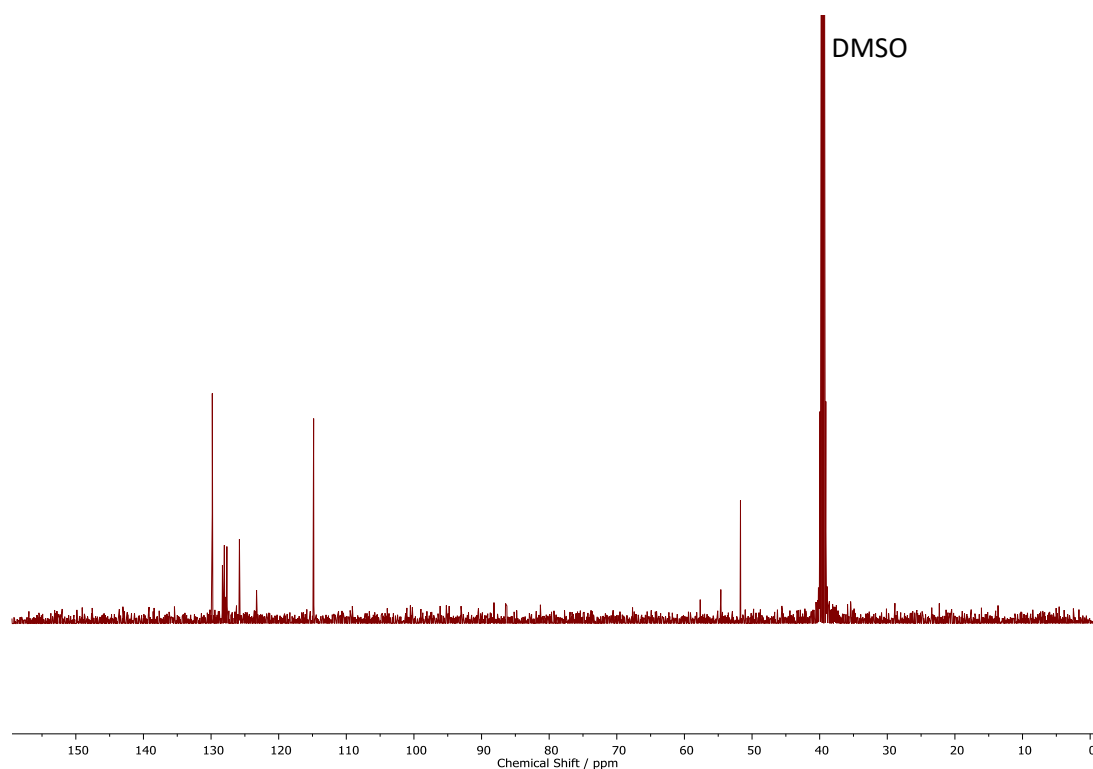


Fig. S6: ^{13}C NMR spectrum (101 MHz) of (Anth)Tyr-OMe. Some peaks were not observed in ^{13}C NMR spectra due to poor solubility of **3** in all available d-solvents; they were located in 2D NMR spectra in DMSO-d_6

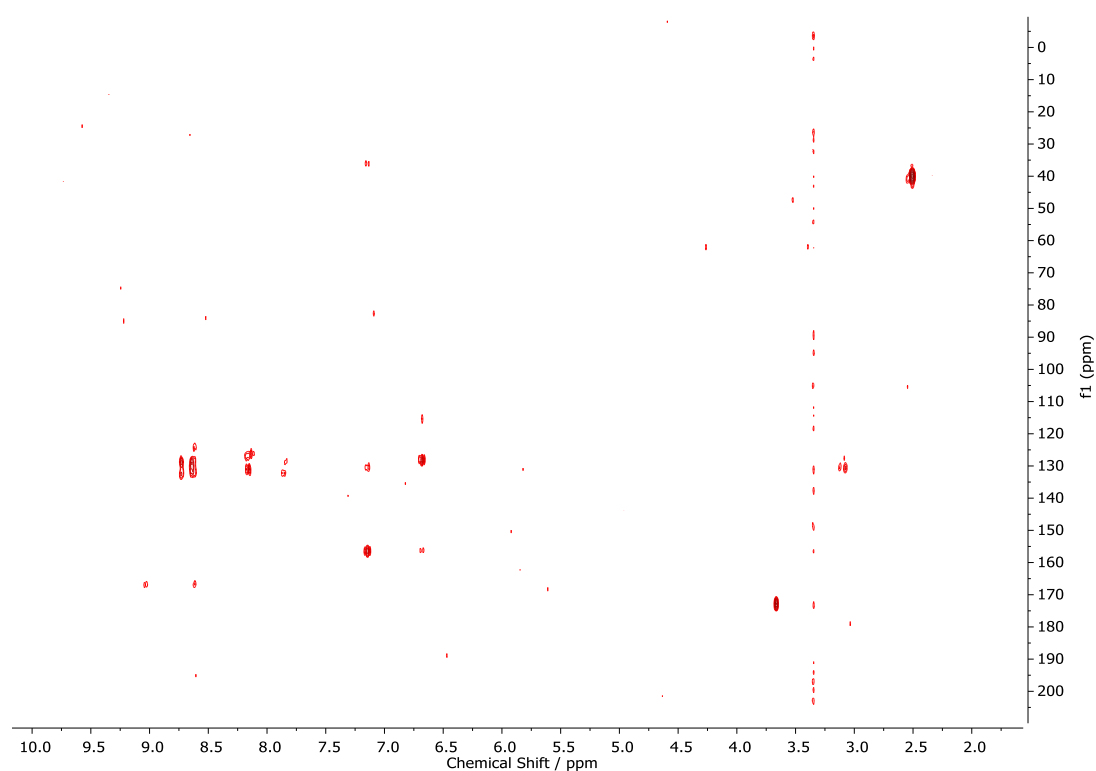


Fig. S7: HMBC (^1H vs ^{13}C) spectrum of (Anth)Tyr-OMe in DMSO-d_6

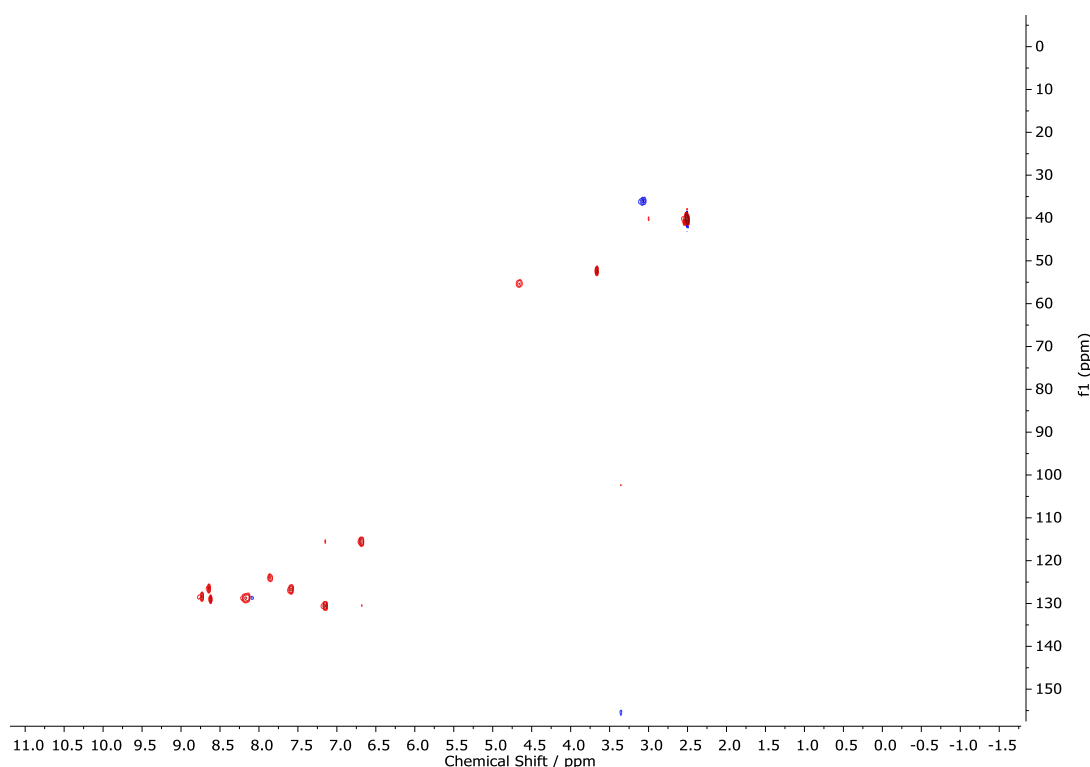
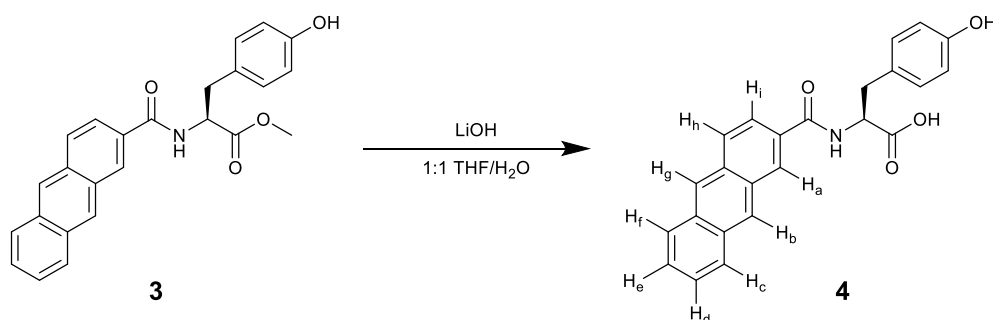


Fig. S8: HSQC (^1H vs ^{13}C) spectrum of (Anth)Tyr-OMe in $\text{DMSO}-d_6$

S2.4. Synthesis of (anthracene-2-carbonyl)tyrosine (**4**)



(Anthracene-2-carbonyl)tyrosine methyl ester (**3**, 150 mg, 0.4 mmol) was stirred in a 1:1 tetrahydrofuran/deionised water mixture. Lithium hydroxide (19 mg, 1 mmol) was added and the reaction stirred at room temperature for 16 h. The tetrahydrofuran was removed on a rotary evaporator, upon which a clear, pale-yellow gel formed in the round-bottomed flask. The gel was diluted with further deionised H_2O (ca. 20 mL) and shaken to break down the gel. The resulting solution was washed thoroughly with diethyl ether. The aqueous layer was carefully acidified to ca. pH 4 with 0.1 M HCl, resulting in the precipitation of an off-white solid. This solid was extracted into ethyl acetate and dried *in vacuo* to yield small, yellow crystals of **2** (110 mg, 71%).

^1H NMR (400 MHz, $\text{DMSO-}d_6$): δ 12.89 (br s, COOH), 9.13 (s, 1H, OH), 8.72 (s, 1H, H_g), 8.62 (s, 1H, H_b), 8.54 (d, $J = 1.5$ Hz, 1H, H_a), 8.46 (br s, 1H, NH), 8.18 – 8.09 (m, 3H, H_d , H_f , H_h), 7.81 (dd, $J = 9, 1.5$ Hz, 1H, H_i), 7.62 – 7.52 (m, 2H, H_c , H_e), 7.08 (d, $J = 8.5$ Hz, 2H, Ar-H), 6.62 (d, $J = 8.5$ Hz, 2H, Ar-H), 4.40 (br, 1H, CH), 3.14 (dd, $J = 13.5, 1.5$ Hz, 1H, CHH'), 3.01 (dd, $J = 13.5, 8.5$ Hz, 1H, CHH'). ^{13}C NMR (101 MHz, $\text{DMSO-}d_6$): δ 173.8 (COOH), 166.9 (CONH), 156.3 (Ar-C), 132.6 (Anth-C), 132.1 (Anth-C), 132.1 (Anth-C), 131.2 (Anth-C), 130.5 (Anth-C), 130.5 (Ar-C), 128.9 (Ar-CH), 128.8 (Anth-CH), 128.7 (Anth-CH), 128.7 (Anth-CH), 128.6 (Anth-CH), 128.3 (Anth-CH), 126.9 (Anth-CH), 126.5 (Anth-CH), 126.4 (Anth-CH), 124.0 (Anth-CH), 115.5 (Ar-CH), 55.2 (CH), 36.1 (CH_2). ν_{max} (cm^{-1}): 3667w, 2960m, 2884w, 724s, 1643m, 1513m. HRMS: $[(\text{C}_{24}\text{H}_{19}\text{NO}_4) - \text{H}^+]^-$ expected 384.1241, found 384.1244. Anal: Calcd for $\text{C}_{24}\text{H}_{19}\text{NO}_4 \cdot 3\text{H}_2\text{O}$: C, 65.59; H, 5.73; N, 3.19. Found: C 65.85, H 5.13, N 3.50.

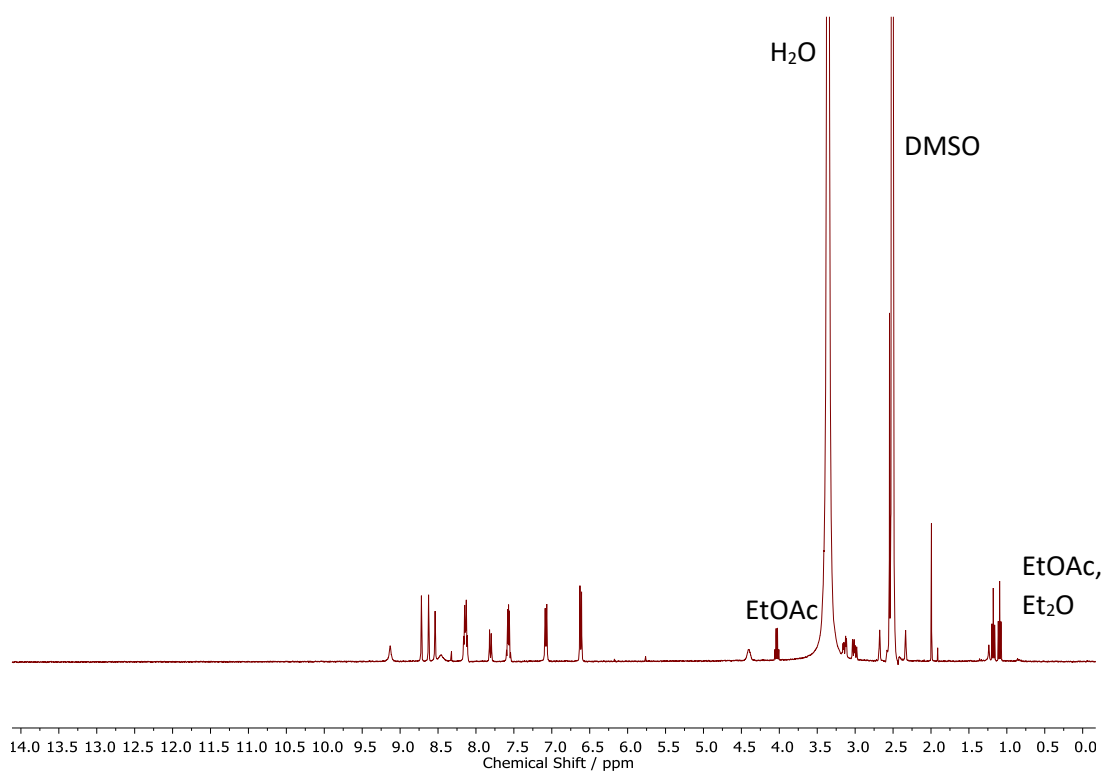


Fig. S9: ^1H NMR spectrum (400 MHz) of (Anth)Tyr-OH in $\text{DMSO-}d_6$. Sample contains small amounts of residual solvent (ethyl acetate and diethyl ether).

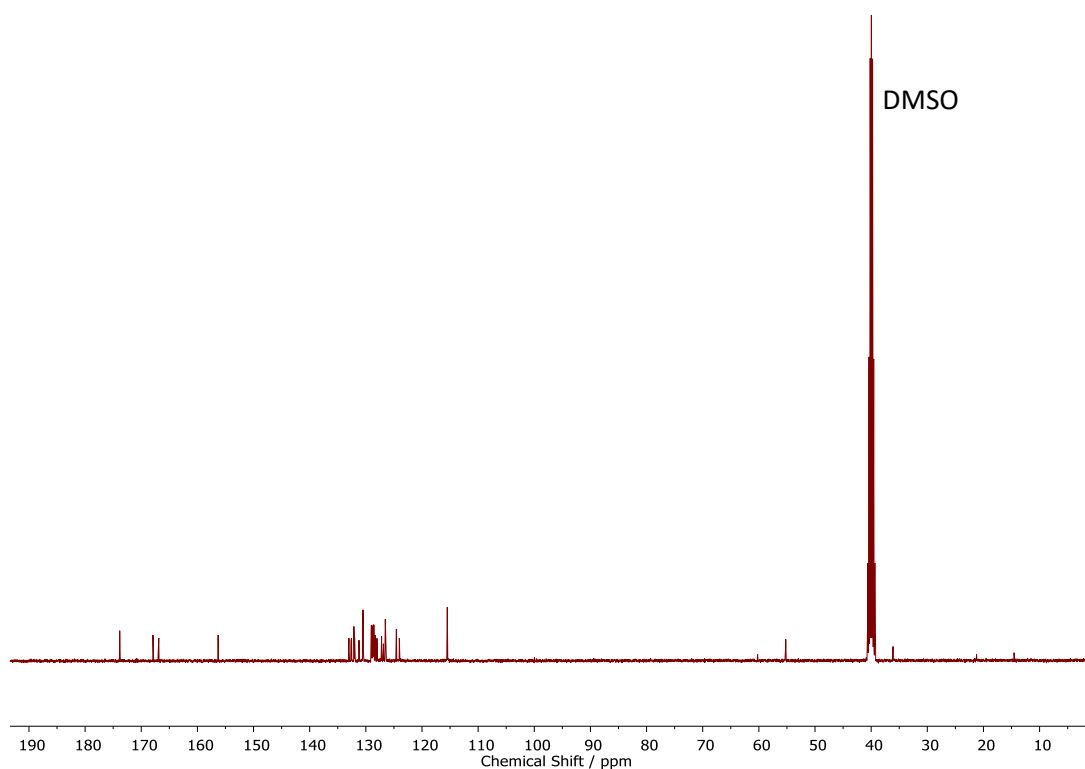
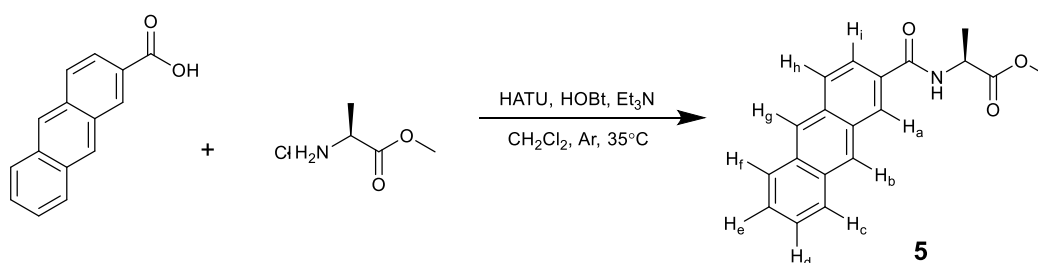


Fig. S10: ^{13}C NMR spectrum (101 MHz) of (Anth)Tyr-OH in DMSO-d_6

S2.5. Synthesis of (anthracene-2-carbonyl)alanine methyl ester (**5**)



Anthracene-2-carboxylic acid (222 mg, 1 mmol), 1-[bis(dimethylamino)methylene]-1H-1,2,3-triazolo[4,5-b]pyridinium 3-oxide hexafluorophosphate (HATU, 380 mg, 1 mmol) and 1-hydroxybenzotriazole (HOBt, 63 mg, 0.5 mmol) were charged into a dry flask and stirred in dry dichloromethane (5 mL) at 0°C under nitrogen gas. Triethylamine (0.5 mL, 3.6 mmol) was added *via* syringe and the solution stirred for a further 15 min at 0°C.

Separately, alanine methyl ester hydrochloride (140 mg, 1 mmol) was stirred in dry dichloromethane (5 mL) in an oven-dried flask under nitrogen gas. Triethylamine (0.5 mL, 3.6 mmol) was added *via* syringe and the solution stirred at room temperature for 30 min. The clear, colourless solution was then transferred *via* syringe to the reaction mixture and stirred for 1 h at 0°C before heating to 35°C and stirring for a further 16 h. During this time the formation of a yellow precipitate was evident.

Upon reaction completion, the solvent was removed *in vacuo*. The resulting crude solid was resuspended in a separating funnel with ethyl acetate (*ca.* 20 mL) and washed sequentially with aqueous HCl (0.1 M, 3 × 10 mL) and saturated NaCl solution (3 × 10 mL). The solid was filtered and washed with further portions of ethyl acetate (3 × 20 mL) before drying *in vacuo* to yield a pale yellow, dusty solid (193 mg, 63%).

^1H NMR (400 MHz, CDCl_3): δ 8.54 (s, 1H, H_g), 8.52 (s, 1H, H_b), 8.45 (d, $J = 1.5$ Hz, 1H, H_a), 8.07-8.02 (m, 3H, H_d , H_f , H_h), 7.82 (dd, $J = 9$, 2 Hz, 1H, H_i), 7.56 – 7.49 (m, 2H, H_c , H_e), 6.94 (d, $J = 7.5$ Hz, 1H, NH), 4.90 (dq, $J = 7.5$, 7.5 Hz, 1H, CH), 3.8 (s, 3H, OCH_3) 3.26 (dd, $J = 14$, 6 Hz, 1H, CHH'), 1.60 (d, $J = 7.5$ Hz, 3H CH_3). ^{13}C NMR (101 MHz, CDCl_3): δ 174.0 (COOH), 167.0 (CONH), 133.0 (Anth-C), 132.4 (Anth-C), 132.3 (Anth-C), 130.7 (Anth-C), 130.6 (Anth-C), 129.0 (Anth-CH), 128.6 (Anth-CH), 128.5 (Anth-CH), 128.4 (Anth-CH), 128.3 (Anth-CH), 126.5 (Anth-CH), 126.4 (Anth-CH), 126.1 (Anth-CH), 122.9 (Anth-CH), 52.8 (CH_3), 48.9 (CH), 19.0 (CH_3). ν_{max} (cm^{-1}): 3309m, 3048w, 2951w, 1744s, 1636m, 1525m. HRMS: $[(\text{C}_{19}\text{H}_{17}\text{NO}_3) + \text{Na}^+]^-$ expected 330.1101, found 330.1091.

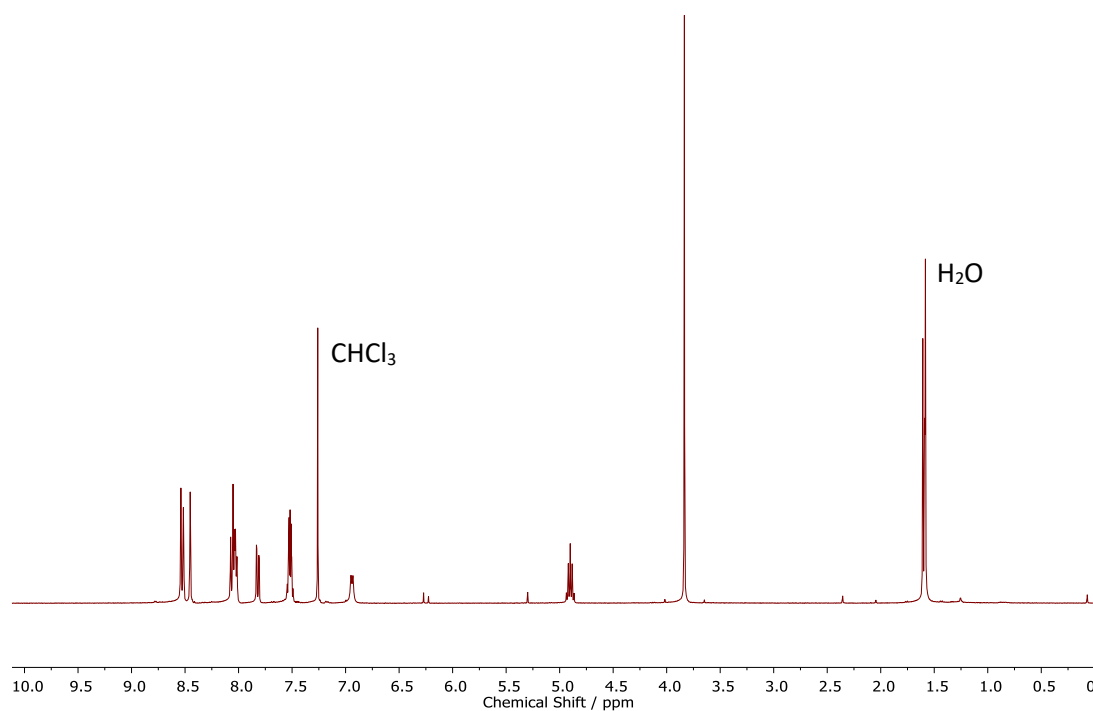


Fig. S11: ^1H NMR spectrum (400 MHz) of (Anth)Ala-OMe in CDCl_3

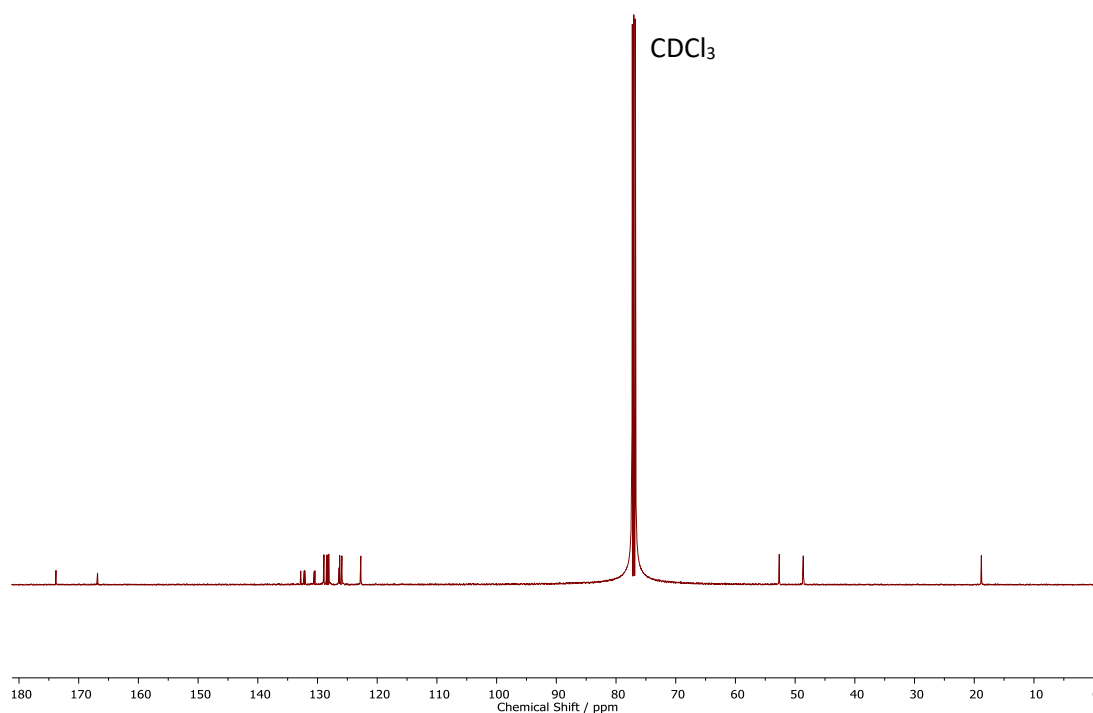
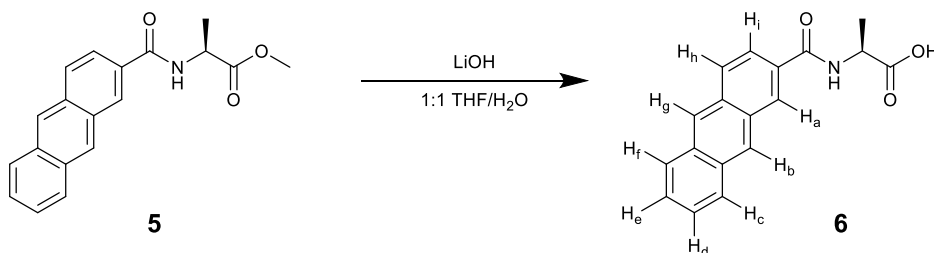


Fig. S12: ^{13}C NMR spectrum (101 MHz) of (Anth)Ala-OMe in CDCl_3

S2.6. Synthesis of (anthracene-2-carbonyl)alanine (**6**)



(Anthracene-2-carbonyl)alanine methyl ester (**5**, 170 mg, 0.6 mmol) was stirred in a 1:1 tetrahydrofuran/deionised water mixture. Lithium hydroxide (28 mg, 1.2 mmol) was added and the reaction stirred at room temperature for 16 h. The tetrahydrofuran was removed on a rotary evaporator to yield an off-white solid which was dissolved in deionised H_2O (*ca.* 20 mL) and washed thoroughly with diethyl ether. The aqueous layer was carefully acidified to *ca.* pH 4 with 0.1 M HCl, resulting in the precipitation of an off-white solid. This solid was extracted into ethyl acetate and dried *in vacuo* to yield off-white powder **6** (153 mg, 90%).

^1H NMR (400 MHz, $\text{DMSO}-d_6$): δ 12.60 (br s, COOH), 8.90 (d, $J = 7$ Hz, 1H, NH), 8.72 (s, 1H, H_g), 8.69 (s, 1H, H_b), 8.64 (d, $J = 1.5$ Hz, 1H, H_a), 8.21 – 8.10 (m, 3H, H_d , H_f , H_h), 7.93 (dd, $J = 9$, 1.5 Hz, 1H, H_i), 7.62 –

¹H NMR spectrum of compound **1** in DMSO-d₆. The x-axis is labeled "Chemical Shift / ppm" and ranges from 13.0 to 0.0. The spectrum shows several peaks: a broad peak around 12.5 ppm, a multiplet between 8.5 and 9.0 ppm, a multiplet between 7.5 and 8.0 ppm, a small peak at 6.5 ppm, a multiplet at 4.5 ppm, a sharp peak at 3.5 ppm labeled "H₂O", a sharp peak at 2.5 ppm labeled "DMSO", and a multiplet between 1.5 and 2.0 ppm.

S16 | Page

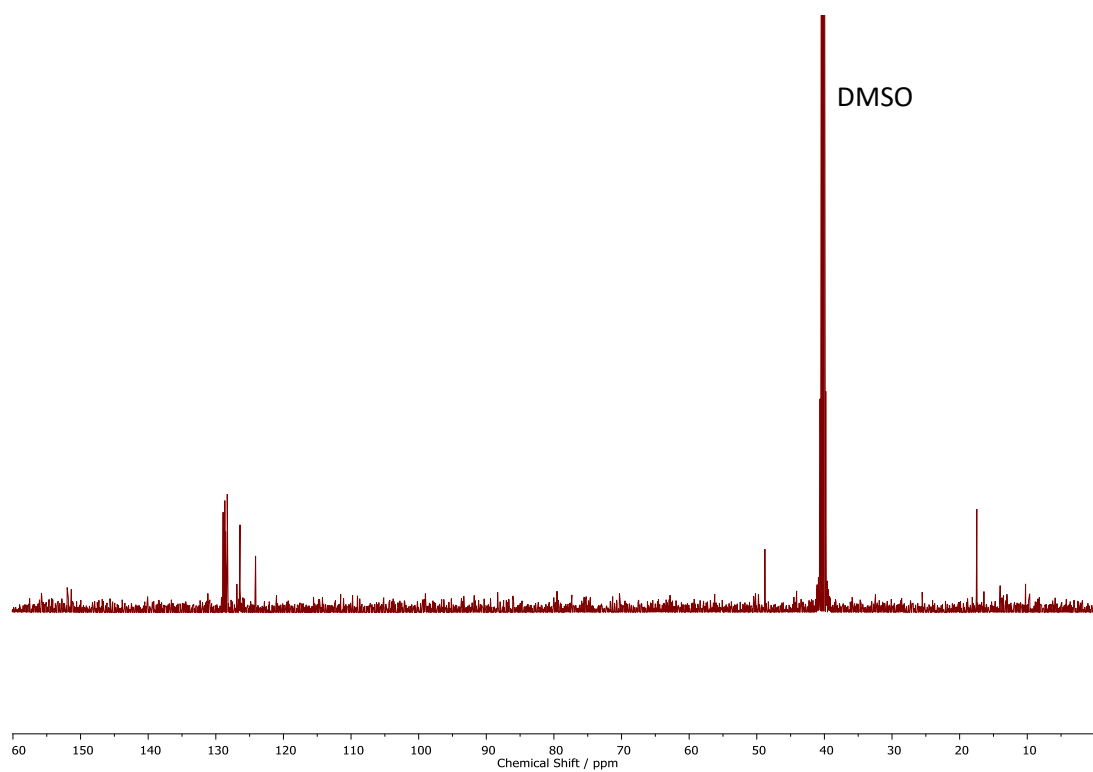


Fig. S14: DEPT NMR spectrum of (Anth)Ala-OH in DMSO- d_6

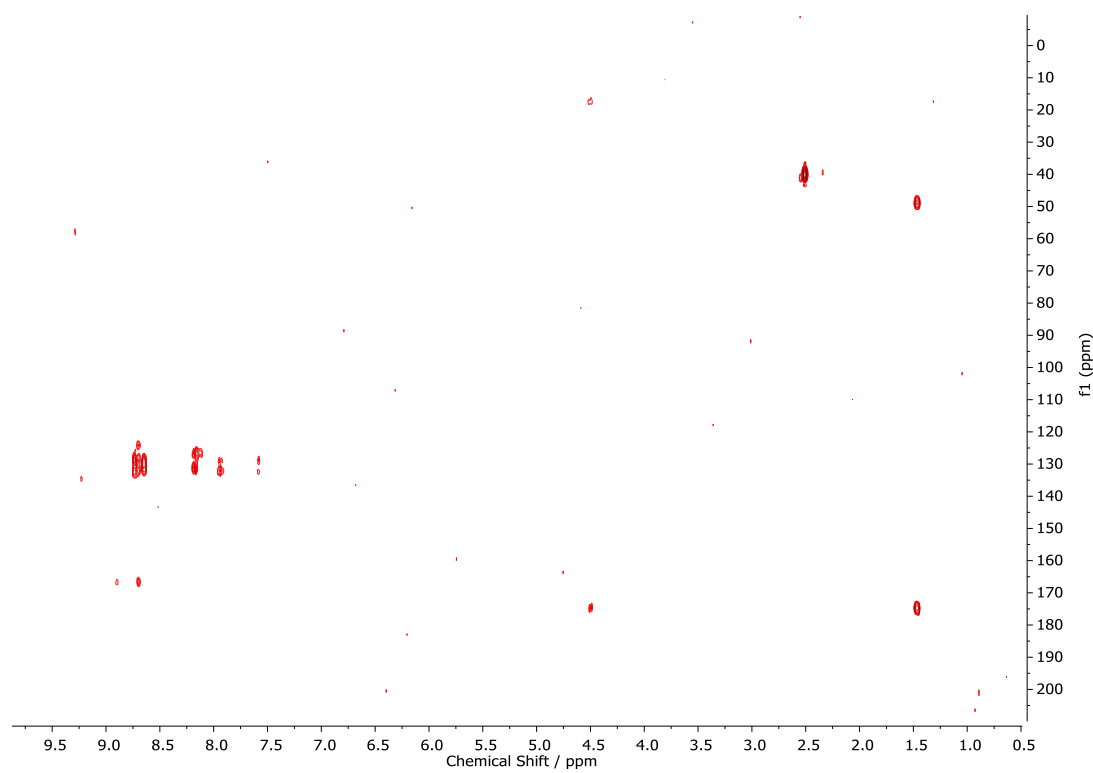


Fig. S15: HMBC (^{13}C vs ^1H) NMR spectrum of (Anth)Ala-OH in DMSO- d_6

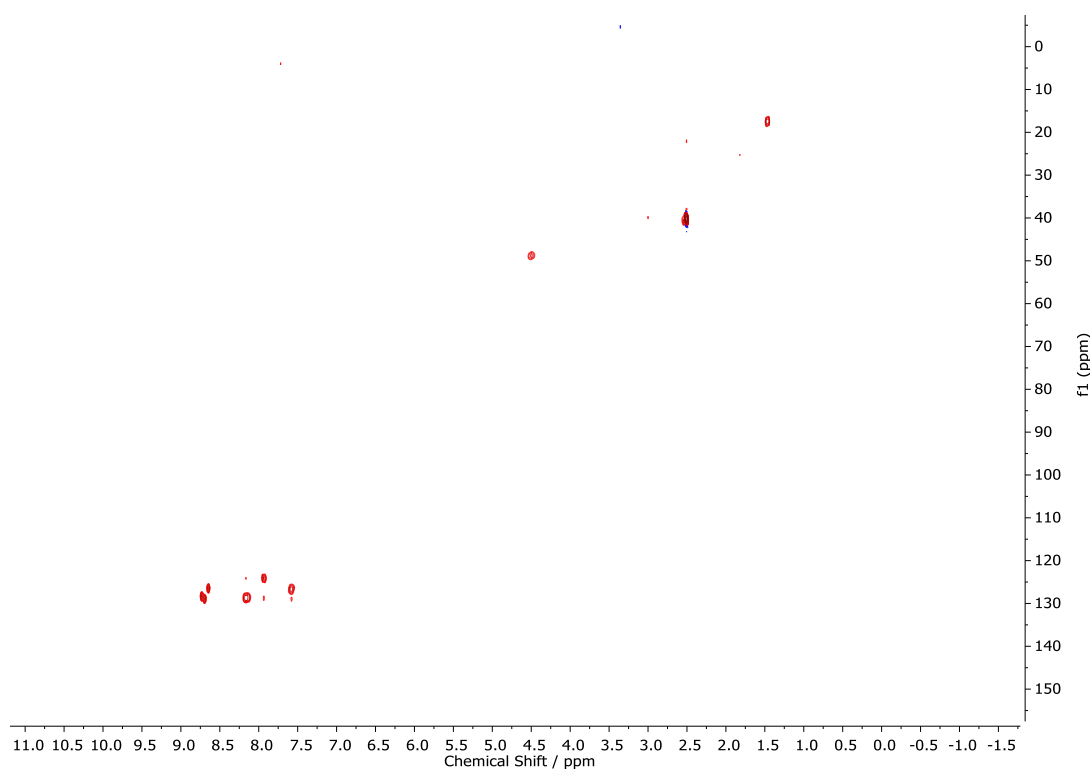
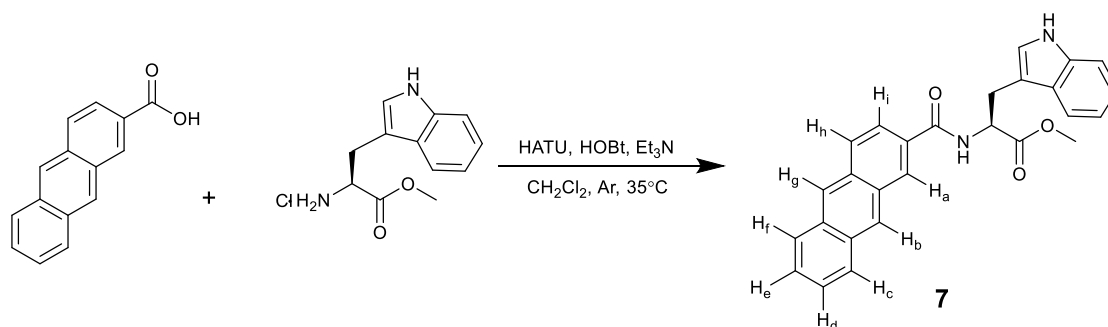


Fig. S16: HSQC (^{13}C vs ^1H) NMR spectrum of (Anth)Ala-OH in $\text{DMSO}-d_6$

S2.7. Synthesis of (anthracene-2-carbonyl)tryptophan methyl ester (**7**)



Anthracene-2-carboxylic acid (222 mg, 1 mmol), 1-[bis(dimethylamino)methylene]-1H-1,2,3-triazolo[4,5-b]pyridinium 3-oxide hexafluorophosphate (HATU, 380 mg, 1 mmol) and 1-hydroxybenzotriazole (HOBt, 63 mg, 0.5 mmol) were charged into a dry flask and stirred in dry dichloromethane (5 mL) at 0°C under nitrogen gas. Triethylamine (0.5 mL, 3.6 mmol) was added *via* syringe and the solution stirred for a further 15 min at 0°C.

Separately, alanine methyl ester hydrochloride (255 mg, 1 mmol) was stirred in dry dichloromethane (5 mL) in an oven-dried flask under nitrogen gas. Triethylamine (0.5 mL, 3.6 mmol) was added *via* syringe and the solution stirred at room temperature for 30 min. The clear, colourless solution was

then transferred *via* syringe to the reaction mixture and stirred for 1 h at 0°C before heating to 35°C and stirring for a further 16 h. During this time the formation of a white precipitate was evident.

Upon reaction completion, the solvent was removed *in vacuo*. The resulting crude solid was resuspended in a separating funnel with ethyl acetate (*ca.* 20 mL) and washed sequentially with aqueous HCl (0.1 M, 3 × 10 mL) and saturated NaCl solution (3 × 10 mL). The solid was filtered and washed with further portions of ethyl acetate (3 × 20 mL) before drying *in vacuo* to yield a white powder (265 mg, 63%).

^1H NMR (400 MHz, $\text{DMSO-}d_6$): δ 10.88 (d, J = 2.5 Hz, 1H, Trp NH), 9.05 (d, J = 7.5 Hz, 1H, CONH), 8.70 (s, 1H, H_g), 8.64-8.61 (m, 2H, H_a , H_b), 8.20 - 8.09 (m, 3H, H_d , H_f , H_h), 7.87 (dd, J = 9, 1.5 Hz, 1H, H_i), 7.62 (d, J = 7.5 Hz, 1H, Trp Ar- H), 7.60 – 7.54 (m, 2H, H_c , H_e), 7.34 (d, J = 7.5 Hz, 1H, Trp Ar- H) 7.28 (d, J = 2.5 Hz, Trp =CH), 7.10 – 7.05 (ddd, J = 7.5, 7.5, 1 Hz, 1H, Trp Ar- H), 7.04 – 6.99 (ddd, J = 7.5, 7.5, 1 Hz, 1H, Trp Ar- H), 4.78 (ddd, J = 9, 7.5, 5.5 Hz, 1H, Trp-CH), 3.67 (s, 3H, OCH_3) 3.37-3.30 (m under HOD peak, 2H, CH_2). ^{13}C NMR (101 MHz, $\text{DMSO-}d_6$): δ 136.1 (Trp-C), 132.2 (Anth-C), 131.7 (Anth-C), 131.6 (Anth-C), 130.5 (Anth-C), 130.0 (Anth-C), 128.6 (Anth-CH), 128.3 (Anth-CH), 128.3 (Anth-CH), 128.1 (Anth-CH), 127.9 (Anth-CH), 127.1 (Trp Ar-C), 126.5 (Anth-CH), 126.1 (Anth-CH), 126.0 (Anth-CH), 123.8 (Trp Ar-CH), 123.6 (Anth-CH), 121.0 (Trp Ar-CH), 118.5 (Trp Ar-CH), 118.1 (Trp =CH), 111.5 (Trp Ar-CH), 110.0 (Trp =C), 53.78 (Trp CH), 51.75 (CH_3), 26.48 (CH_2). ν_{max} (cm^{-1}): 3364w, 2980w, 2884w, 1734s, 1644w, 1507w. HRMS: $[(\text{C}_{27}\text{H}_{21}\text{N}_2\text{O}_3) - \text{H}^+]^+$ expected 421.1558, found 421.1566.

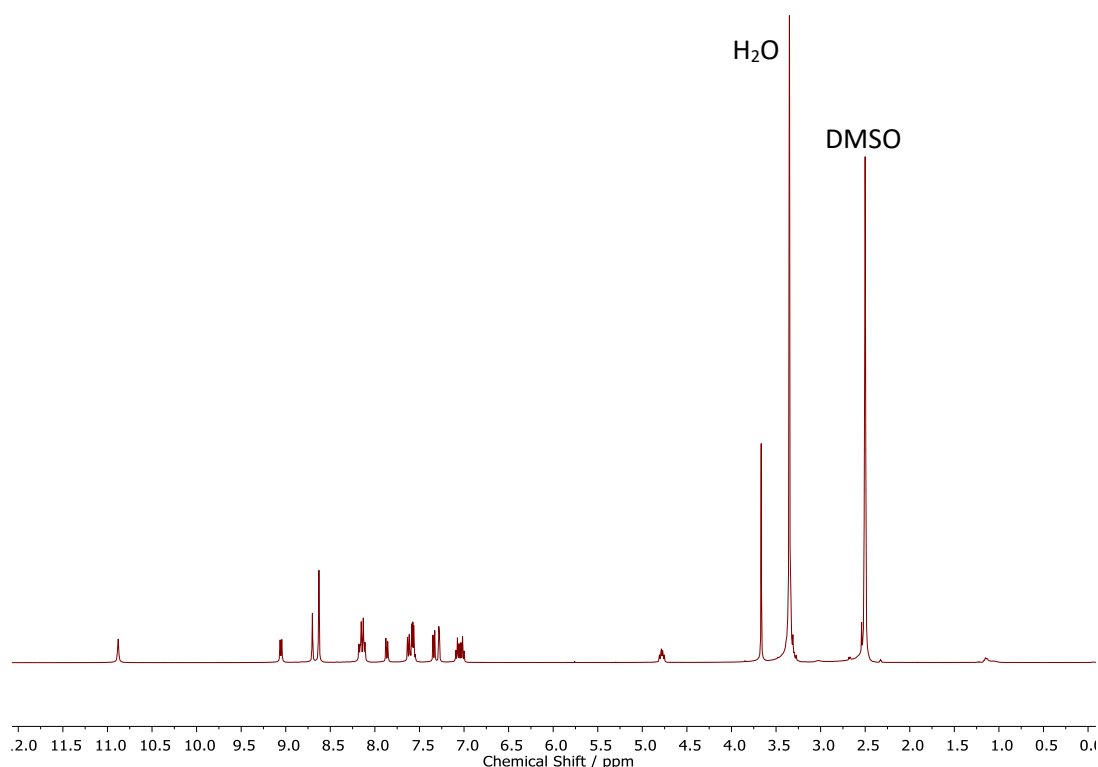


Fig. S17: ^1H NMR spectrum (400 MHz) of (Anth)Trp-OME in $\text{DMSO-}d_6$

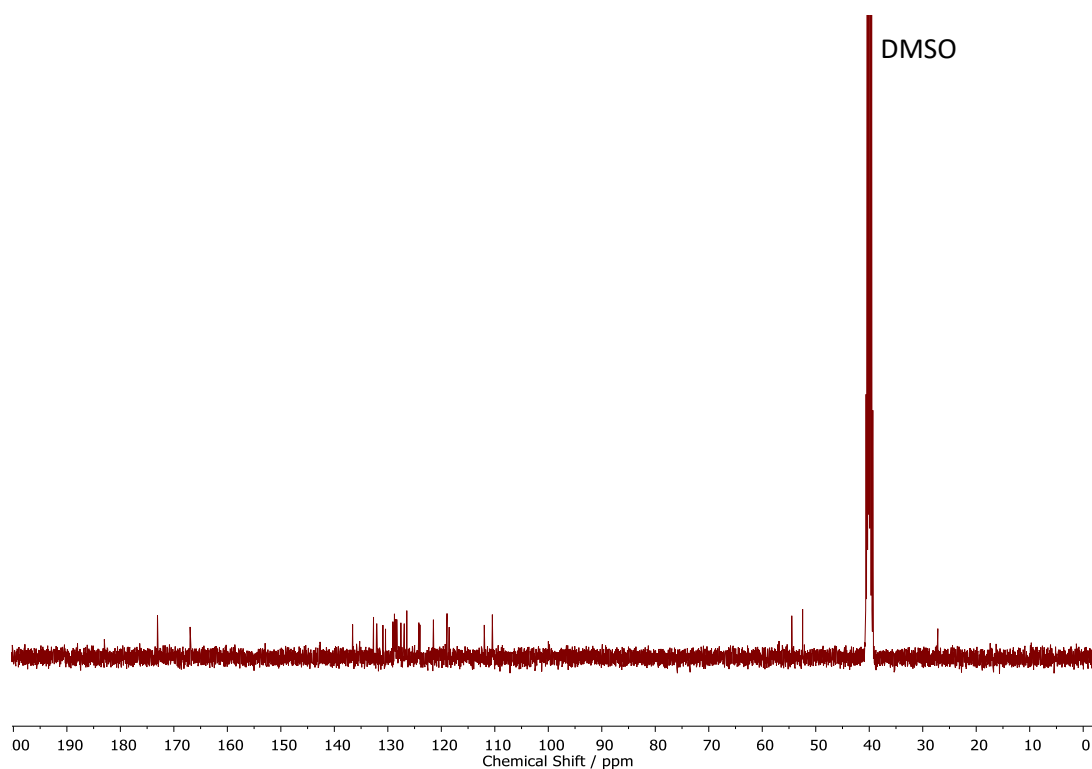
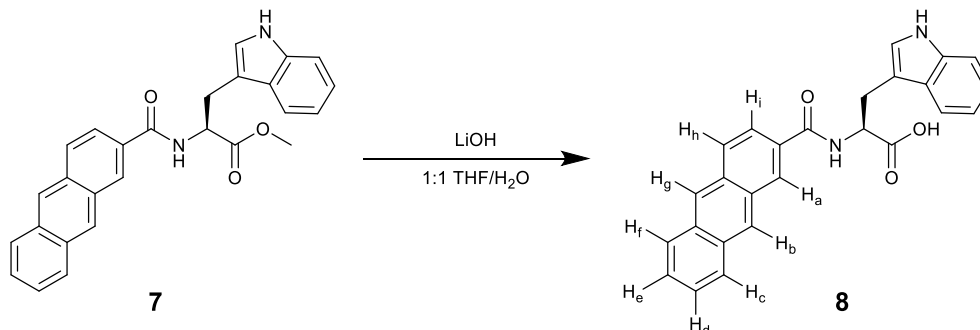


Fig. S18: ^{13}C NMR spectrum (101 MHz) of (Anth)Trp-OMe in $\text{DMSO}-d_6$

S2.8. Synthesis of (anthracene-2-carbonyl)tryptophan (**8**)



(Anthracene-2-carbonyl)tryptophan methyl ester (**7**, 250 mg, 0.6 mmol) was stirred in a 1:1 tetrahydrofuran/deionised water mixture. Lithium hydroxide (28 mg, 1.2 mmol) was added and the reaction stirred at room temperature for 16 h. The tetrahydrofuran was removed on a rotary evaporator to yield an off-white solid, which was dissolved in deionised H_2O (ca. 20 mL) and washed thoroughly with diethyl ether. The aqueous layer was carefully acidified to ca. pH 4 with 0.1 M HCl, resulting in the precipitation of an off-white solid. This solid was extracted into ethyl acetate and dried *in vacuo* to yield off-white powder **8** (177 mg, 72%).

^1H NMR (400 MHz, $\text{DMSO}-d_6$): δ 12.79 (s, 1H, COOH), 10.84 (d, $J = 2.5$ Hz, 1H, Trp NH), 8.87 (d, $J = 8$ Hz, 1H, CONH), 8.70 (s, 1H, H_g), 8.63 (s, 1H, H_b), 8.62 (d, $J = 1.5$ Hz, 1H, H_a), 8.20 – 8.10 (m, 3H, H_d , H_f , H_h), 7.86 (dd, $J = 9, 1.5$ Hz, 1H, H_i), 7.66 (d, $J = 8$ Hz, 1H, Trp Ar-H), 7.62 – 7.54 (m, 2H, H_c , H_e), 7.33 (d, $J = 8$

Hz, 1H, Trp Ar-*H*), 7.27 (d, *J* = 2.5 Hz, Trp =CH), 7.10 – 7.04 (ddd, *J* = 7, 7, 1 Hz, 1H, Trp Ar-*H*), 7.04 – 6.98 (ddd, *J* = 7, 7, 1 Hz, 1H, Trp Ar-*H*), 4.78 (ddd, *J* = 9.5, 8, 4.5 Hz, 1H, Trp-CH), 3.40-3.25 (m, 2H, CH₂). ¹³C NMR (101 MHz, DMSO-*d*₆): δ 171.0 (COOH), 166.6 (CONH₂), 136.3 (Trp Ar-C), 132.5 (Anth-C), 132.2 (Anth-C), 131.6 (Anth-C), 131.5 (Anth-C), 129.6 (Anth-C), 128.9 (Anth-CH), 128.7 (Anth-CH), 128.6 (Anth-CH), 128.5 (Anth-CH), 128.3 (Anth-CH), 127.5 (Trp Ar-C), 126.7 (Trp Ar-CH), 126.5 (Anth-CH), 124.0 (Trp =CH), 121.4 (Trp-Ar-CH), 119.0 (Anth-CH), 118.8 (Trp Ar-CH), 111.8 (Trp Ar-CH), 110.8 (Trp =C), 54.7 (Trp CH), 27.2 (Trp CH₂). Some peaks were not observed in ¹³C NMR spectra due to poor solubility of **8** in DMSO-*d*₆; they were located in 2D NMR spectra. ν_{max} (cm⁻¹): 3209*w*, 2980*m*, 2885*w*, 1730*s*, 1657*m*. HRMS: [(C₂₇H₂₁N₂O₃) – H⁺]⁺ expected 421.1558, found 421.1566.

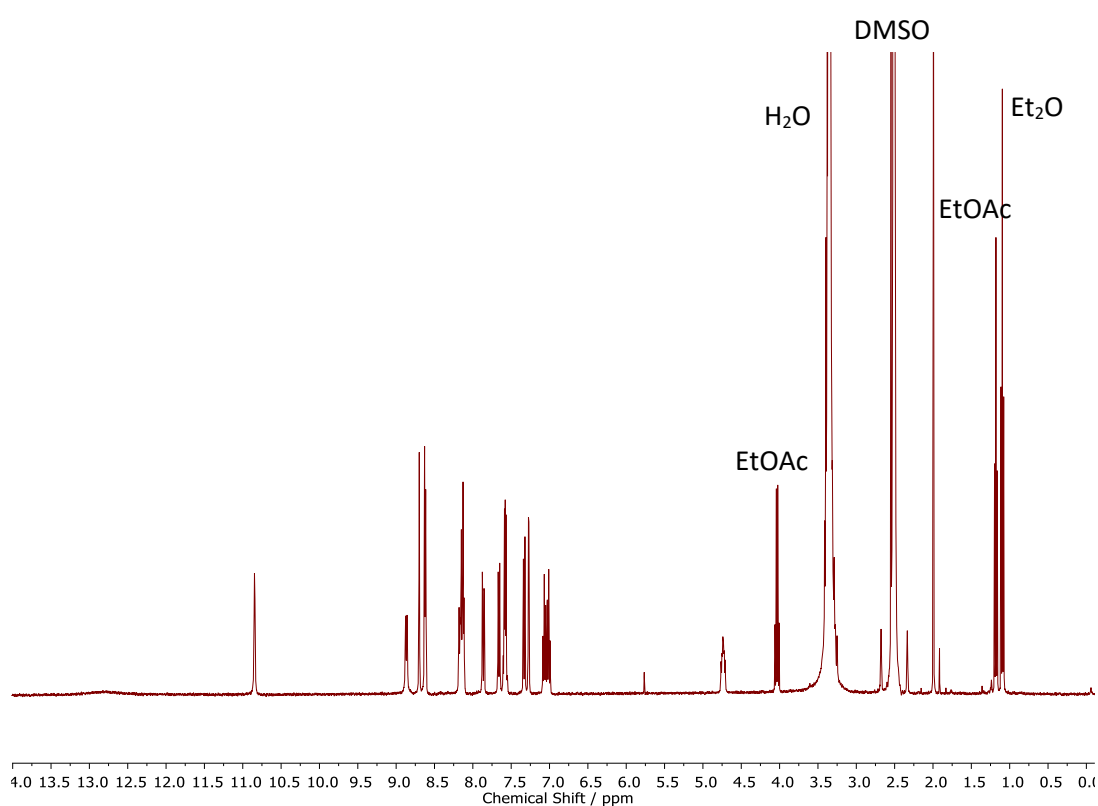


Fig. S19: ¹H NMR spectrum (400 MHz) of (Anth)Trp-OH in DMSO-*d*₆. Sample contains residual solvent (ethyl acetate and diethyl ether).

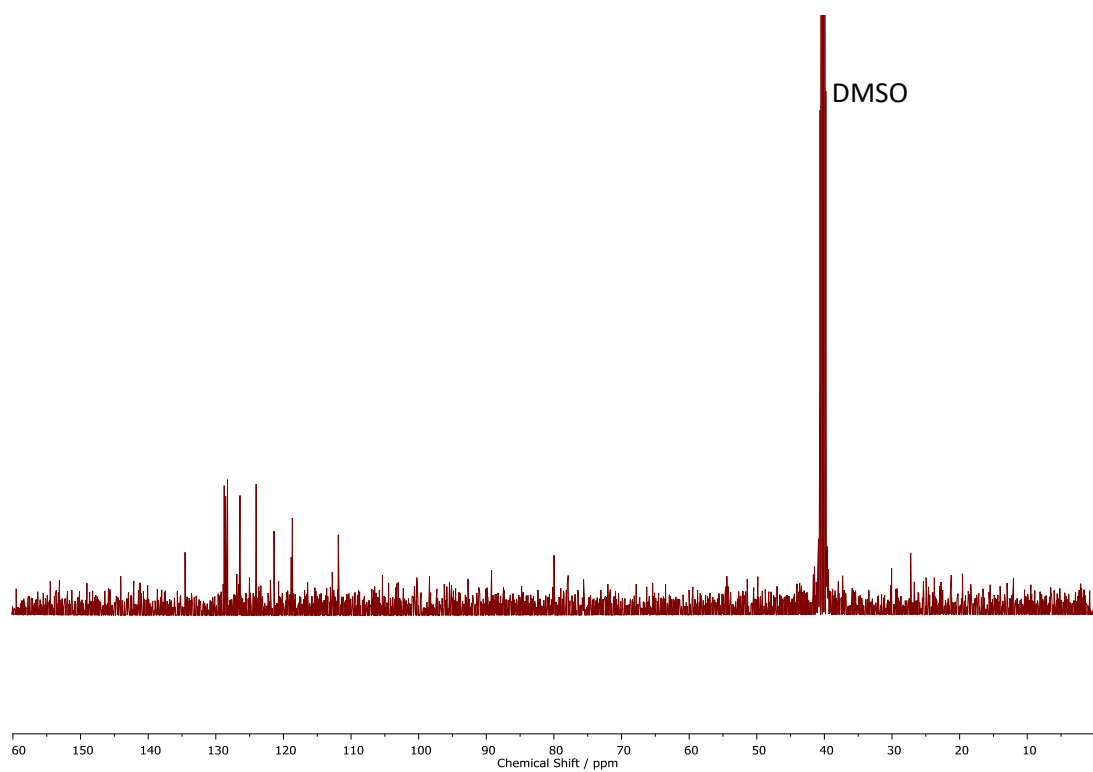


Fig. S20: DEPT NMR spectrum of (Anth)Trp-OH in DMSO-d₆

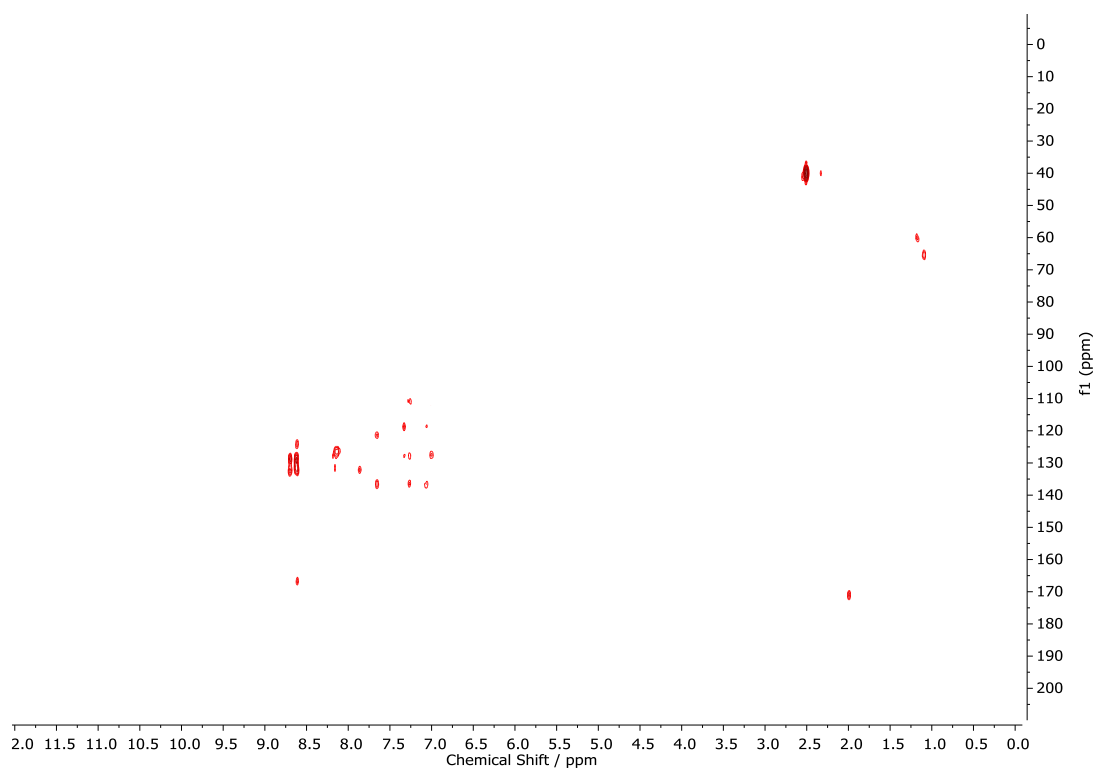


Fig. S21: HMBC (¹³C vs ¹H) NMR spectrum of (Anth)Trp-OH in DMSO-d₆

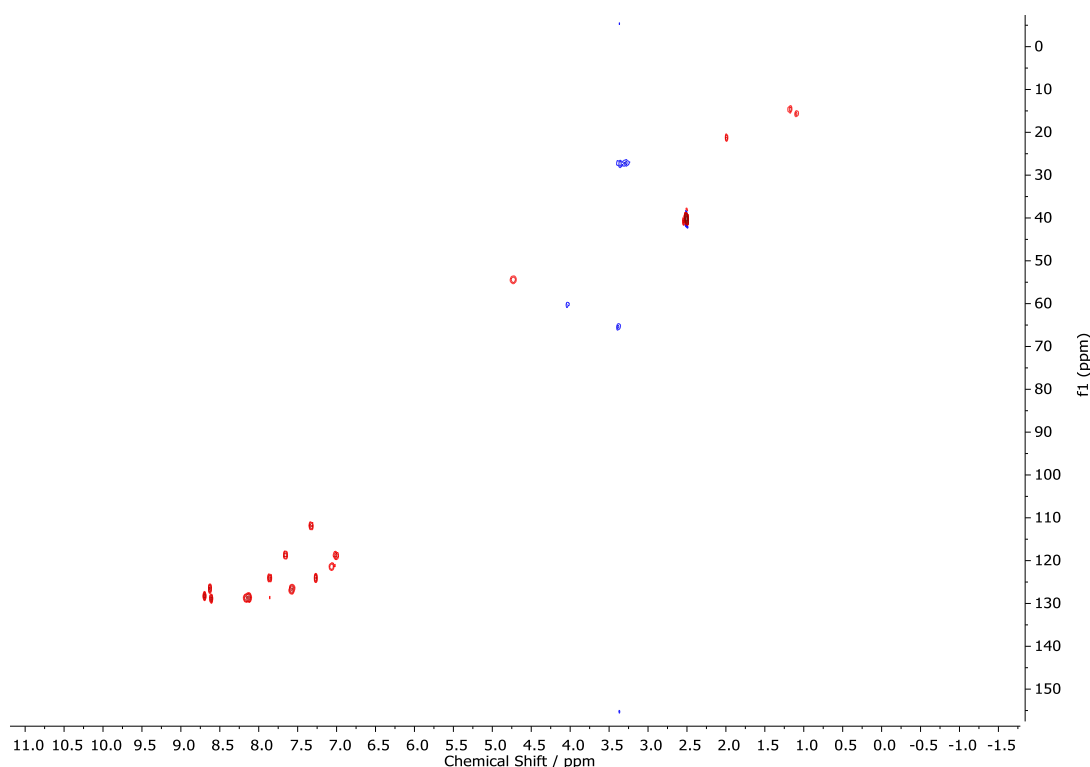


Fig. S22: HSQC (^{13}C vs ^1H) NMR spectrum of (Anth)Trp-OH in $\text{DMSO}-d_6$

S2.9. General procedure for synthesis of (anthracene-9-carbonyl)amino acids

Anthracene-9-carboxylic acid (222 mg, 1 mmol), 1-[bis(dimethylamino)methylene]-1*H*-1,2,3-triazolo[4,5-*b*]pyridinium 3-oxide hexafluorophosphate (HATU, 380 mg, 1 mmol) and 1-hydroxybenzotriazole (HOBt, 63 mg, 0.5 mmol) were charged into a dry flask and stirred in dry dichloromethane (5 mL) at 0°C under nitrogen gas. Triethylamine (0.5 mL, 3.6 mmol) was added *via* syringe and the solution stirred for a further 15 min at 0°C.

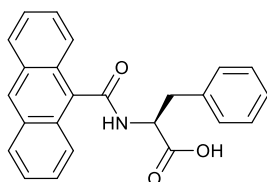
Separately, the appropriate amino acid methyl ester hydrochloride (1 mmol) was stirred in dry dichloromethane (5 mL) in an oven-dried flask under nitrogen gas. Triethylamine (0.5 mL, 3.6 mmol) was added *via* syringe and the solution stirred at room temperature for 30 min. The clear, colourless solution was then transferred *via* syringe to the reaction mixture and stirred for 1 h at 0°C before heating to 35°C and stirring for a further 16 h. During this time the formation of a white precipitate was evident.

Upon reaction completion, the solvent was removed *in vacuo*. The resulting crude solid was dissolved in ethyl acetate and washed sequentially with aqueous HCl (0.1 M, 3 × 10 mL) and saturated NaCl solution (3 × 10 mL). The organic layers were combined, dried over MgSO_4 and dried *in vacuo*. The crude product was purified by flash column chromatography, eluting with 5-20% MeOH in

dichloromethane. Product fractions were combined and dried *in vacuo* to yield the desired (anthracene-9-carbonyl)amino acid methyl ester.

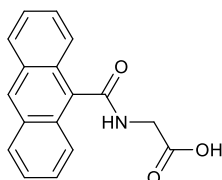
This compound (0.5 mmol) was dissolved in a 1:1 THF/H₂O mixture and stirred with LiOH (28 mg, 1 mmol) for 16 h before removing the THF *in vacuo*. The resulting aqueous solution was washed thoroughly with diethyl ether before acidification to pH 4 using HCl_(aq) (0.1 M), resulting in precipitation of the desired product. The solid was extracted into ethyl acetate and dried over MgSO₄ and *in vacuo* to yield the final product.

S2.10 Synthesis of (anthracene-9-carbonyl)phenylalanine



Isolated as yellow powder (42% yield over two steps). ¹H NMR (400 MHz, DMSO-*d*₆): 13.06 (s, 1H, COOH), 9.25 (d, *J* = 8.5 Hz, 1H, CONH), 8.66 (s, 1H, Anth-CH), 8.27 – 8.22 (m, 2H, Anth-CH), 8.18 – 8.09 (m, 4H, Anth-CH), 7.62 – 7.55 (m, 2H, Anth-CH), 7.52 (t, *J* = 7 Hz, 1H, *para* Phe-CH), 7.26 (dd, *J* = 8, 7 Hz, 2H, *meta* Phe-CH), 7.07 (d, *J* = 8 Hz, 2H, *ortho* Phe-CH), 5.13 (ddd, *J* = 12, 8.5, 4 Hz, 1H, Phe-CH), 3.39 (m, 1H, Phe CHH'), 2.98 (dd, *J* = 14, 12 Hz, 1H, Phe CHH'). ¹³C NMR (101 MHz, DMSO-*d*₆): 173.5 (COOH), 168.7 (CONH), 138.6 (2 × Anth-C), 133.3 (2 × Anth-C), 131.0 (Anth-C), 129.7 (2 × Anth-CH), 129.4 (Anth-C), 128.8 (2 × Anth-CH), 128.6 (Anth-CH), 128.5 (Anth-CH), 128.0 (Phe-C), 127.5 (Anth-CH), 126.9 (Anth-CH), 126.5 (Phe-CH), 126.4 (Anth-CH), 126.2 (Phe-CH), 126.0 (Phe-CH), 125.9 (Phe-CH), 125.8 (Phe-CH), 54.2 (Phe-CH), 36.7 (Phe CH₂). LRMS [(C₂₄H₁₉NO₃) – H⁺]⁺ expected 368.14, found 368.1.

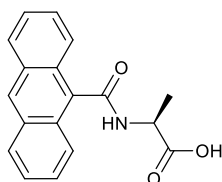
S2.11. Synthesis of (anthracene-9-carbonyl)glycine



Isolated as pale yellow powder (53% yield over two steps). ¹H NMR (400 MHz, DMSO-*d*₆): 12.78 (s, 1H, COOH), 9.20 (t, *J* = 6 Hz, 1H, CONH), 8.67 (s, 1H, Anth-CH), 8.24 – 8.19 (m, 2H, Anth-CH), 8.15 – 8.10

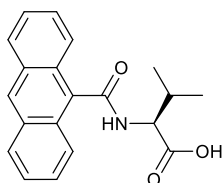
(m, 2H, Anth-CH), 7.59 – 7.52 (m, 4H, Anth-CH), 4.13 (d, $J = 6$ Hz, 2H, CH_2). ^{13}C NMR (101 MHz, $\text{DMSO-}d_6$): 171.8 (COOH), 169.3 (CONH), 157.1 (Anth-C), 133.2 (2 \times Anth-C), 131.1 (2 \times Anth-C), 128.7 (2 \times Anth-CH), 128.0 (2 \times Anth-CH), 127.8 (2 \times Anth-C), 126.8 (2 \times Anth-CH), 126.1 (2 \times Anth-CH), 41.8 (CH_2). LRMS $[(\text{C}_{17}\text{H}_{13}\text{NO}_3) - \text{H}^+]^-$ expected 278.09, found 278.1.

S2.12. Synthesis of (anthracene-9-carbonyl)alanine



Isolated as pale yellow powder (50% yield over two steps). ^1H NMR (400 MHz, $\text{DMSO-}d_6$): 12.7 (s, 1H, COOH), 9.10 (d, $J = 7.5$ Hz, 1H, CONH), 8.66 (s, 1H, Anth-CH), 8.38 – 8.33 (m, 1H, Anth-CH), 8.15 – 8.10 (m, 2H, Anth-CH), 8.01 – 7.96 (m, 1H, Anth-CH), 7.59 – 7.52 (m, 4H, Anth-CH), 4.58 (dq, $J = 7.5, 7.5$ Hz, 1H, Ala-CH), 1.43 (d, $J = 7.5$ Hz, 3H, CH_3). ^{13}C NMR (101 MHz, $\text{DMSO-}d_6$): 174.7 (COOH), 168.7 (CONH), 150.7 (Anth-C), 133.3 (2 \times Anth-C), 131.1 (2 \times Anth-C), 128.8 (Anth-CH), 128.6 (Anth-CH), 127.7 (Anth-CH), 126.9 (Anth-CH), 126.6 (Anth-CH), 126.3 (Anth-CH), 126.1 (Anth-CH), 126.0 (Anth-CH), 125.8 (Anth-CH), 48.8 (Ala-CH), 17.1 (Ala- CH_3). LRMS $[(\text{C}_{18}\text{H}_{15}\text{NO}_3) - \text{H}^+]^-$ expected 292.11, found 292.1.

S2.13. Synthesis of (anthracene-9-carbonyl)valine



Isolated as pale yellow powder (39% yield over two steps). ^1H NMR (400 MHz, $\text{DMSO-}d_6$): 12.8 (s, 1H, COOH), 9.10 (d, $J = 7.5$ Hz, 1H, CONH), 8.66 (s, 1H, Anth-CH), 8.27 – 8.21 (m, 1H, Anth-CH), 8.16 – 8.10 (m, 2H, Anth-CH), 7.97 – 7.92 (m, 1H, Anth-CH), 7.59 – 7.52 (m, 4H, Anth-CH), 4.58 (dd, $J = 7.5, 6$ Hz, 1H, Val-CH*), 2.24 (dh, $J = 7.5, 6$ Hz, Val-CH(CH_3) $_2$), 1.08 (d, $J = 7.5$ Hz, 3H, Val- CH_3), 1.08 (d, $J = 7.5$ Hz, 3H, Val- CH_3). ^{13}C NMR (101 MHz, $\text{DMSO-}d_6$): 173.5 (COOH), 169.4 (CONH), 143.3 (Anth-C), 131.2 (2 \times Anth-C), 130.9 (2 \times Anth-C), 128.8 (Anth-CH), 128.6 (Anth-CH), 127.5 (Anth-CH), 126.8 (Anth-CH), 126.5 (Anth-CH), 126.3 (Anth-CH), 126.0 (Anth-CH), 126.0 (Anth-CH), 125.7 (Anth-CH), 58.9 (Val-CH), 33.8 (Val-CH), 19.9 (Val- CH_3), 18.8 (Val- CH_3). LRMS $[(\text{C}_{20}\text{H}_{19}\text{NO}_3) - \text{H}^+]^-$ expected 320.14, found 320.1.

S3. Hydrogelation procedures

S3.1. Using glucono- δ -lactone (GdL) to trigger hydrogelation

A known quantity of gelator (either (Anth)Phe-OH **2** or (Anth)Tyr-OH **4**) was weighed into a mass spectrometry vial. Deionised water (480 μ L) and NaOH solution (*ca.* 2 equiv. 20 μ L of 0.5 M NaOH) was added. The vial was sonicated for a few seconds until the gelator dissolved. The solution was then transferred to a second mass spectrometry vial containing a known quantity of GdL. The vial was swirled to disperse the GdL and the sample left undisturbed to allow gel formation.

Table S1: Gelation tests via the GdL hydrolysis method.¹

Gelator	Concentration / mg mL ⁻¹	[GdL] / mg mL ⁻¹	Gel?
(Anth)Phe-OH 2	1	4	Syn
	3	4	Syn
	5	4	G \rightarrow Syn
	5	2	G \rightarrow Syn
	5	1	G \rightarrow OG
(Anth)Tyr-OH 4	5	4	OG

G = Gel, OG = Opaque gel, S = Sol, P = Precipitate, Syn = Syneresis (expulsion of liquid from a gel)

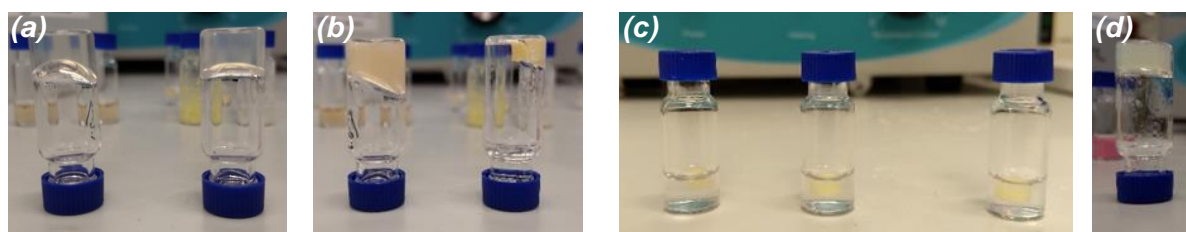


Fig. S23: (a) (Anth)Phe-OH gel-like materials (5 mg mL⁻¹) formed through addition of 1 mg mL⁻¹ (left) and 2 mg mL⁻¹ (right) GdL after 4 h. (b) (Anth)Phe-OH gel-like materials (5 mg mL⁻¹) formed through addition of 1 mg mL⁻¹ (left) and 2 mg mL⁻¹ (right) GdL after 24 h. (c) (Anth)Phe-OH gel-like materials (left = 1 mg mL⁻¹, middle = 3 mg mL⁻¹, right = 5 mg mL⁻¹) triggered with 4 mg mL⁻¹ GdL after 24 h. (d) (Anth)Tyr-OH gel-like materials (5 mg mL⁻¹) triggered using 4 mg mL⁻¹ GdL after 24 h.

S3.2. *Using salts to trigger hydrogelation*

A known quantity of gelator (either (Anth)Phe-OH **2** or (Anth)Tyr-OH **4**) was weighed into a mass spectrometry vial. Deionised water (380 μL) and NaOH solution (*ca.* 2 equiv., 20 μL of 0.5 M NaOH) was added. The vial was sonicated for a few seconds until the gelator dissolved. In a separate vial, a known quantity of the salt compound of interest was dissolved in deionised water (100 μL). The gelator solution was pipetted into the salt solution and the sample left undisturbed to allow gel formation.

S3.3. *Using media to trigger hydrogelation*

A known quantity of gelator (either (Anth)Phe-OH **2** or (Anth)Tyr-OH **4**) was weighed into a mass spectrometry vial. Deionised water (230 μL) and NaOH solution (*ca.* 2 equiv., 20 μL of 0.5 M NaOH) was added. The vial was sonicated for a few seconds until the gelator dissolved. Media (250 μL) was added to the gelator solution, resulting in near instantaneous gel formation.

S3.4. *Using heating/cooling to trigger hydrogelation*

A known quantity of gelator was suspended in a mass spectrometry vial in either deionised water or phosphate buffered saline (PBS). The sample was heated to dissolution and allowed to cool at room temperature.



Fig. S24: Images of (Anth)Phe-OH gel-like materials. From left to right, formation of these self-supporting materials was triggered by: NaCl, NH_4Cl , KCl, Cys-OMe-HCl, Mannosamine-HCl, $\text{GlyNH}_2\text{-HCl}$, heat/cool cycle in H_2O , heat/cool cycle in PBS.

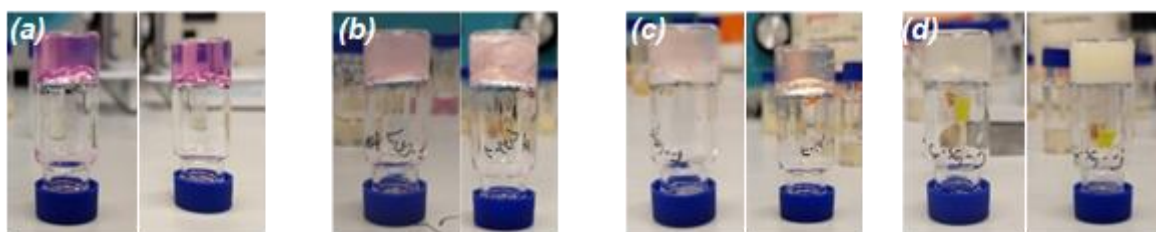


Fig. S25: Images of (Anth)Phe-OH (5 mg mL⁻¹) gel-like materials/hydrogels triggered by addition of (a) media, (b) media with 2 eq. GlyNH₂·HCl, (c) media with 2 eq. GlcN·HCl, (d) media with 2 eq. Cys-OMe·HCl. Images taken after 4 h (left) and 24 h (right).

Table S2: Gelation tests with (Anth)Phe-OH **2** at a concentration of 5 mg mL⁻¹. Approximate time to gelation given in brackets (o/n = overnight). ^aTwo equivalents in all cases

Method	Note	Gel?	Final pH
Salt ^a	NH ₄ Cl	G (15 min)	8.2
	NaCl	G (o/n)	9.3
	KCl	G (o/n)	10.1
	ZnCl ₂	P	6.2
	Lysine	S	11.2
	Spermine	S	11.2
	Arginine	S	11.0
	Cys-OMe·HCl	G (2h) → OG (o/n)	6.7
	Dopamine·HCl	P	8.9
	Mannosamine·HCl	G (2 h)	7.5
	Cysteine	S	7.9
	Cys-OH·HCl	P	5.4
	Lys·HCl	PG	9.0
	Lys·2HCl	P	5.5
Heat/cool	H ₂ O	OG	4.4
	PBS	OG	7.2
Media	Media only	G (instant)	11
	Media + 2 equiv. GlcN·HCl	G (instant)	6.8
	Media + 2 equiv. GlyNH ₂ ·HCl	G (instant)	7.5
	Media + 2 equiv. Cys-OMe·HCl	G (3 min) → OG (o/n)	6.4

G = Gel, OG = Opaque gel, PG = Partial gel (the trigger did not result in gelation of the whole solvent volume), S = Sol, P = Precipitate.

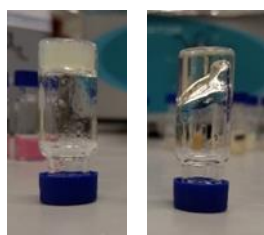


Fig. S26: Images of (Anth)Tyr-OH (5 mg mL⁻¹) gel-like materials /hydrogels triggered by addition of GdL (left) and NH₄Cl (right).

Table S3: Gelation tests with (Anth)Tyr-OH **4**. Approximate time to formation of self-supporting gel-like materials/hydrogels given in brackets (o/n = overnight). ^aTwo equivalents in all cases

Method	Note	Gel?	Final pH
Salt ^a	NH ₄ Cl	G (o/n)	8.1
	Lysine	S	11.1
	Spermine	P (o/n)	10.9
	Arginine	P (o/n)	11.1
	CaCl ₂	P	11.2
	GlcN·HCl	PG (o/n)	7.0
	GlyNH ₂ ·HCl	G (o/n)	7.4
Media	Media only	G (o/n)	11.0
	Media + 2 equiv. GlcN·HCl	G (o/n)	6.8

G = Gel, OG = Opaque gel, PG = Partial gel (the trigger did not result in gelation of the whole solvent volume), S = Sol, P = Precipitate.

Table S4: Effect of salt and gelator concentration on (Anth)Phe-OH gelation. Where relevant, approximate time to formation of a self-supporting gel-like material given in brackets (o/n = overnight).

Trigger	Equivalents	Gelator concentration / mg mL ⁻¹		
		1	3	5
GlyNH ₂ ·HCl	0.5	S	S	PG (o/n)
	1	S	S	PG (o/n)
	2	S	PG (o/n)	G (0.5 h)
	6	-	-	-
	10	S	G (5 min)	G (instant)
	20	PG (2 h)	-	-
GlcN·HCl	1	-	S	PG (3 h)
	2	S	PG (o/n)	G (o/n)
	6	-	-	G (instant)
	10	-	G (3 h)	-
	20	PG (3 h)	-	-
CaCl ₂	0.5	-	-	G (3 h)
	1	-	-	OG (instant)
	2	-	-	P

G = Gel, OG = Opaque gel, PG = Partial gel (the trigger did not result in gelation of the whole solvent volume), S = Sol, P = Precipitate, - = Not evaluated

S4. NMR spectroscopy studies of (Anth)Phe-OH gelation

A known quantity of (Anth)Phe-OH **2** was weighed into a mass spectrometry vial. D₂O (380 μ L) and NaOH solution in D₂O (*ca* 2 equiv., 20 μ L of 0.5 M NaOH in D₂O) was added. The vial was sonicated for a few seconds until the gelator dissolved. In a separate vial, a known quantity of a salt compound was dissolved in D₂O (100 μ L). DMSO was added as internal standard to each solution at a concentration of 0.056 M. The gelator solution was pipetted into the salt solution and the mixture transferred quickly into an NMR tube where it was left overnight to allow complete gelation (gelator concentration = 5 mg mL⁻¹). In the case of the basic gelator solution, the gelator solution was added directly to the NMR tube without the addition of salt. ¹H NMR spectra of the gel-like materials (weak gels or true gels) were recorded and the percentage of mobile gelator and salt estimated based on the integrals of known peaks compared to the internal standard.² In calculating these values, we assume that all N-H and O-H peaks are completely suppressed through H/D exchange with D₂O and therefore do not contribute to any signals in the aromatic region.

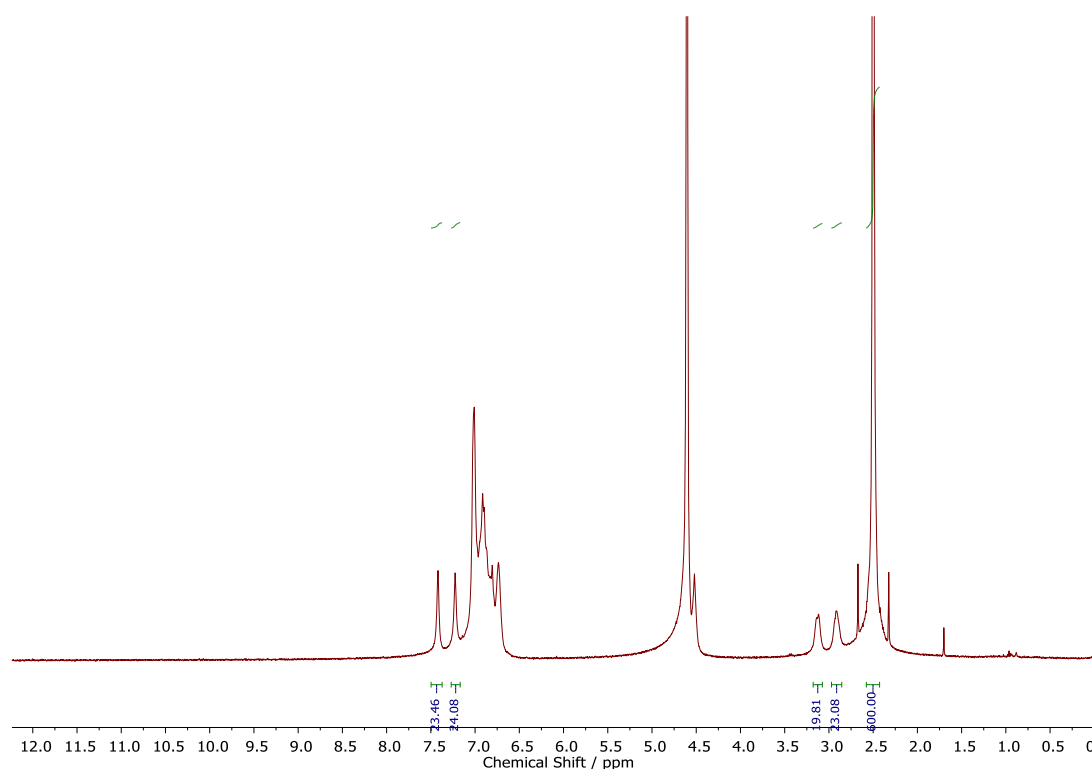


Fig S27: ¹H NMR spectrum (400 MHz) of (Anth)Phe-OH dissolved in aqueous (D₂O) sodium hydroxide solution.

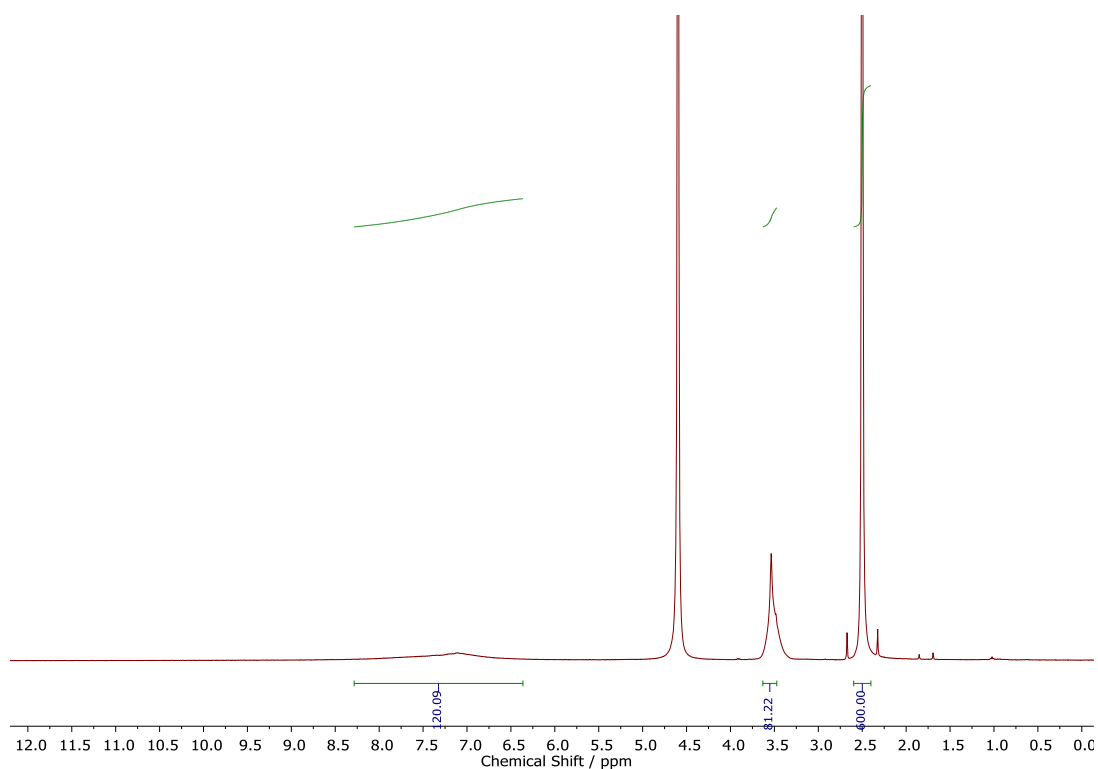


Fig S28: ^1H NMR spectrum (400 MHz) of $\text{GlyNH}_2\cdot\text{HCl}$ (2 equiv.) triggered (Anth)Phe-OH gel-like materials formed in D_2O . Broad aromatic signal is considered to represent fourteen protons (anthracene and phenylalanine aromatics). Peak at ca 3.6 ppm is assigned as glycnamide methylene protons.

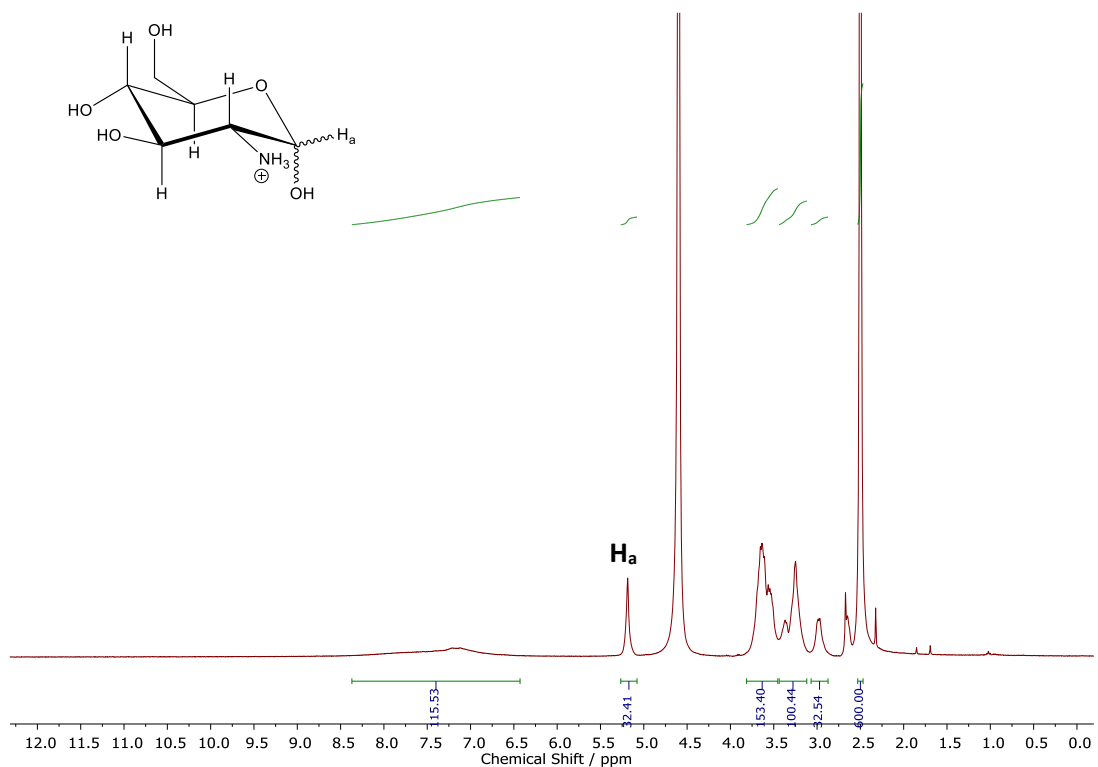


Fig S29: ^1H NMR spectrum (400 MHz) of $\text{GlcN}\cdot\text{HCl}$ (2 equiv.) triggered (Anth)Phe-OH weak gel formed in D_2O . Broad aromatic signal is considered to represent 14 protons (anthracene and phenylalanine aromatics). The peak at ca 5.2 ppm represents one glucosamine methylene proton H_a . Peaks from ca 4 - 2.8 ppm represent the six other glucosamine methylene protons.³

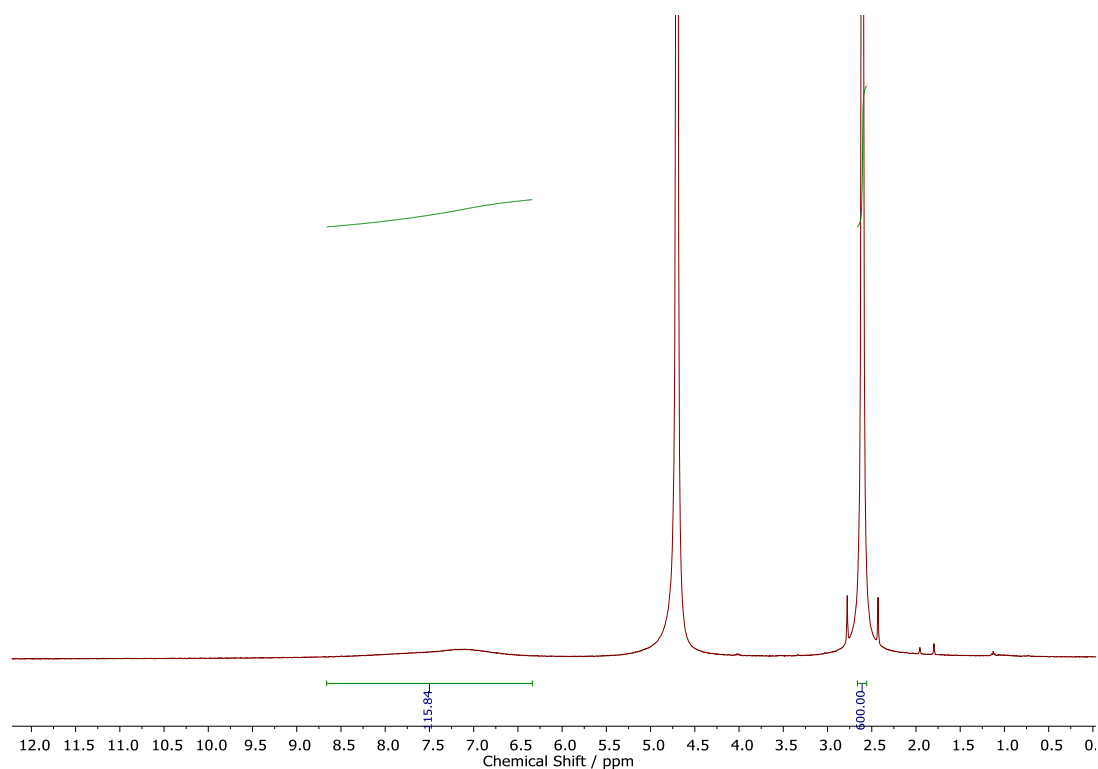


Fig S30: ^1H NMR spectrum (400 MHz) of $\text{GlcN} \cdot \text{HCl}$ (2 equiv.) triggered $(\text{Anth})\text{Phe-OH}$ weak gel formed in D_2O . Broad aromatic signal is considered to represent 14 protons (anthracene and phenylalanine aromatics). NH_4Cl peaks are not visible due to H/D exchange.

Table S5: Proportion of mobile gelator and salt in $(\text{Anth})\text{Phe-OH}$ samples estimated by ^1H NMR spectroscopy. Mobile salt may represent molecules free in solution or those in rapid exchange between bound and unbound states.

Salt	% mobile gelator	% mobile salt
None	95	N/A
$\text{GlyNH}_2 \cdot \text{HCl}$	36	84
$\text{GlcN} \cdot \text{HCl}$	34	68
NH_4Cl	34	-

S5. T_{gel} experiments

Gels were prepared as described in Section S3. The samples were submerged in a paraffin oil bath on a temperature controlled hot plate. The temperature of the oil bath was raised by 1 $^{\circ}\text{C}$ increments, and the temperature allowed to equilibrate for 5 min prior to assessing the condition of the gels. The T_{gel} was defined as the temperature at which the gel was no longer self-supporting, whilst the aggregation temperature (T_{agg}) was defined as the temperature at which the gel clouded and appeared to phase separate from the bulk solution.

Table S6: Gelation and aggregation temperatures of (Anth)Phe-OH **2** gel-like materials/hydrogels

Sample	[Gelator] / mg mL ⁻¹	Trigger (equivalents)	T_{gel}	T_{agg}	Notes
A	5	GlyNH ₂ ·HCl (2 eq.)	105	70	Gel reforms on cooling
B	5	GlyNH ₂ ·HCl (6 eq.)	110	70	Gel reforms on cooling
C	3	GlyNH ₂ ·HCl (2 eq.)	35	-	Remains sol on cooling
D	3	GlyNH ₂ ·HCl (10 eq.)	35	-	Gel reforms on cooling
E	5	GlcN·HCl (2 eq.)	115	90	Gel reforms on cooling
F	5	GlcN·HCl (6 eq.)	>120	95	Remains phase-separated on cooling
G	3	GlcN·HCl (2 eq.)	35	-	Gel reforms on cooling
H	3	GlcN·HCl (10 eq.)	>120	50	Remains phase-separated on cooling
I	5	Media	>120	-	-
J	5	Media + GlcN·HCl (2 eq.)	>120	-	-

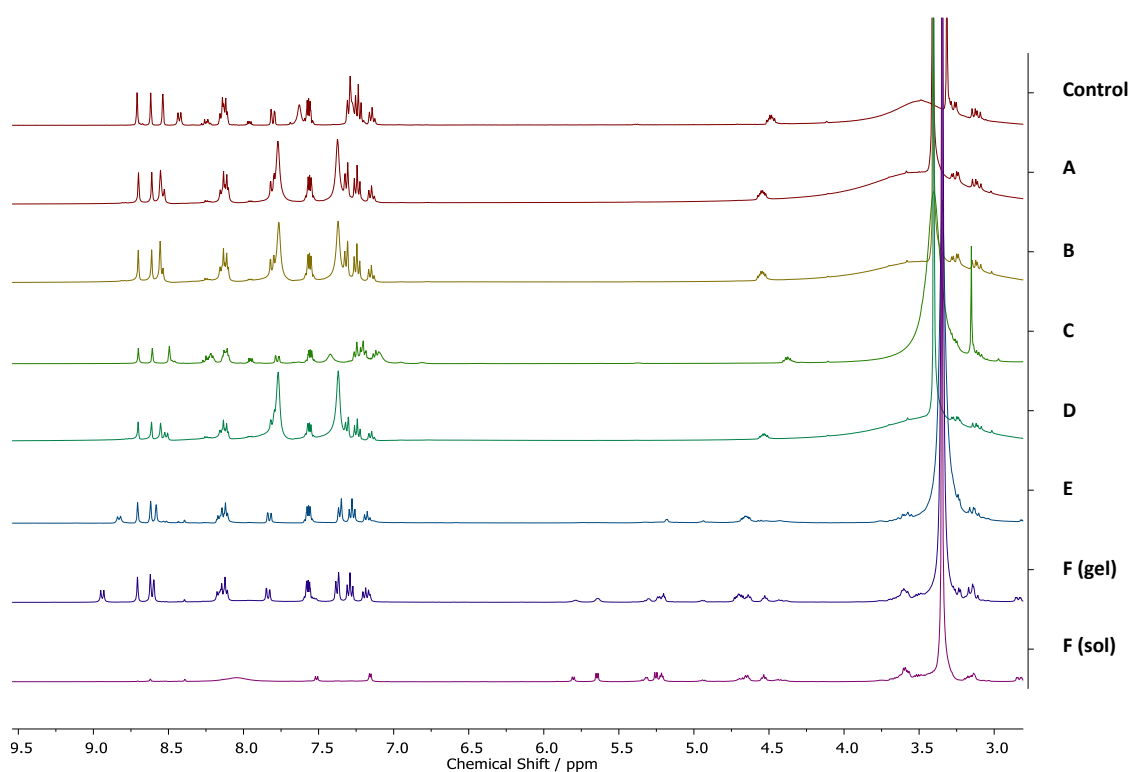


Fig. S31: NMR spectra of lyophilised (Anth)Phe-OH **2** hydrogels after heating to 120 °C and cooling. For F (gel) and F (sol) the solid-like and liquid portions of the cooled samples were separated prior to lyophilisation. Spectra recorded in DMSO-d₆.

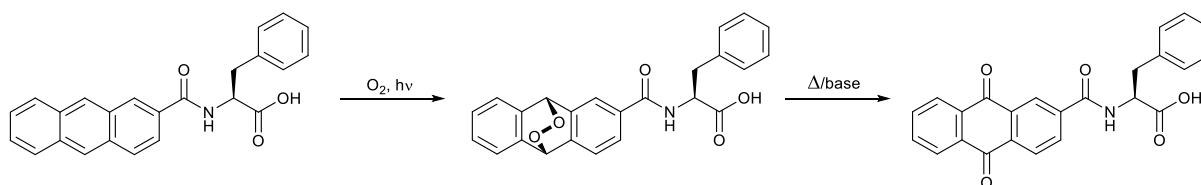
S6. Gel ageing study

Gels formed *via* addition of GlyNH₂·HCl (2 equiv.) underwent a change in colour over time from almost colourless to orange/brown. We reasoned that this may be the result of structural changes to the self-assembled gelator through either photochemical or oxidative processes. To study this, we prepared and stored gels under different exposure to air and light. Gels were prepared closely following the procedures outlined in Section S3 (0.5 mL volume), using GlyNH₂·HCl (2 equiv.) as the triggering stimulus. Gels excluding argon were prepared using water and solutions which had been sparged with argon for 1 h prior to use, and in vials which had been purged with argon gas. Gels excluding light were prepared and stored in vials wrapped in aluminium foil and kept in a dark cupboard. Samples exposed to light were kept out on a bench with no foil wrapping. Any changes in visual appearance of the gels were noted and after 5 days the samples were lyophilised and dissolved in DMSO-*d*₆ for analysis by NMR spectroscopy.

Discoloration of all the hydrogels/gel-like materials was observed over time. This process appeared faster for gels exposed to both air and light and slowest for gels incubated in the absence of both (Fig. S32). We used NMR spectroscopy to monitor changes in the (Anth)Phe-OH **2** gelators under the different preparation and storage conditions. In the discolored samples, the appearance of new peaks in the aromatic region and a small singlet at *ca.* 4.5 ppm indicated chemical changes to the gelator (Fig. S33). These new peaks closely match those reported for anthraquinones.⁴ Consistent with previous reports, we propose that oxidation of (Anth)Phe-OH **2** in these hydrogels to the corresponding anthraquinone *via* an endoperoxide intermediate (Scheme S2) accounts for the observed changes.

Comparison of peak integrals corresponding to the (Anth)Phe-OH **2** gelator and the oxidised by-product allowed us to estimate the proportion of gelator which had been oxidised in each sample (Fig. S33). Consistent with the changes in appearance, air and light exclusion limited oxidation (8%) compared to those samples exposed to one or both stimuli (*ca.* 30% conversion). The degree of oxidation in air and light exposed samples was similar to the proportion of free gelator calculated above (Table S5, 36%). It is possible that self-assembly of (Anth)Phe-OH **2** into nanofibers confers some resistance to oxidation and that degradation occurs only in the solution state, but further studies are required to confirm whether this is the case.

Informed by this study, subsequent experiments were carried out using freshly prepared gels to avoid confounding data from any anthraquinone



Scheme S2: Proposed degradation of (Anth)Phe-OH to the corresponding anthraquinone via an endoperoxide intermediate. The second step occurs spontaneously at room temperature in related compounds, but can also be catalysed by trace amounts of base.⁵

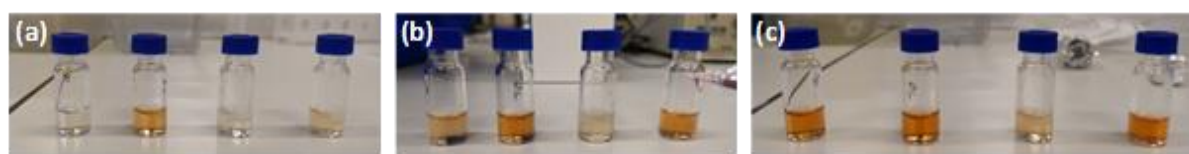


Fig. S32: Images of aged gels after (a) 24 h, (b) 48 h and (c) 120 h. In each image, gel samples from left to right are exposed to: [+ air, - light]; [+ air, + light]; [- air, - light]; [- air, + light].

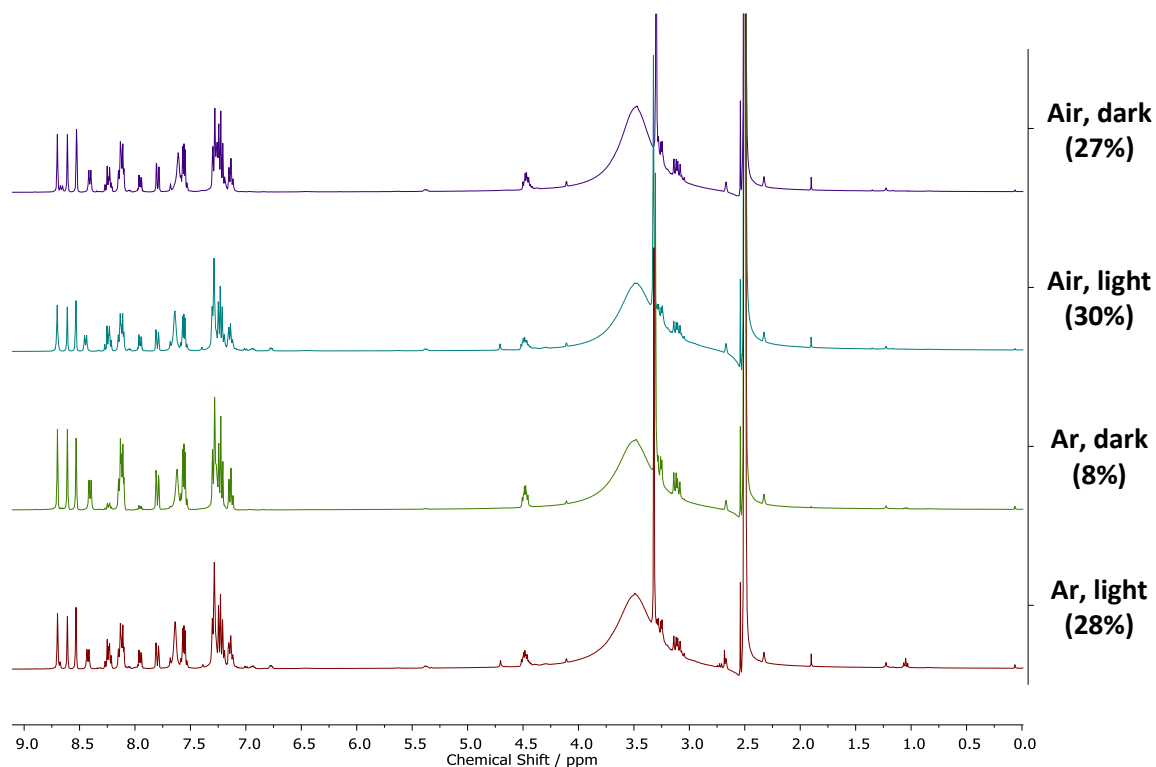


Fig. S33: NMR spectra of lyophilised (Anth)Phe-OH 2 hydrogels after 5 days of ageing. Approximate conversion to endoperoxide, calculated by comparison of the integrals of peaks corresponding to the starting and oxidised material ($\delta = 8.61$ and 7.95 ppm respectively) are given with each spectrum. Spectra were recorded in DMSO-d_6 .

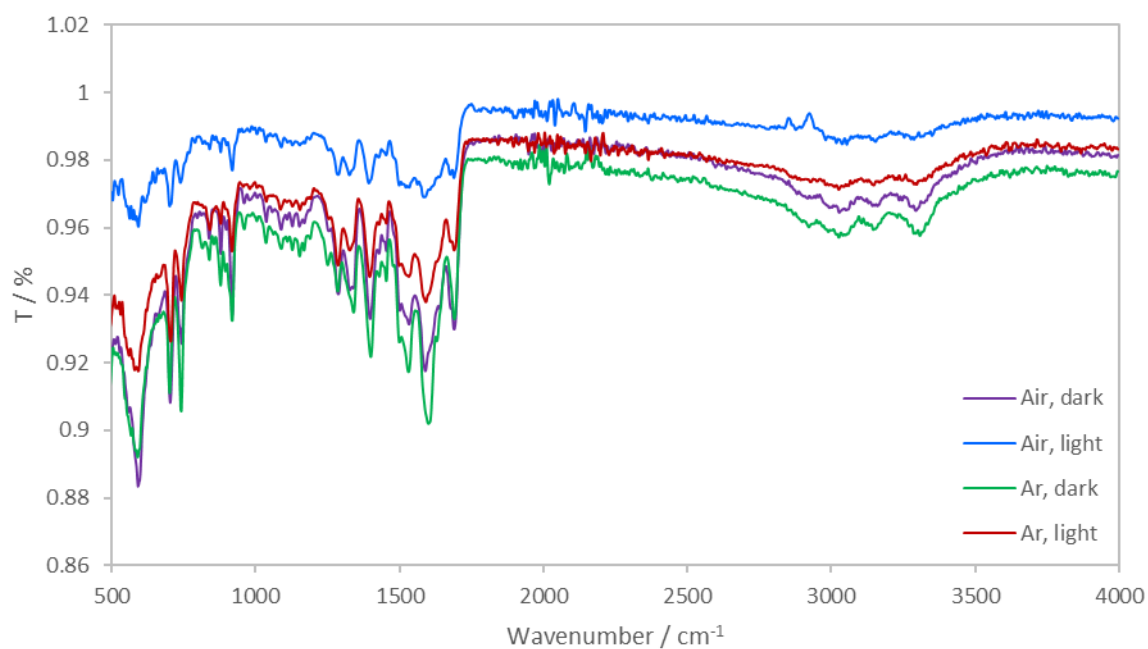


Fig. S34: IR spectra of lyophilised (Anth)Phe-OH 2 hydrogels after 5 days of ageing.

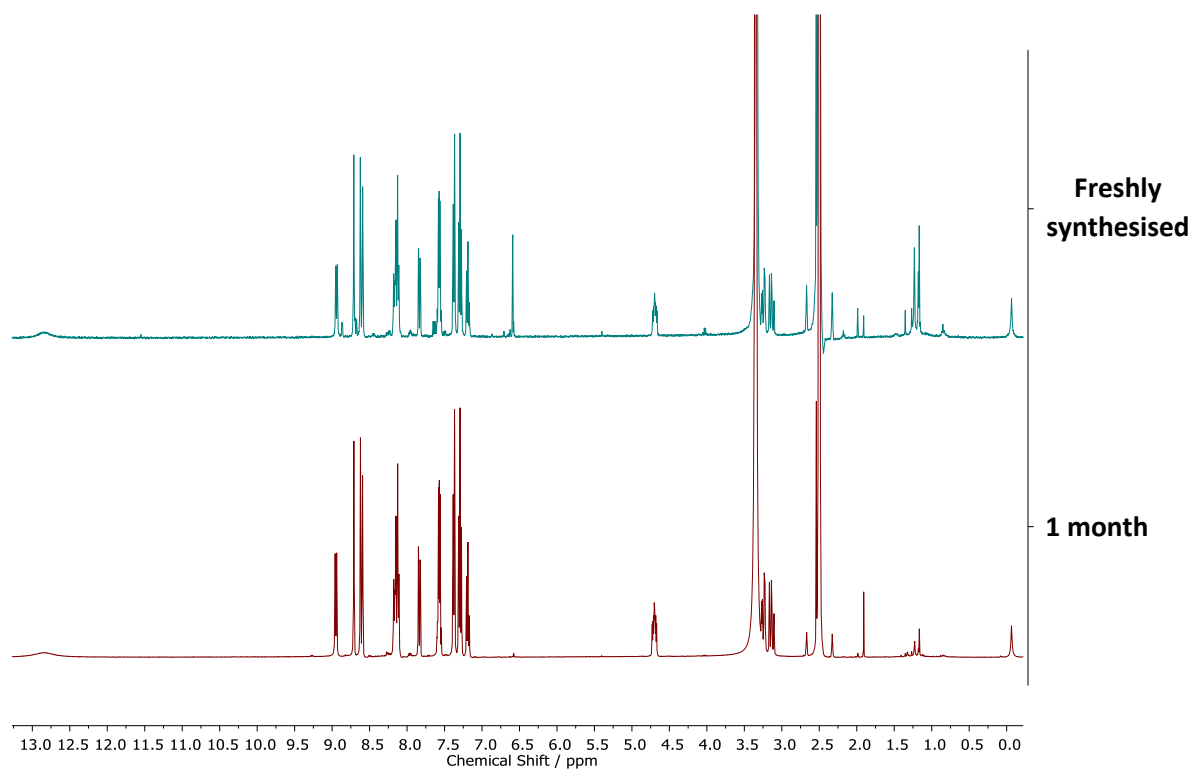


Fig. S35: ¹H NMR spectra of (Anth)Phe-OH 2 powders in DMSO-d₆

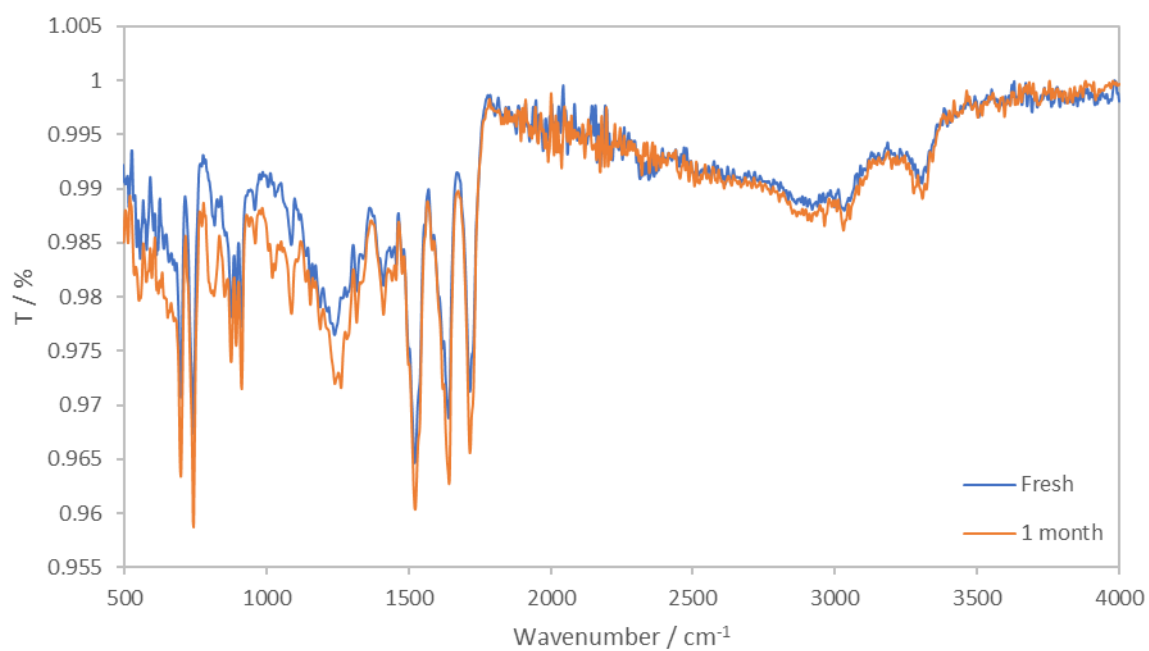


Fig. S36: IR spectra of (Anth)Phe-OH 2 powder when freshly prepared and after 1 month's exposure to light and air

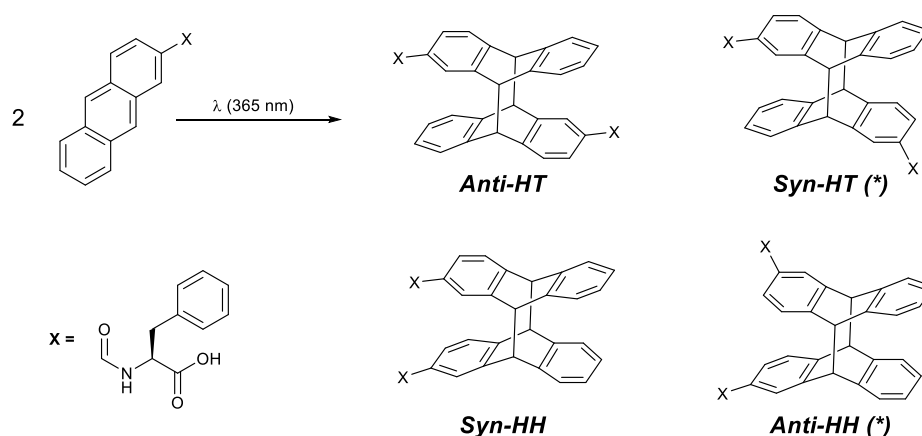
S7. Photo-dimerisation reactions

All photo-dimerisation reactions were carried out in fluorescence cuvettes at a gelator concentration of 5 mg mL⁻¹. Samples were placed in a cuvette holder (ThorLabs CVH100) which was directly coupled to an LED. Samples were exposed to electromagnetic irradiation (λ = 365 nm) at an intensity of 750 mAh for known lengths of time.

We studied the photoirradiation of (Anth)Phe-OH **2** in both the solution and gel phase. Mass spectrometry confirmed the presence of dimerised **2** in all samples (Table S7). Reaction conversion was estimated using NMR spectroscopy. Characteristic peaks associated with bridgehead protons of the (Anth)Phe-OH **2** dimer were observed at 4.7 ppm in the ¹H NMR spectra of all photoreactions (e.g. Figs. S37 and S59), whilst resonances associated with anthracene aromatic protons significantly reduced in intensity. These peak integrals were compared to calculate conversion in samples irradiated using 365 nm light for 1 h (Table S7). Reasonable conversion to the dimer was observed in both solution and gel phase samples. Reaction in the media-triggered hydrogel (63%) was significantly less efficient than in the glycineamide gel (81%), but both are comparable with dimerisation in previous, more structurally complex anthracene-based hydrogels.⁶ Differences in the self-assembled structures (Fig. S77) may be responsible for the lower conversion in media-triggered hydrogels. For Glyc-HCl triggered hydrogels/gel-like materials, the region of the gel shielded from irradiation was also lyophilised and analysed by NMR spectroscopy. A significant percentage (ca. 36%) of the lyophilised material was dimerised gelator – presumably due to diffusion from the irradiated region – suggesting that the photoreaction conversion may be higher than estimated here.

Anthracene cycloaddition can lead to the formation of four regioisomers (Scheme S3), the distribution of which can, in theory, yield information regarding the orientation of Anth-2-Phe-OH in the gel nanofibres. Splitting patterns for resonances associated with bridgehead (δ = 4.7 ppm) and vicinal aromatic (7.4 ppm) protons are diagnostic of the syn/anti and head-to-head (HH)/head-to-tail (HT) arrangements with respect to the arrangement of phenylalanine moieties.⁷ Unfortunately, even at 800 MHz these peaks were insufficiently resolved to elucidate the structures (Fig. S38). Differences in the peak structure at 4.7 ppm do suggest, again, different (Anth)Phe-OH **2** packing in Glyc-HCl and media-triggered gels. Interestingly, three new cross-coupling peaks between amide NH and Phe CH are observed in COSY NMR spectra on irradiation of both gels, suggesting the formation of at least three distinct cycloaddition products. Shouldering in the COSY peaks at 4.7 ppm (Fig. S53) suggest that in at least one of these products the Phe groups are arranged in an anti-fashion, a notion supported by the presence of apparent 'self-coupling' in the HMBC spectra. HPLC separation of the products – to enable identification and yield comparisons – were unsuccessful.

Conditions of solvent have been shown to have a significant influence on the regioisomer distribution of anthracene photodimerisations. Previous studies on anthracene-2-carboxylic acid dimerisation suggest that in dichloromethane there is a slight preference for the formation of HT dimers, whereas in polar solvents such as methanol a HH arrangement is favoured.^{6,8} Anthracene-containing supramolecular gels typically demonstrate the inverse behaviour, with H-T stacking preferred in aqueous conditions.⁹ For (Anth)Phe-OH **2**, similar bridgehead proton peak shapes are seen in spectra for reactions in Glyc·HCl gel and dichloromethane, whilst a very different structure is observed in the more polar solvents (MeOH and aqueous NaOH). We tentatively suggest that H-T stacking is preferred in (Anth)Phe-OH **2** hydrogels.



Scheme S3: General gelator photo-dimerisation scheme

S7.1. Photo-dimerisation in the solution-phase

(Anth)Phe-OH **2** was dissolved or suspended in the desired solvent (aq. NaOH, CH₂Cl₂ or MeOH, 2 mL) in a fluorescence cuvette. The cuvette was capped prior to reaction to prevent solvent evaporation. After reaction the solvent was removed from the whole sample by rotary evaporation, the residue acidified with HCl (1 M, 1 mL) and extracted into EtOAc (5 mL). This solution was dried *in vacuo* and the resulting solid taken for analysis.

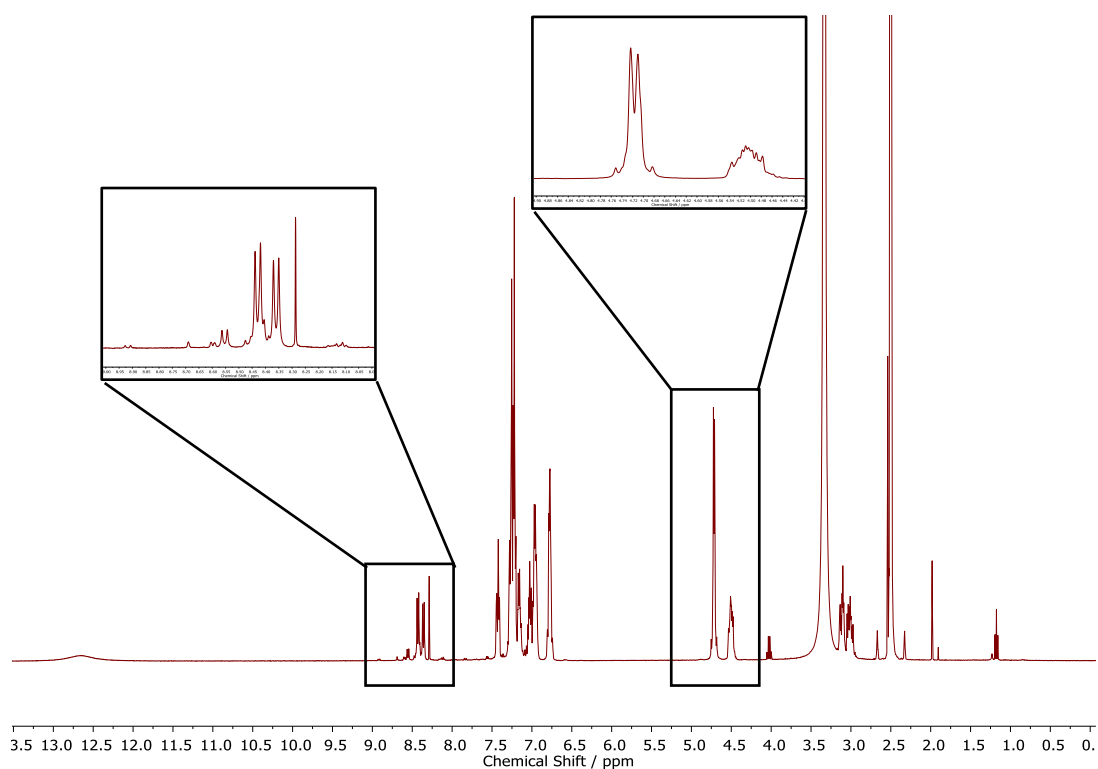


Fig S37: ^1H NMR spectrum (400 MHz) of irradiated (Anth)Phe-OH in $\text{DMSO}-d_6$. Sample had been dissolved in aqueous NaOH solution (5 mg mL^{-1}), subjected to 1 h irradiation using 365 nm light then acidified using 1 M HCl prior to drying. Expansions show regions with new amide NH (9.0 - 8.0ppm) and bridgehead CH (4.7 ppm) peaks formed after irradiation.

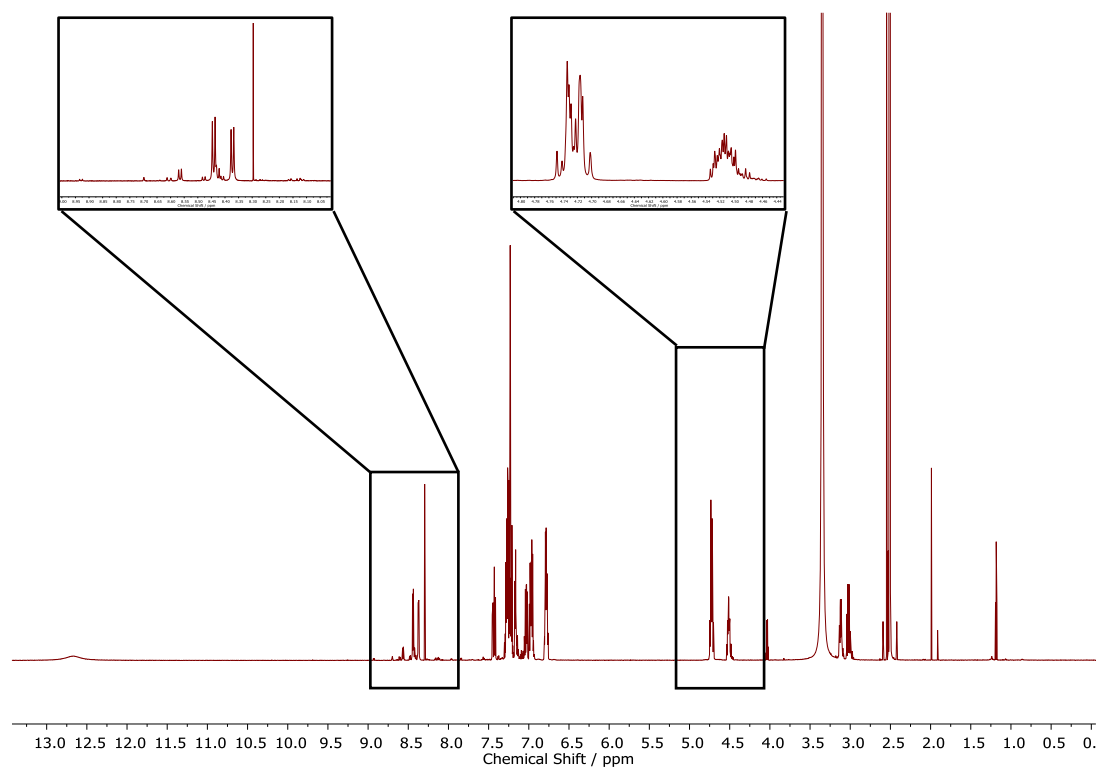


Fig S38: ^1H NMR spectrum (800 MHz) of irradiated (Anth)Phe-OH in $\text{DMSO}-d_6$. Sample had been dissolved in aqueous NaOH solution (5 mg mL^{-1}), subjected to 1 h irradiation using 365 nm light then acidified using 1 M HCl prior to drying. Expansions show regions with new amide NH (9.0 - 8.0ppm) and bridgehead CH (4.7 ppm) peaks formed after irradiation.

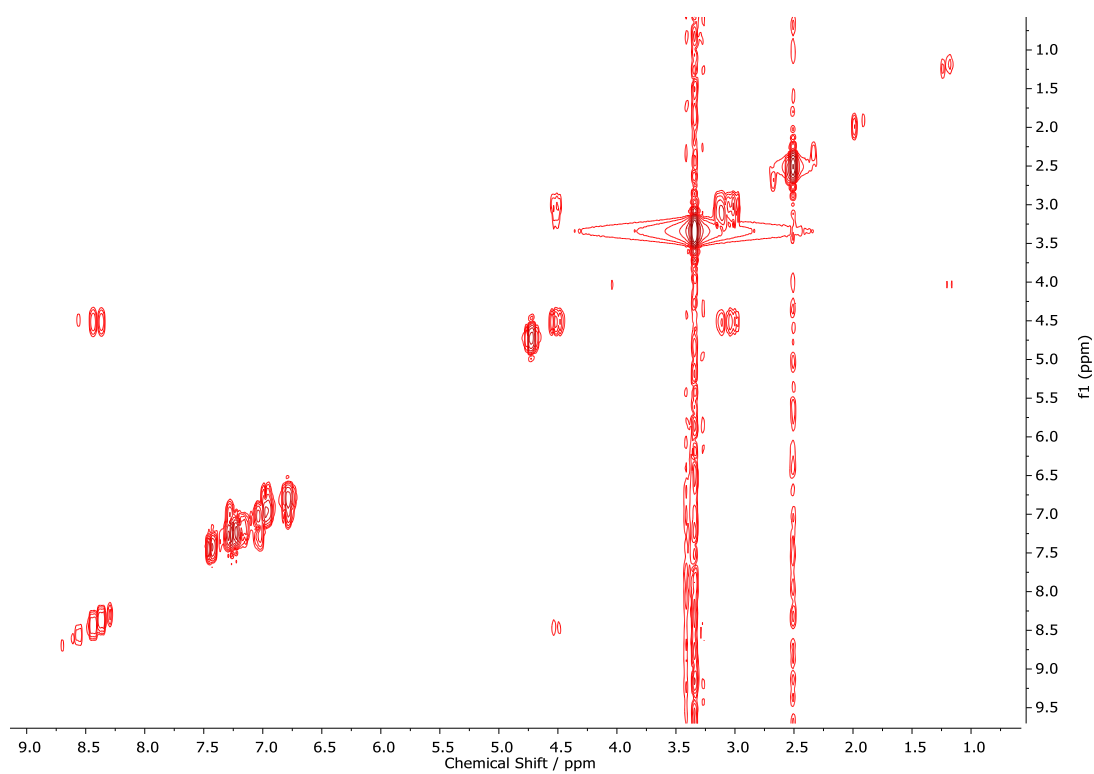


Fig S39: ^1H NMR spectrum (400 MHz) of irradiated (Anth)Phe-OH in DMSO-d_6 . Sample had been dissolved in aqueous NaOH solution (5 mg mL^{-1}), subjected to 1 h irradiation using 365 nm light then acidified using 1 M HCl prior to drying.

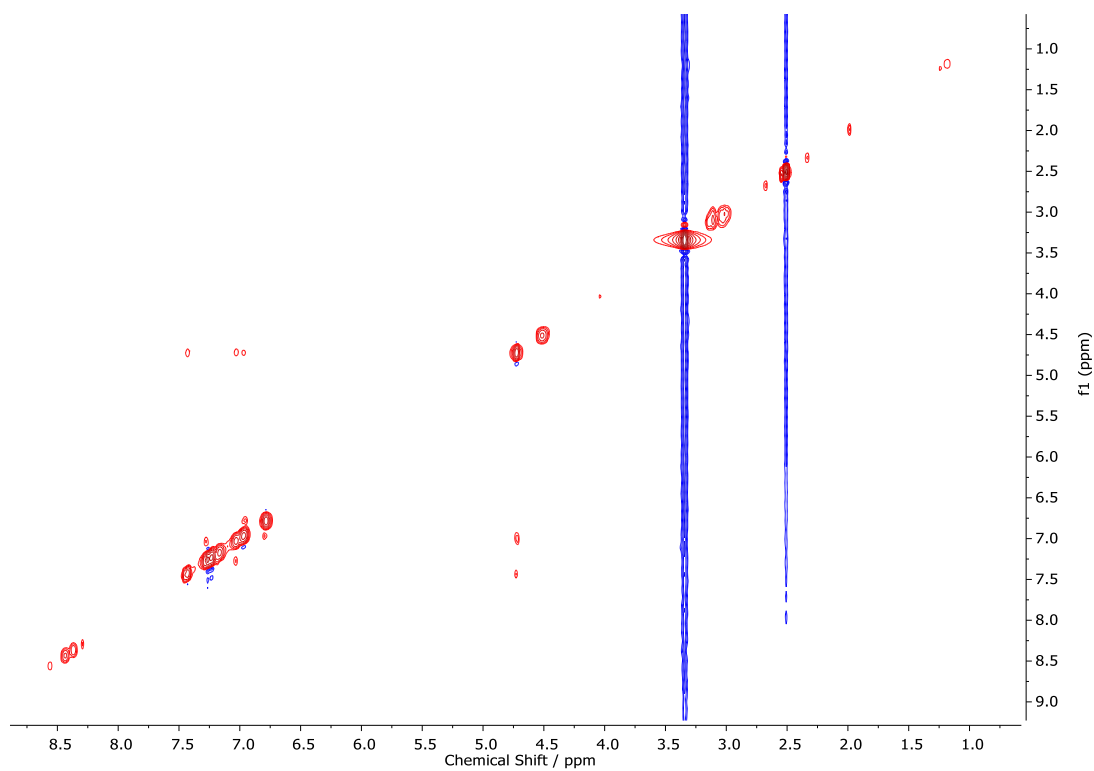


Fig S40: NOESY NMR spectrum of irradiated (Anth)Phe-OH in DMSO-d_6 . Sample had been dissolved in aqueous NaOH solution (5 mg mL^{-1}), subjected to 1 h irradiation using 365 nm light then acidified using 1 M HCl prior to drying.

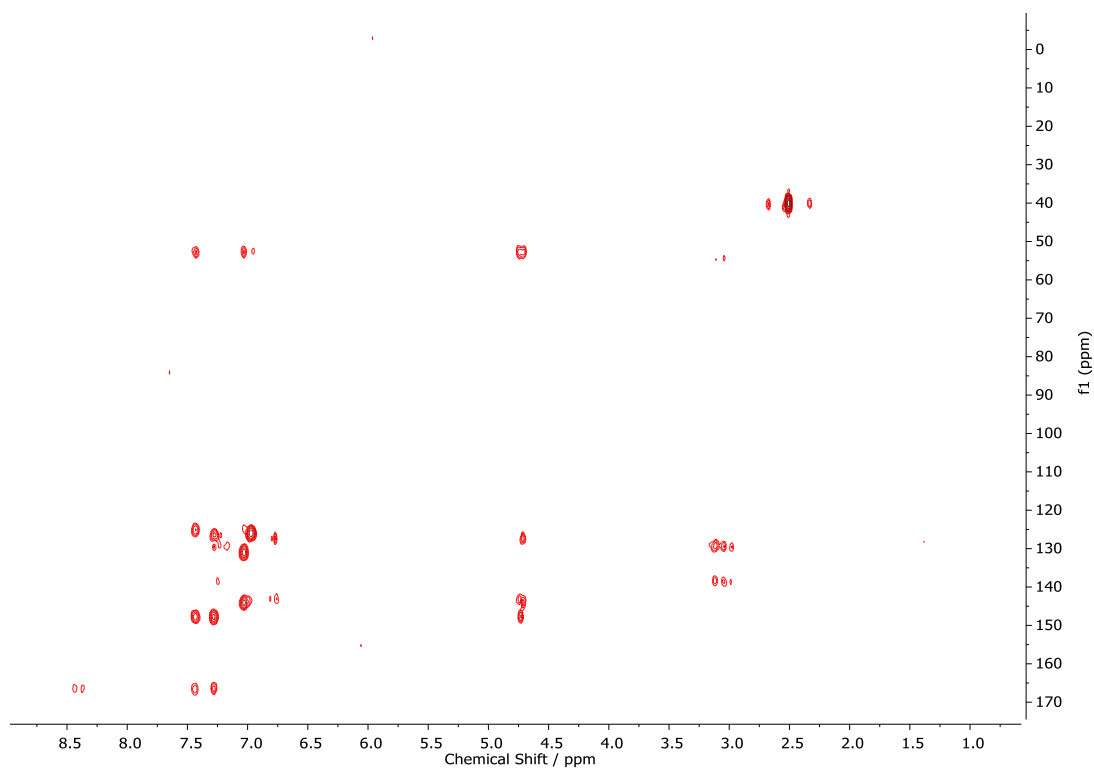


Fig S41: $^1\text{H}/^{13}\text{C}$ HMBC spectrum of irradiated (Anth)Phe-OH in DMSO-d_6 . Sample had been dissolved in aqueous NaOH solution (5 mg mL^{-1}), subjected to 1 h irradiation using 365 nm light then acidified using 1 M HCl prior to drying.

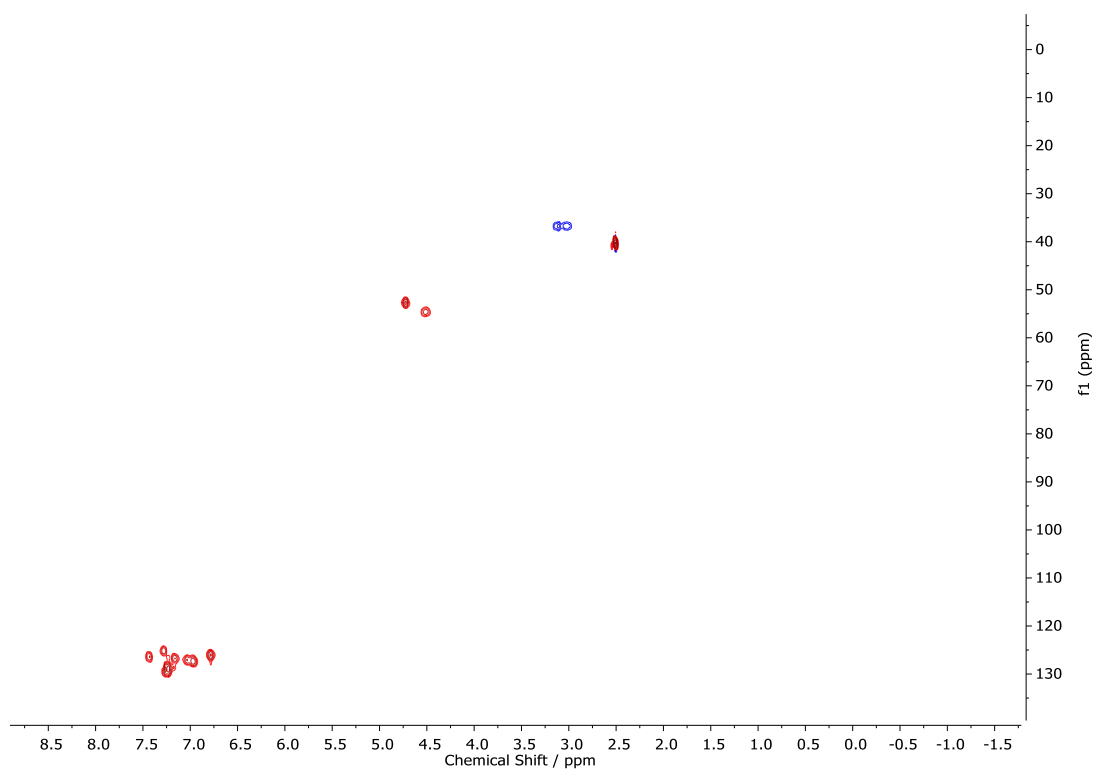


Fig S42: $^1\text{H}/^{13}\text{C}$ HSQC spectrum of irradiated (Anth)Phe-OH in DMSO-d_6 . Sample had been dissolved in aqueous NaOH solution (5 mg mL^{-1}), subjected to 1 h irradiation using 365 nm light then acidified using 1 M HCl prior to drying.

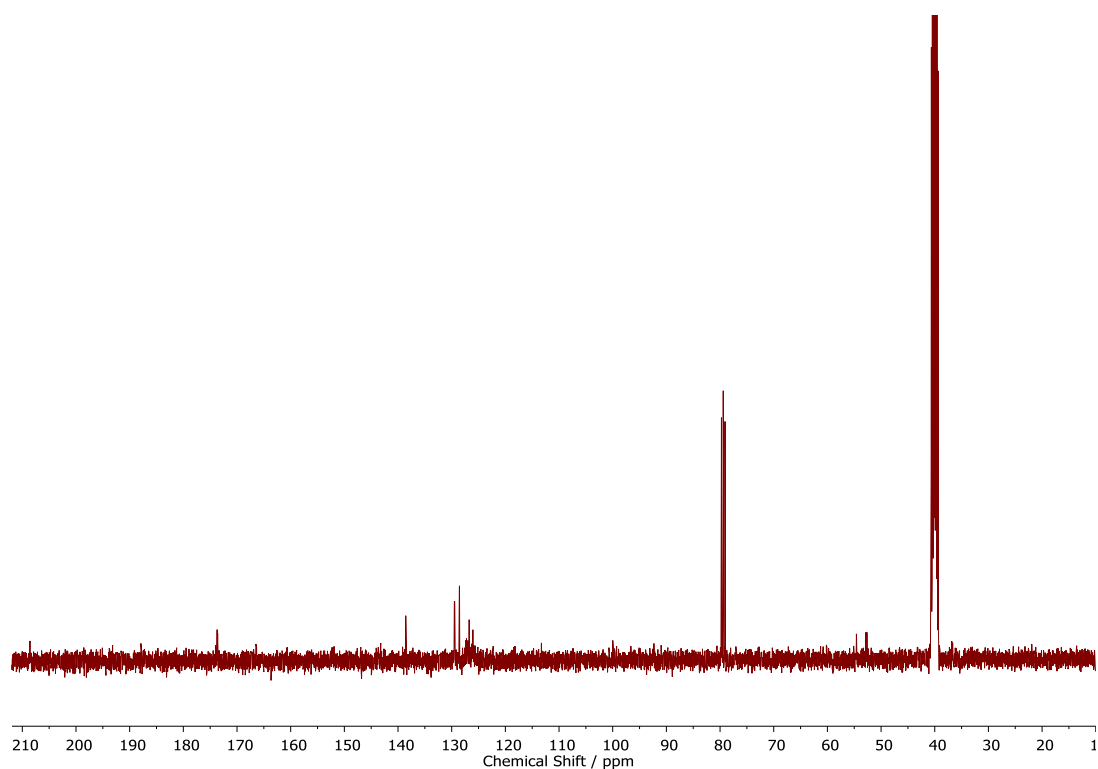


Fig S43: ^{13}C NMR spectrum of irradiated (Anth)Phe-OH in DMSO-d_6 . Sample had been dissolved in aqueous NaOH solution (5 mg mL^{-1}), subjected to 1 h irradiation using 365 nm light then acidified using 1 M HCl prior to drying.

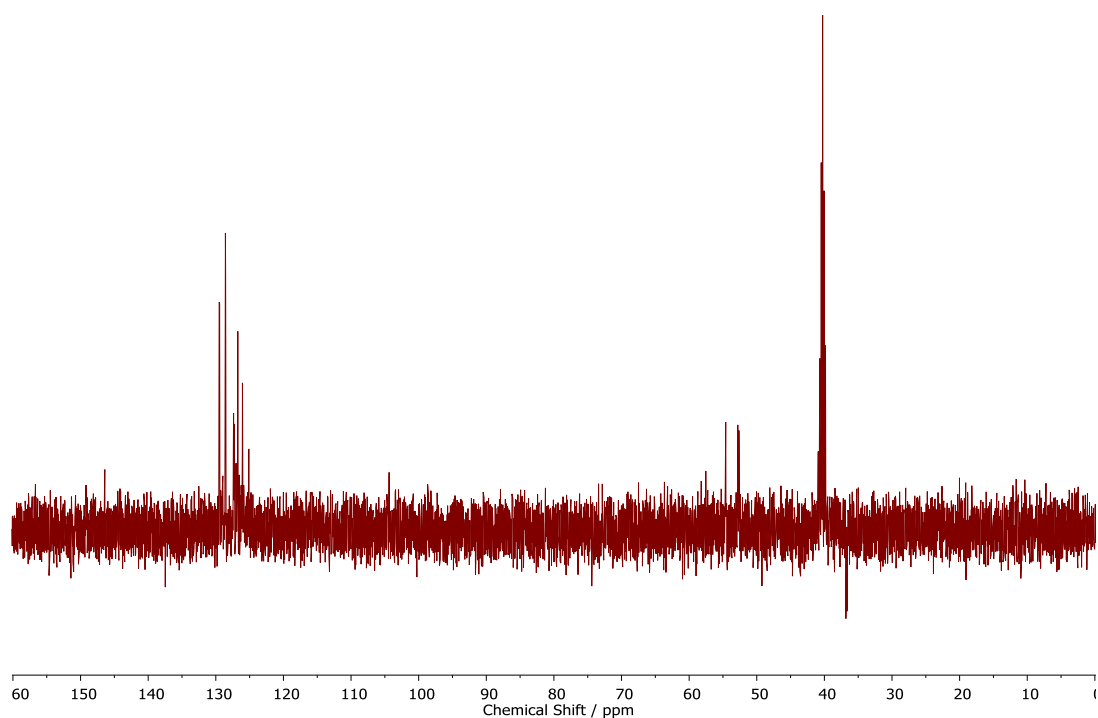


Fig S44: DEPT spectrum of irradiated (Anth)Phe-OH in DMSO-d_6 . Sample had been dissolved in aqueous NaOH solution (5 mg mL^{-1}), subjected to 1 h irradiation using 365 nm light then acidified using 1 M HCl prior to drying.

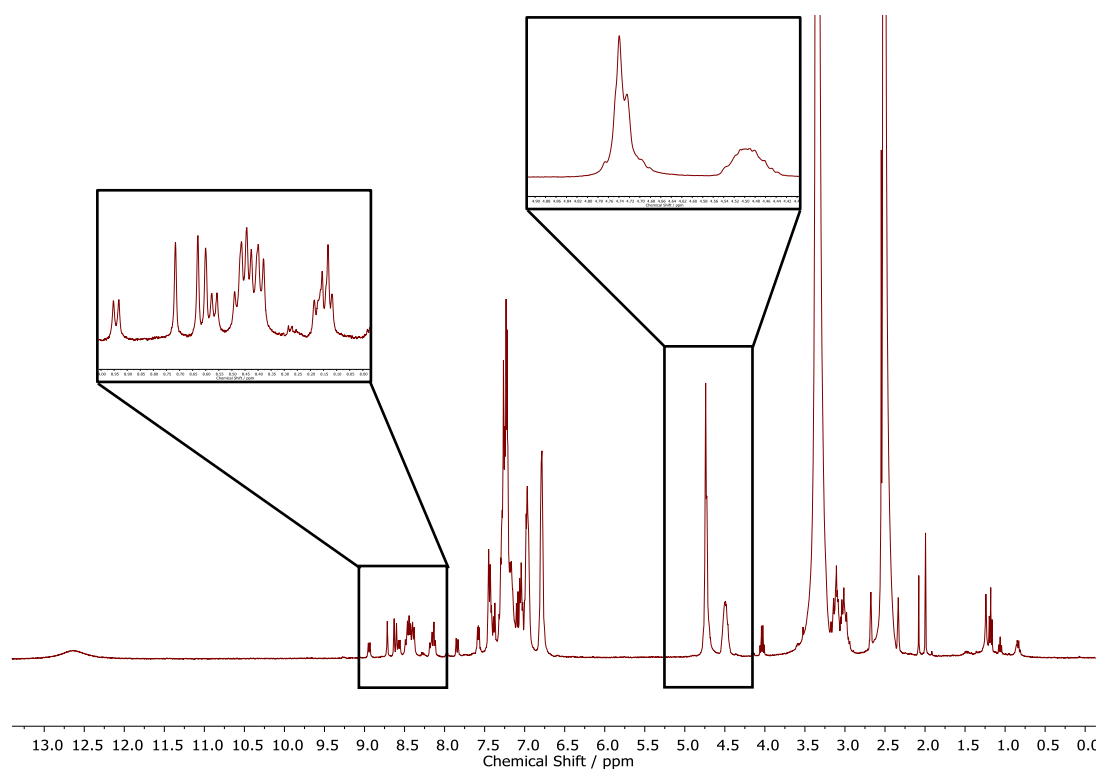


Fig S45: ^1H NMR spectrum (400 MHz) of irradiated (Anth)Phe-OH in DMSO-d_6 . Sample had been suspended in CH_2Cl_2 (5 mg mL^{-1}), subjected to 1 h irradiation using 365 nm light then acidified using 1 M HCl prior to drying. Expansions show regions with new amide NH (9.0 - 8.0 ppm) and bridgehead CH (4.7 ppm) peaks formed after irradiation.

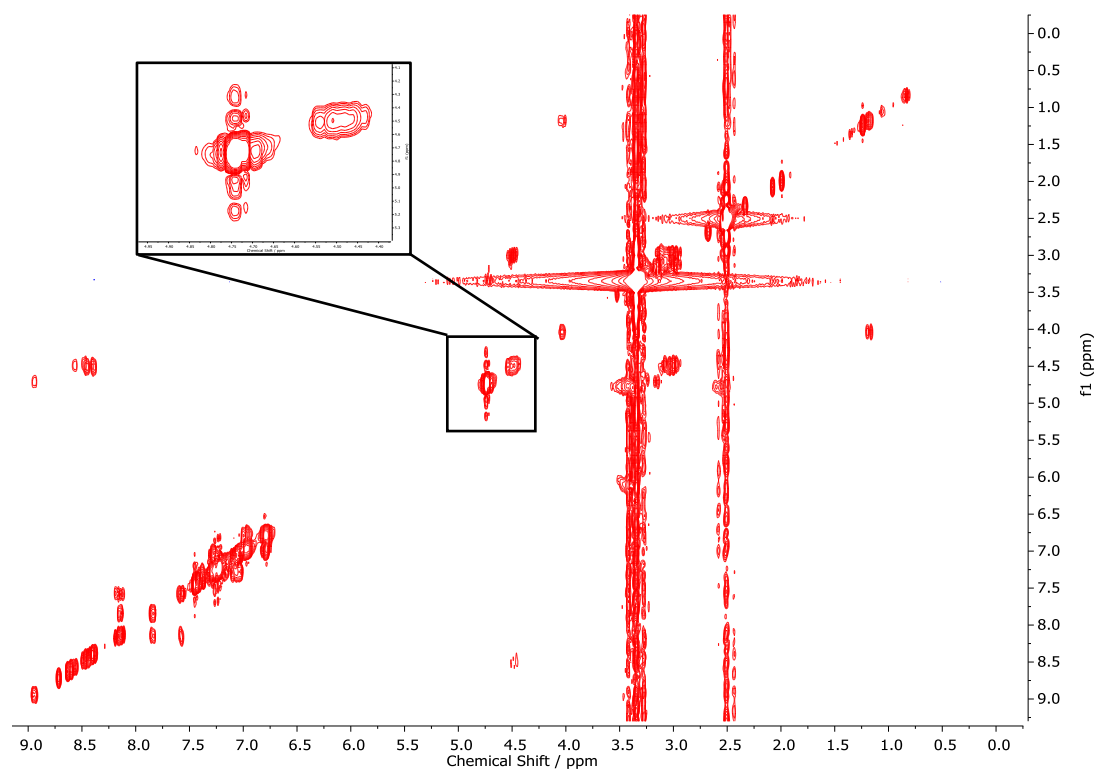


Fig S46: COSY spectrum of irradiated (Anth)Phe-OH in DMSO-d_6 . Sample had been suspended in CH_2Cl_2 (5 mg mL^{-1}), subjected to 1 h irradiation using 365 nm light then acidified using 1 M HCl prior to drying. Expansion shows the fine structure of the dimer bridgehead (4.7 ppm) and Phe CH (4.5 ppm) cross-peaks.

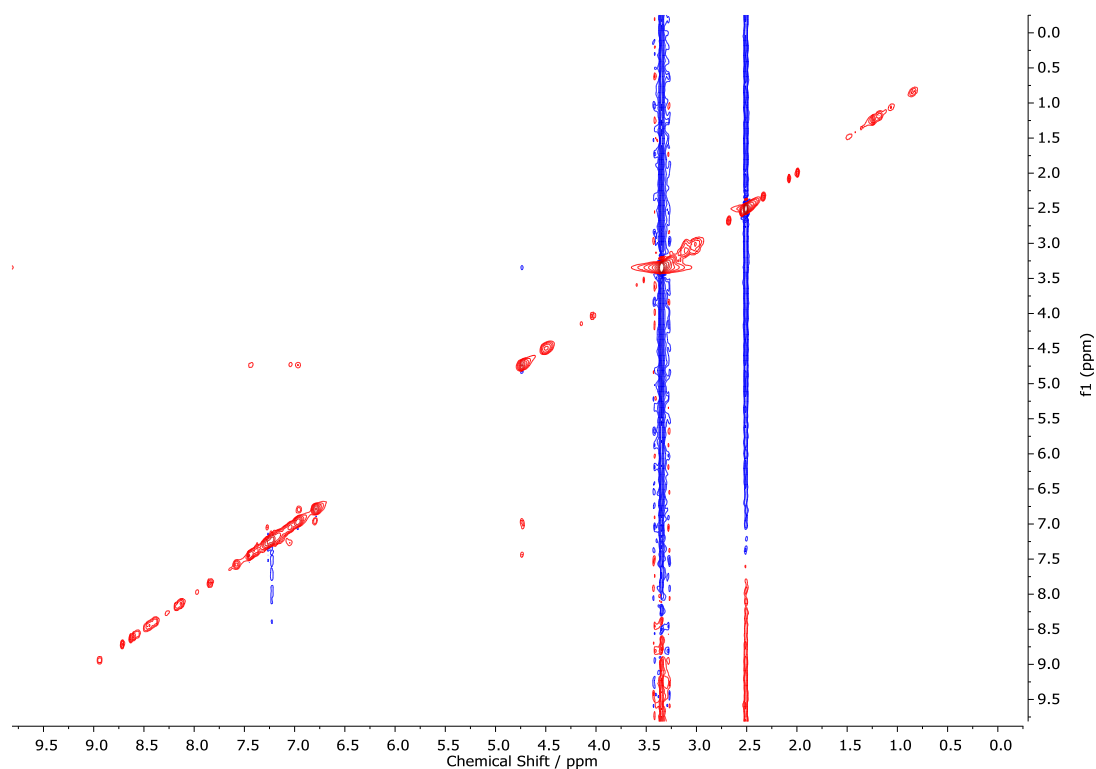


Fig S47: NOESY spectrum of irradiated (Anth)Phe-OH in DMSO- d_6 . Sample had been suspended in CH_2Cl_2 (5 mg mL^{-1}), subjected to 1 h irradiation using 365 nm light then acidified using 1 M HCl prior to drying.

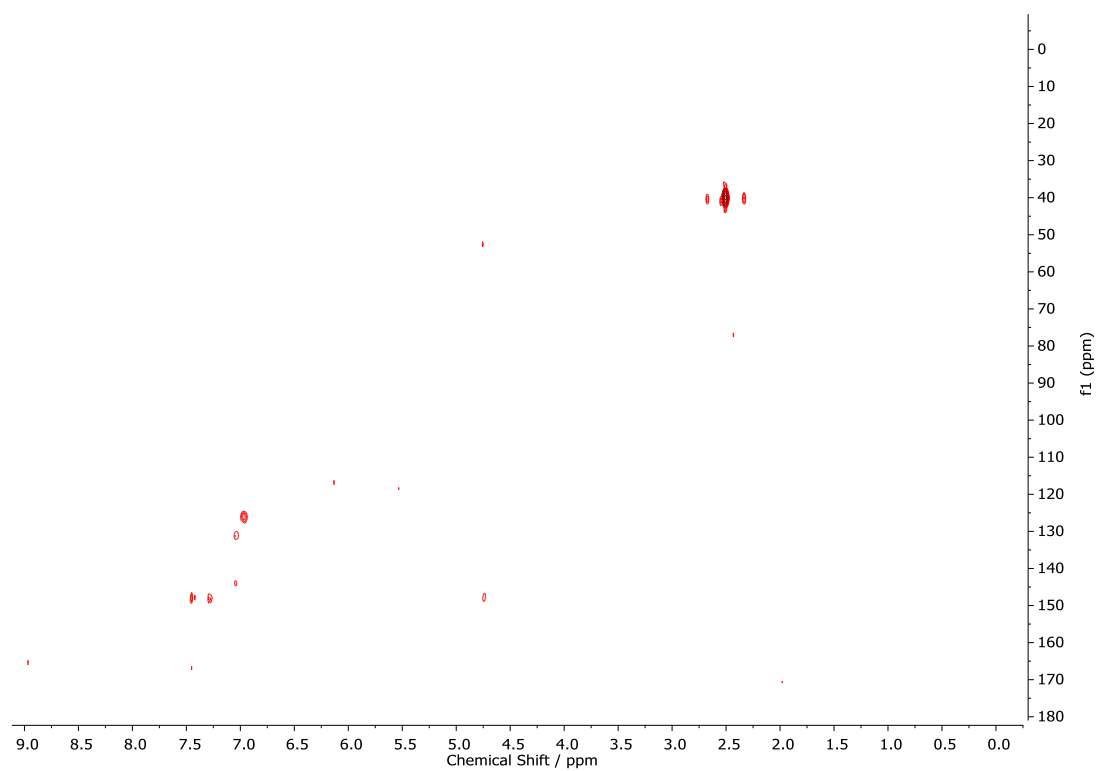


Fig S48: $^1H/^{13}C$ HMBC spectrum of irradiated (Anth)Phe-OH in DMSO- d_6 . Sample had been suspended in CH_2Cl_2 (5 mg mL^{-1}), subjected to 1 h irradiation using 365 nm light then acidified using 1 M HCl prior to drying.

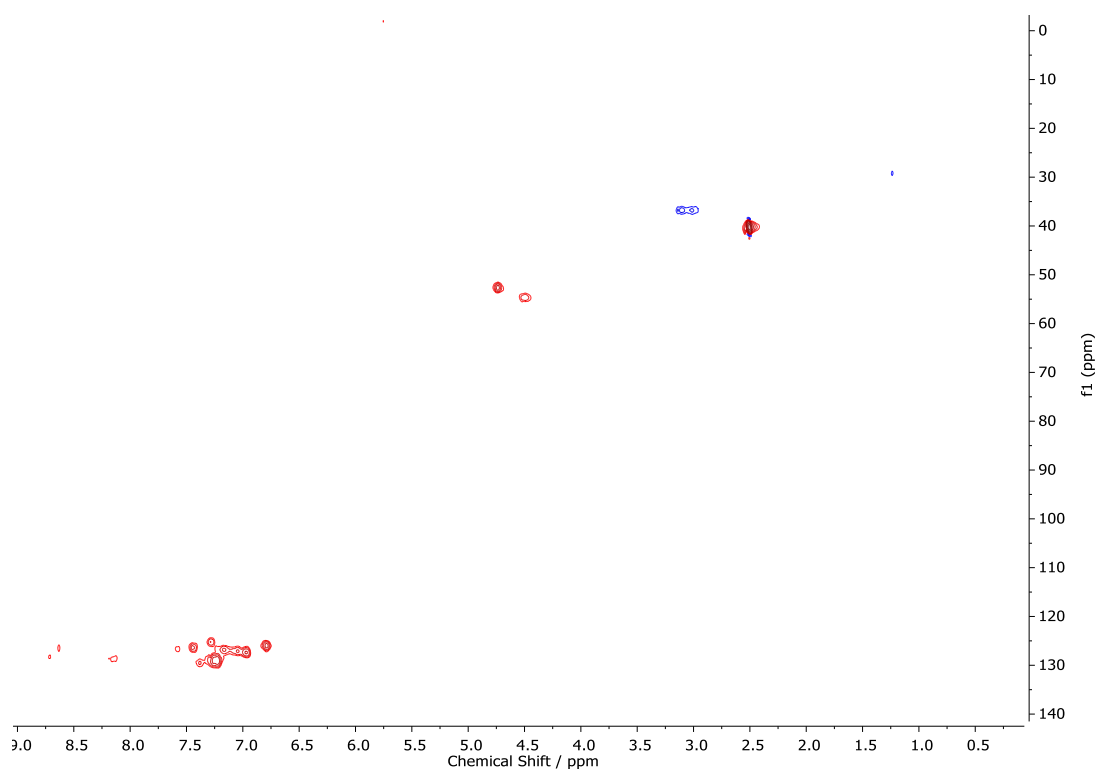


Fig S49: $^1\text{H}/^{13}\text{C}$ HSQC spectrum of irradiated (Anth)Phe-OH in DMSO- d_6 . Sample had been suspended in CH_2Cl_2 (5 mg mL^{-1}), subjected to 1 h irradiation using 365 nm light then acidified using 1 M HCl prior to drying.

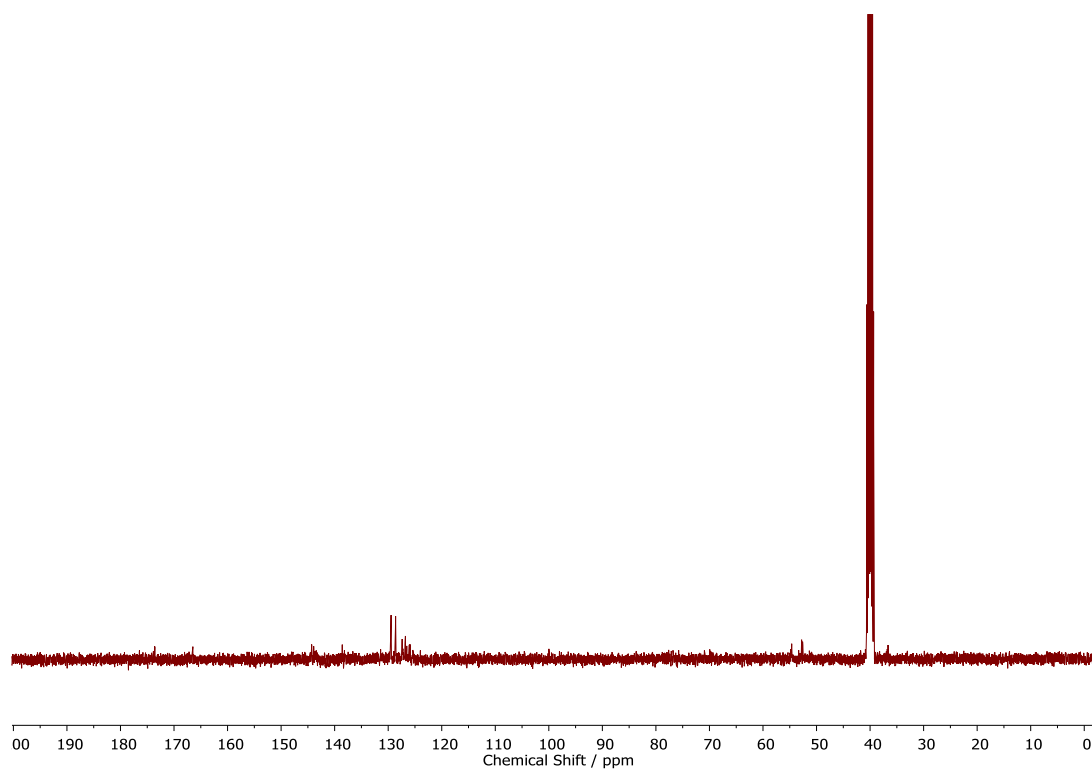


Fig S50: ^{13}C NMR spectrum of irradiated (Anth)Phe-OH in DMSO- d_6 . Sample had been suspended in CH_2Cl_2 (5 mg mL^{-1}), subjected to 1 h irradiation using 365 nm light then acidified using 1 M HCl prior to drying.

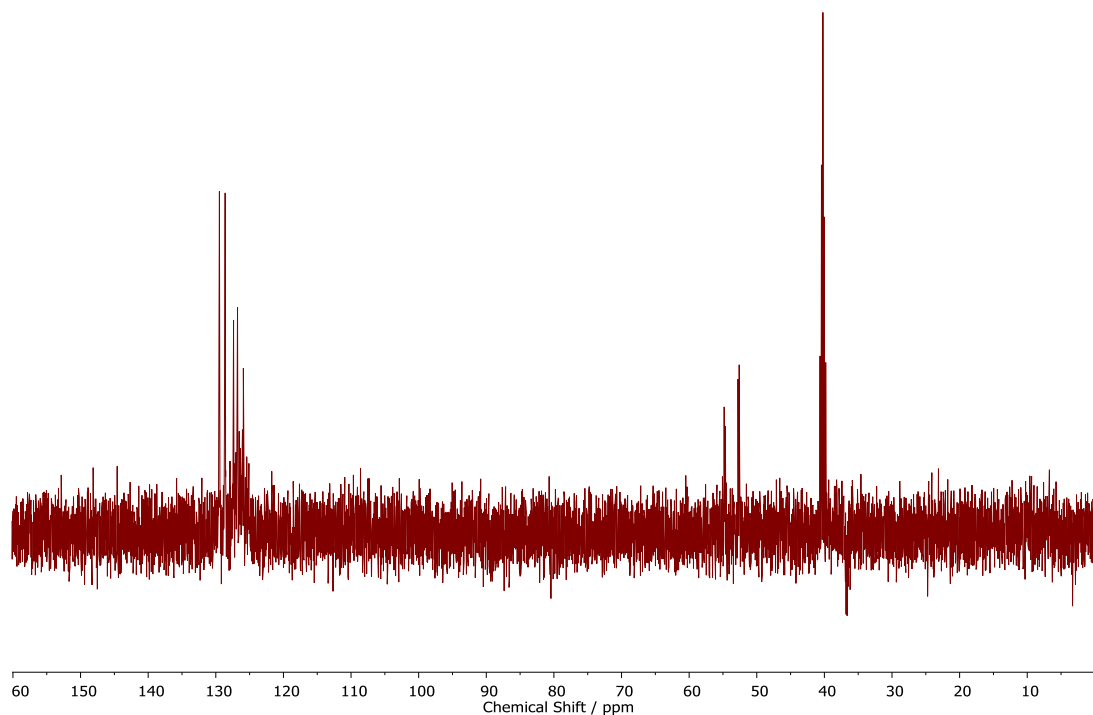


Fig S51: DEPT spectrum of irradiated (Anth)Phe-OH in DMSO- d_6 . Sample had been suspended in CH_2Cl_2 (5 mg mL^{-1}), subjected to 1 h irradiation using 365 nm light then acidified using 1 M HCl prior to drying.

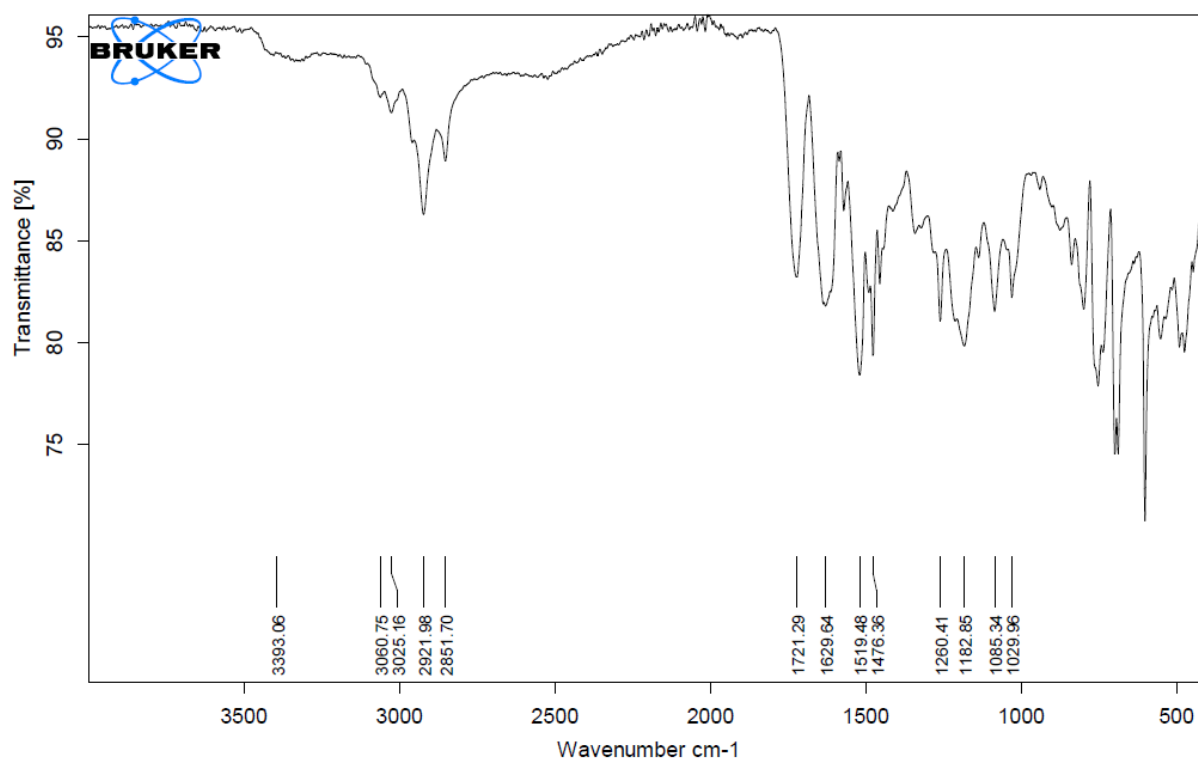


Fig S52: IR spectrum of irradiated (Anth)Phe-OH in DMSO- d_6 . Sample had been suspended in CH_2Cl_2 (5 mg mL^{-1}), subjected to 1 h irradiation using 365 nm light then acidified using 1 M HCl prior to drying.

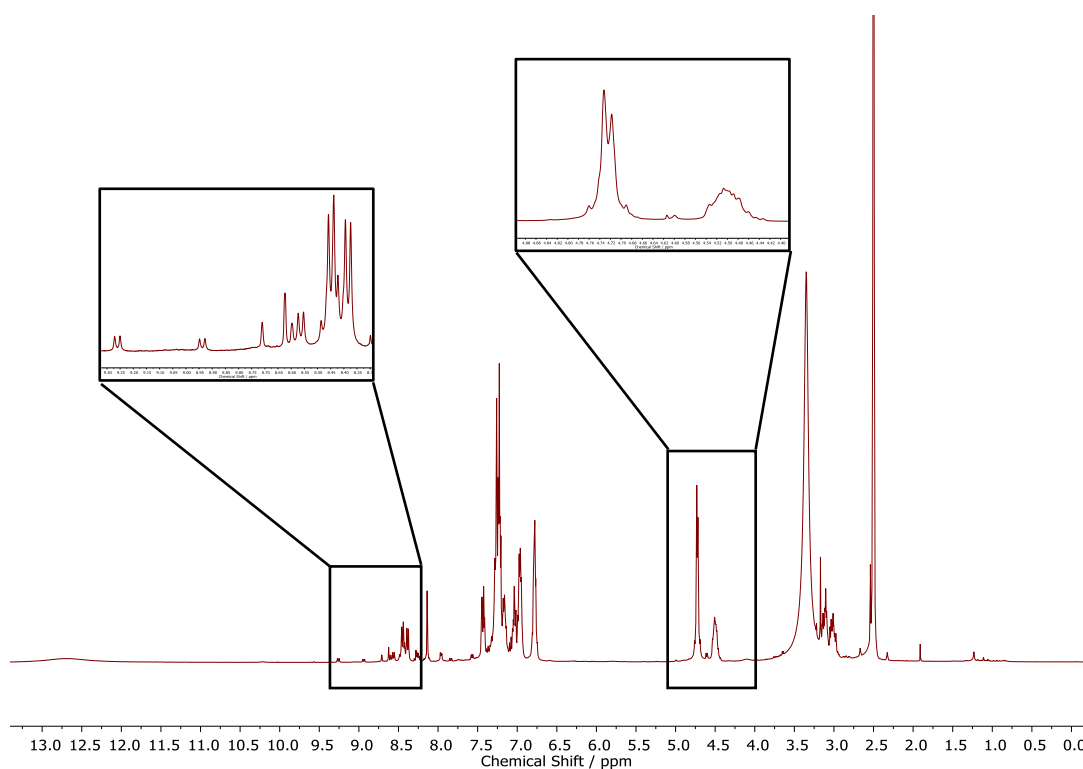


Fig S53: ^1H NMR spectrum (400 MHz) of irradiated (Anth)Phe-OH in DMSO-d_6 . Sample had been dissolved in MeOH (5 mg mL^{-1}), subjected to 1 h irradiation using 365 nm light then acidified using 1 M HCl prior to drying. Expansions show regions with new amide NH (9.0 - 8.0 ppm) and bridgehead CH (4.7 ppm) peaks formed after irradiation.

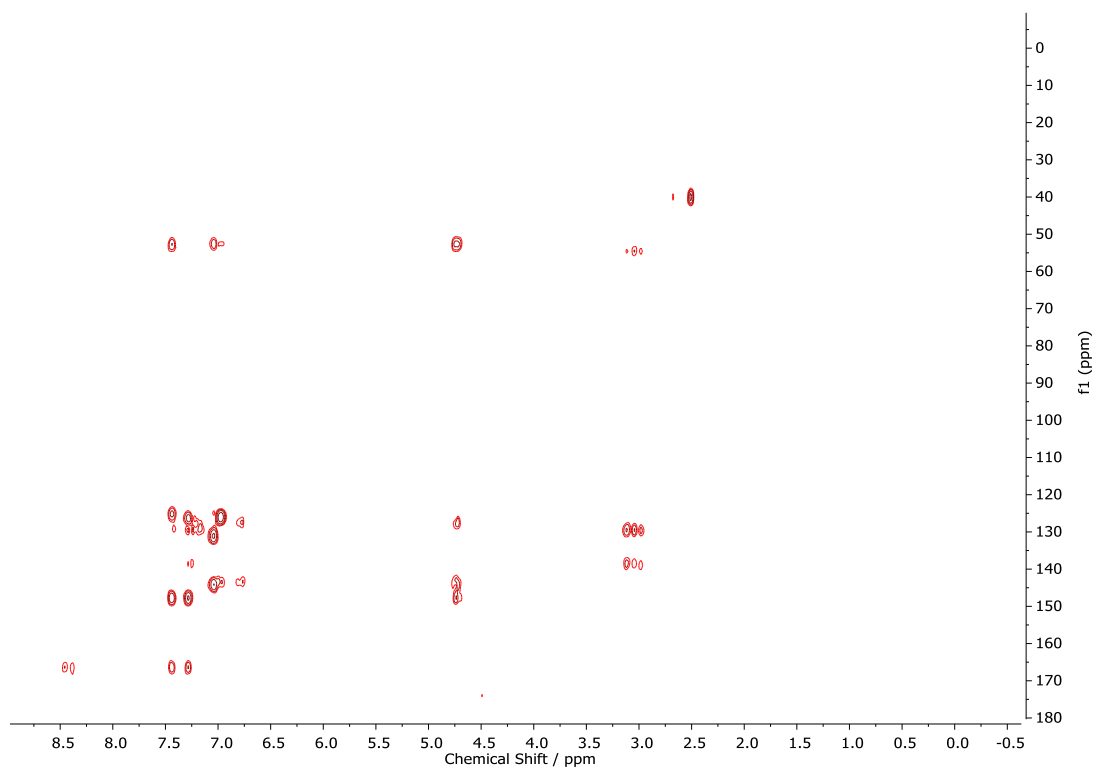


Fig S54: $^1\text{H}/^{13}\text{C}$ HMBC spectrum of irradiated (Anth)Phe-OH in DMSO-d_6 . Sample had been dissolved in MeOH (5 mg mL^{-1}), subjected to 1 h irradiation using 365 nm light then acidified using 1 M HCl prior to drying.

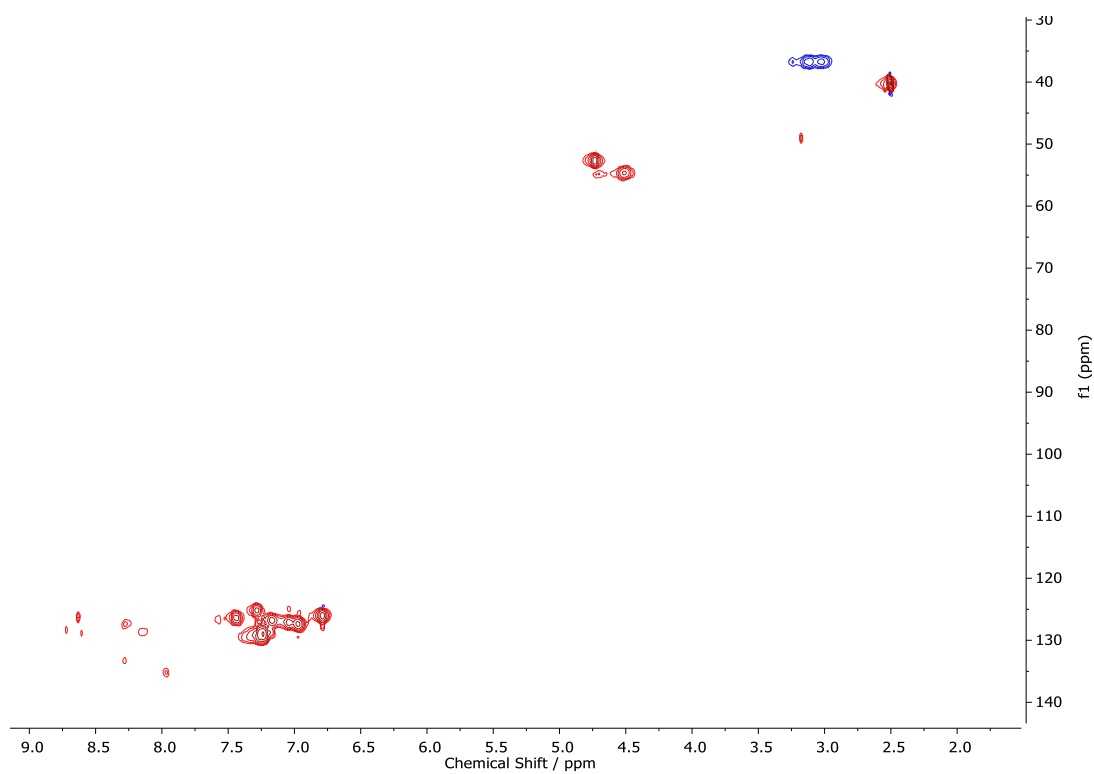


Fig S55: $^1\text{H}/^{13}\text{C}$ HSQC spectrum of irradiated (Anth)Phe-OH in DMSO-d_6 . Sample had been dissolved in MeOH (5 mg mL^{-1}), subjected to 1 h irradiation using 365 nm light then acidified using 1 M HCl prior to drying.

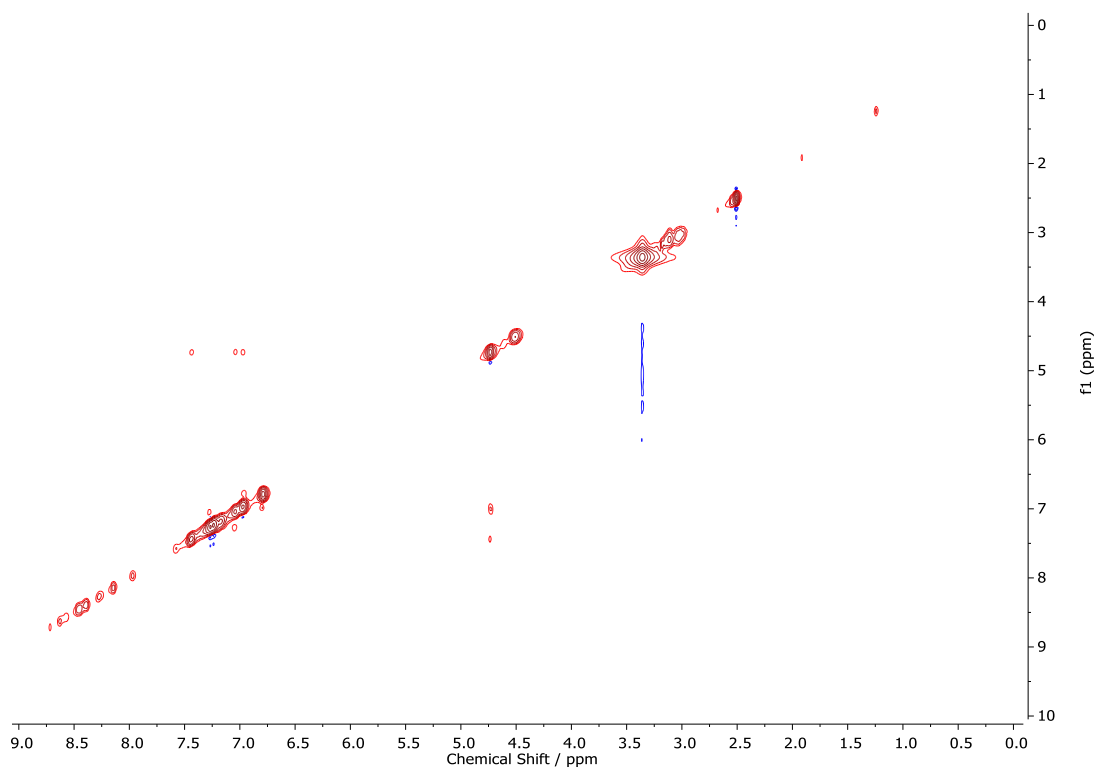


Fig S56: COSY spectrum of irradiated (Anth)Phe-OH in DMSO-d_6 . Sample had been dissolved in MeOH (5 mg mL^{-1}), subjected to 1 h irradiation using 365 nm light then acidified using 1 M HCl prior to drying.

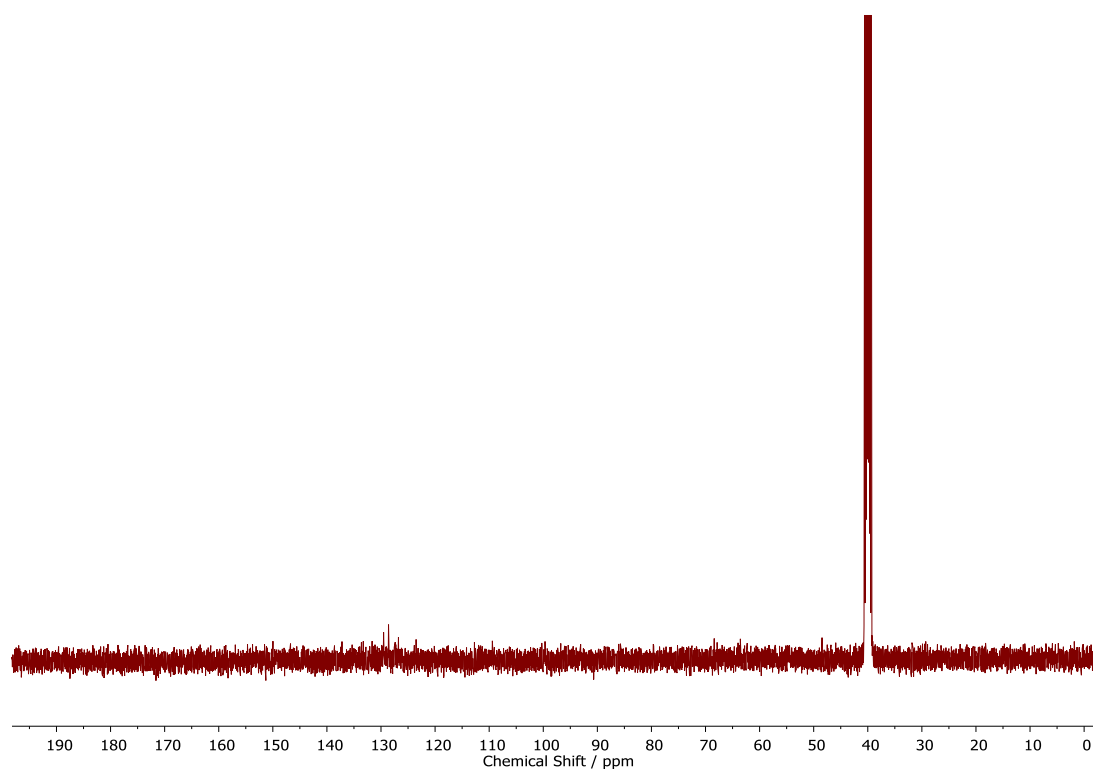


Fig S57: ^{13}C NMR spectrum of irradiated (Anth)Phe-OH in DMSO-d_6 . Sample had been dissolved in MeOH (5 mg mL^{-1}), subjected to 1 h irradiation using 365 nm light then acidified using 1 M HCl prior to drying.

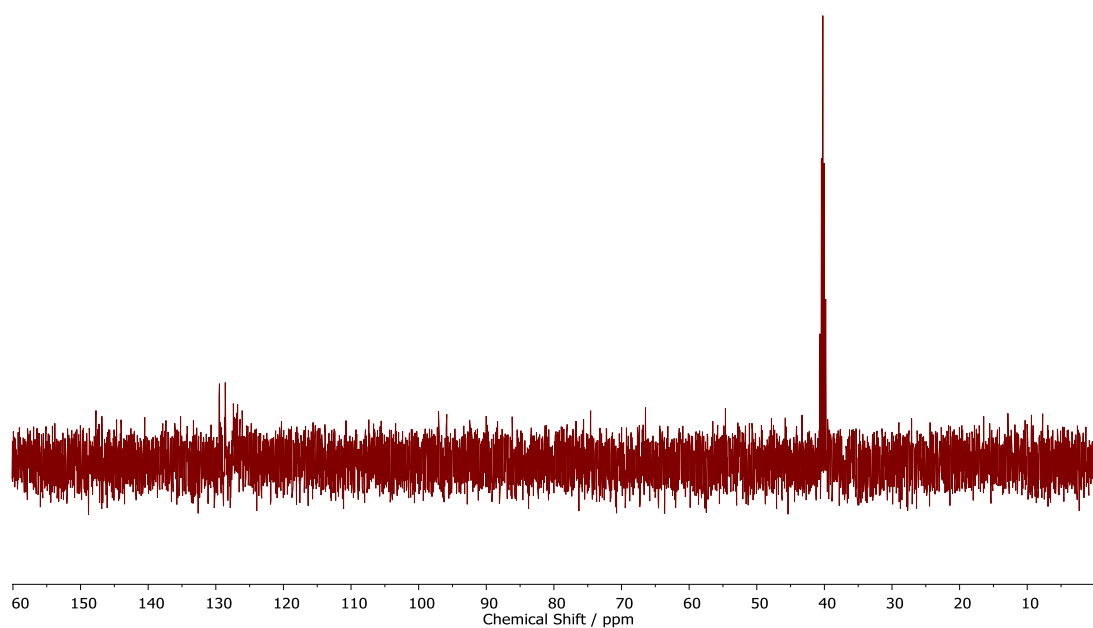


Fig S58: DEPT spectrum of irradiated (Anth)Phe-OH in DMSO-d_6 . Sample had been dissolved in MeOH (5 mg mL^{-1}), subjected to 1 h irradiation using 365 nm light then acidified using 1 M HCl prior to drying.

S7.2. Gel-phase reactions

Gels were prepared in fluorescence cuvettes according to the procedure outlined in Section S3 (scaled up to a total volume of 2 mL). The cuvette was capped prior to reaction to prevent solvent evaporation. After reaction the liquid and gel portions were separated, and the solvent removed from each portion by rotary evaporation. The portions were each acidified with HCl (1 M, 1 mL) and extracted into EtOAc (5 mL). The solvent was removed from the resulting solutions *in vacuo* and the resulting solids taken for analysis.

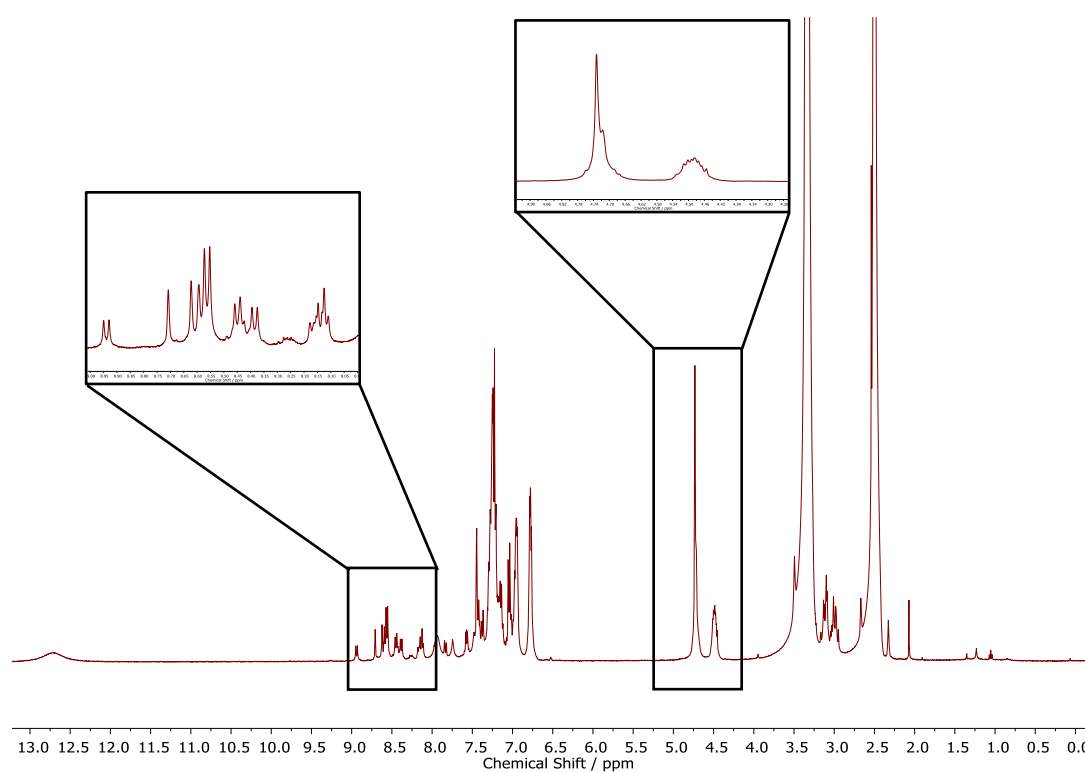


Fig S59: ¹H NMR spectrum (400 MHz) of irradiated (Anth)Phe-OH in DMSO-d₆. Sample was a self-supporting weak gel of (Anth)Phe-OH (5 mg mL⁻¹) formed by addition of GlyNH₂·HCl (2 equiv.), subjected to 1 h irradiation using 365 nm light then acidified using 1 M HCl prior to drying. Expansions show regions with new amide NH (9.0 - 8.0 ppm) and bridgehead CH (4.7 ppm) peaks formed after irradiation.

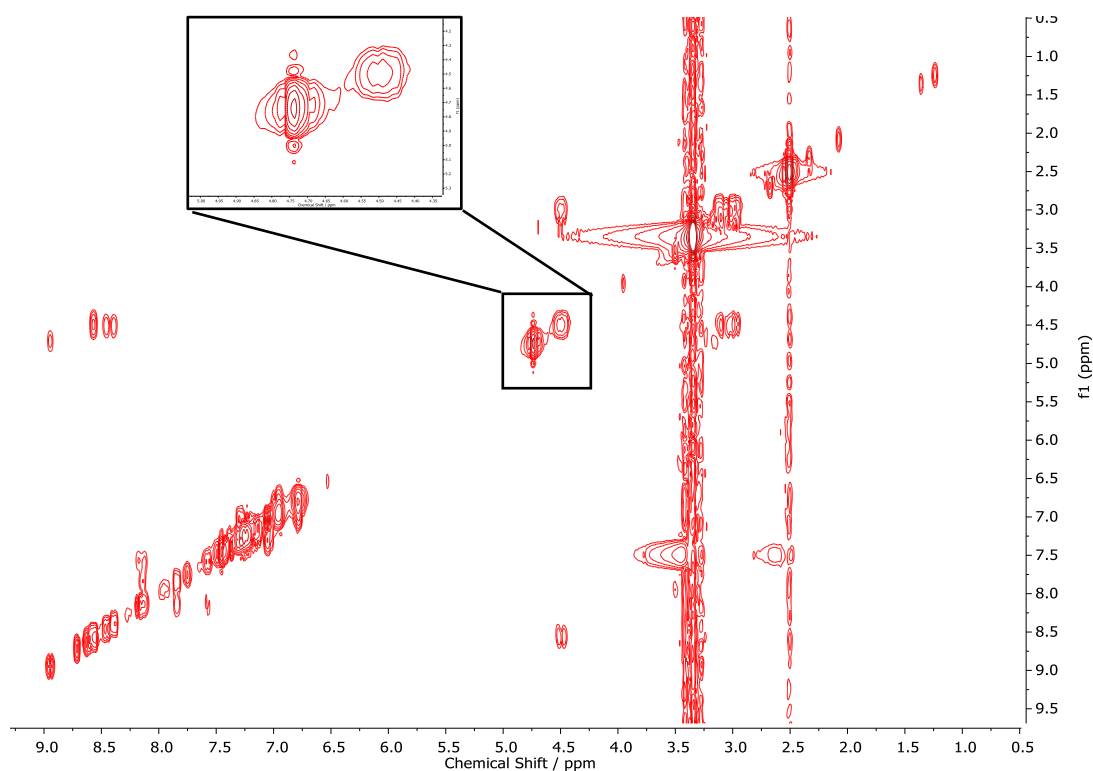


Fig S60: COSY spectrum of irradiated (Anth)Phe-OH in DMSO- d_6 . Sample was a self-supporting weak gel of (Anth)Phe-OH (5 mg mL^{-1}) formed by addition of GlyNH $_2$ ·HCl (2 equiv.), subjected to 1 h irradiation using 365 nm light then acidified using 1 M HCl prior to drying. Expansion shows the fine structure of the dimer bridgehead (4.7 ppm) and Phe CH (4.5 ppm) cross-peaks.

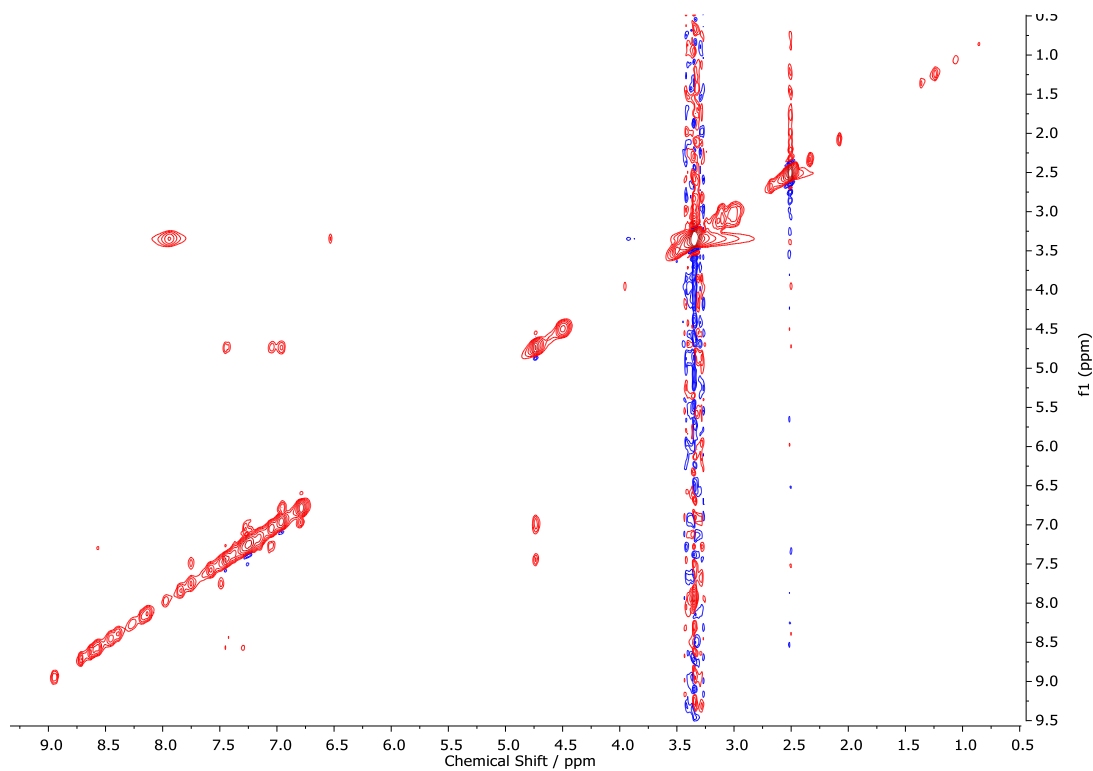


Fig S61: NOESY spectrum of irradiated (Anth)Phe-OH in DMSO- d_6 . Sample was a self-supporting weak gel of (Anth)Phe-OH (5 mg mL^{-1}) formed by addition of GlyNH $_2$ ·HCl (2 equiv.), subjected to 1 h irradiation using 365 nm light then acidified using 1 M HCl prior to drying.

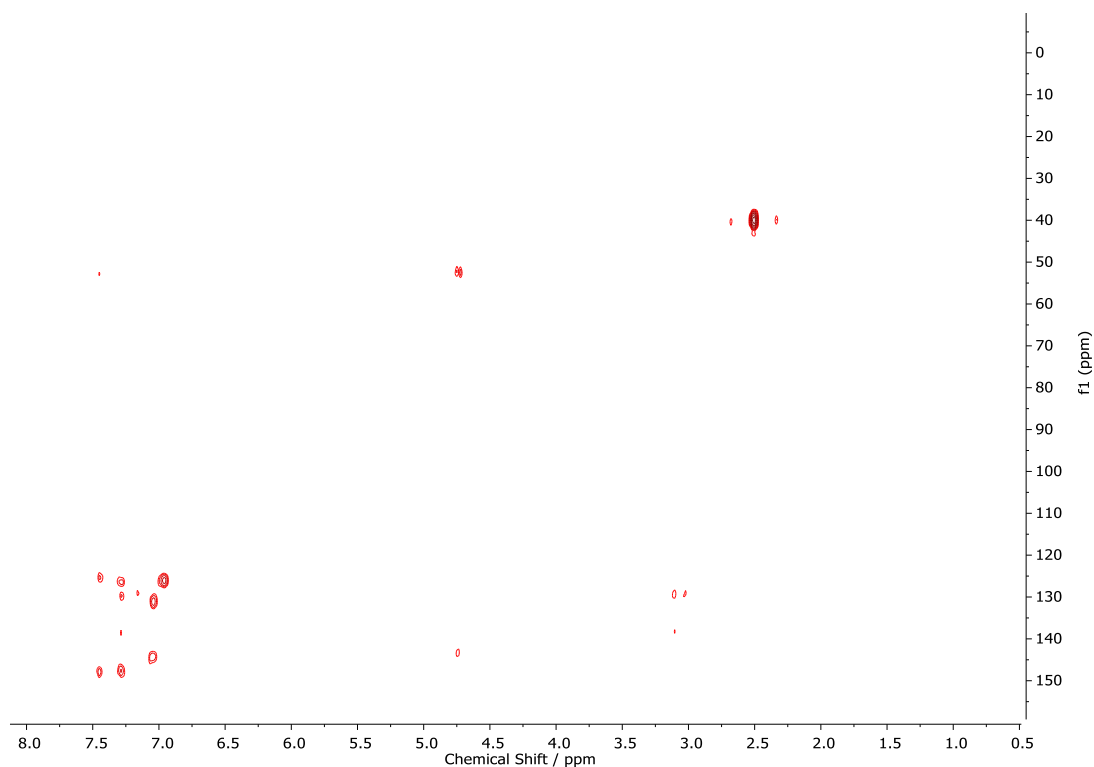


Fig S62: $^1\text{H}/^{13}\text{C}$ HMBC spectrum of irradiated (Anth)Phe-OH in $\text{DMSO}-d_6$. Sample was a self-supporting weak gel of (Anth)Phe-OH (5 mg mL^{-1}) formed by addition of $\text{GlyNH}_2\cdot\text{HCl}$ (2 equiv.), subjected to 1 h irradiation using 365 nm light then acidified using 1 M HCl prior to drying.

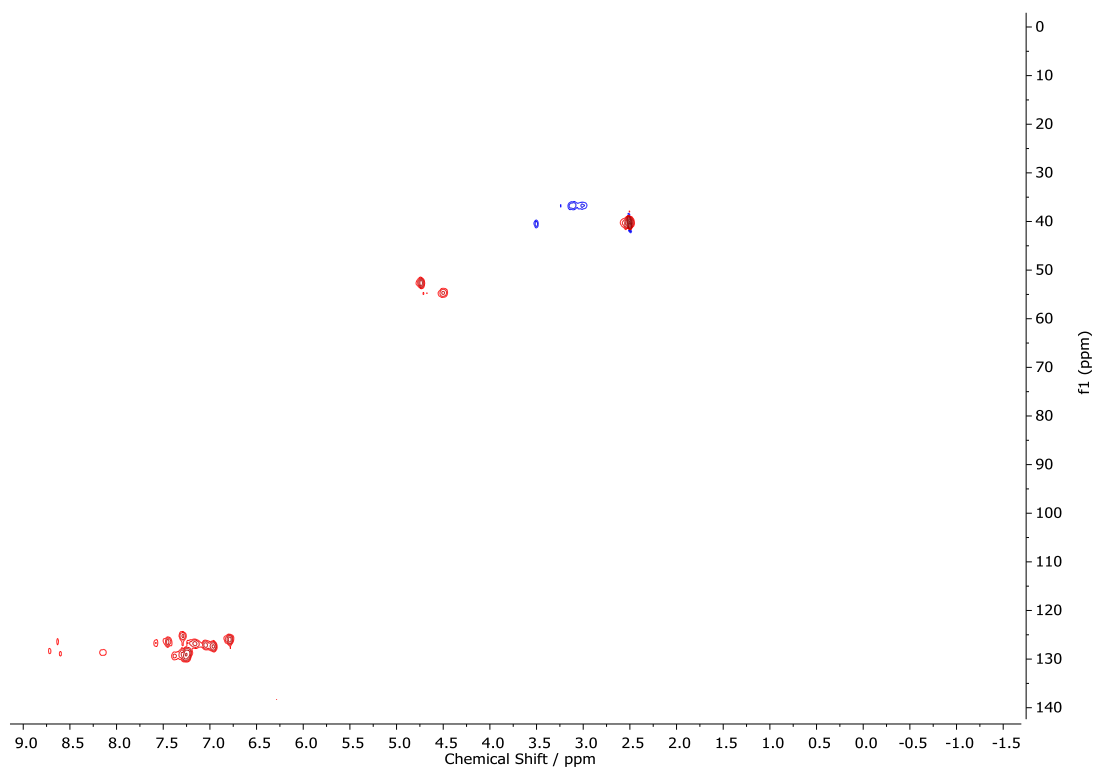


Fig S63: $^1\text{H}/^{13}\text{C}$ HSQC spectrum of irradiated (Anth)Phe-OH in $\text{DMSO}-d_6$. Sample was a self-supporting weak gel of (Anth)Phe-OH (5 mg mL^{-1}) formed by addition of $\text{GlyNH}_2\cdot\text{HCl}$ (2 equiv.), subjected to 1 h irradiation using 365 nm light then acidified using 1 M HCl prior to drying.

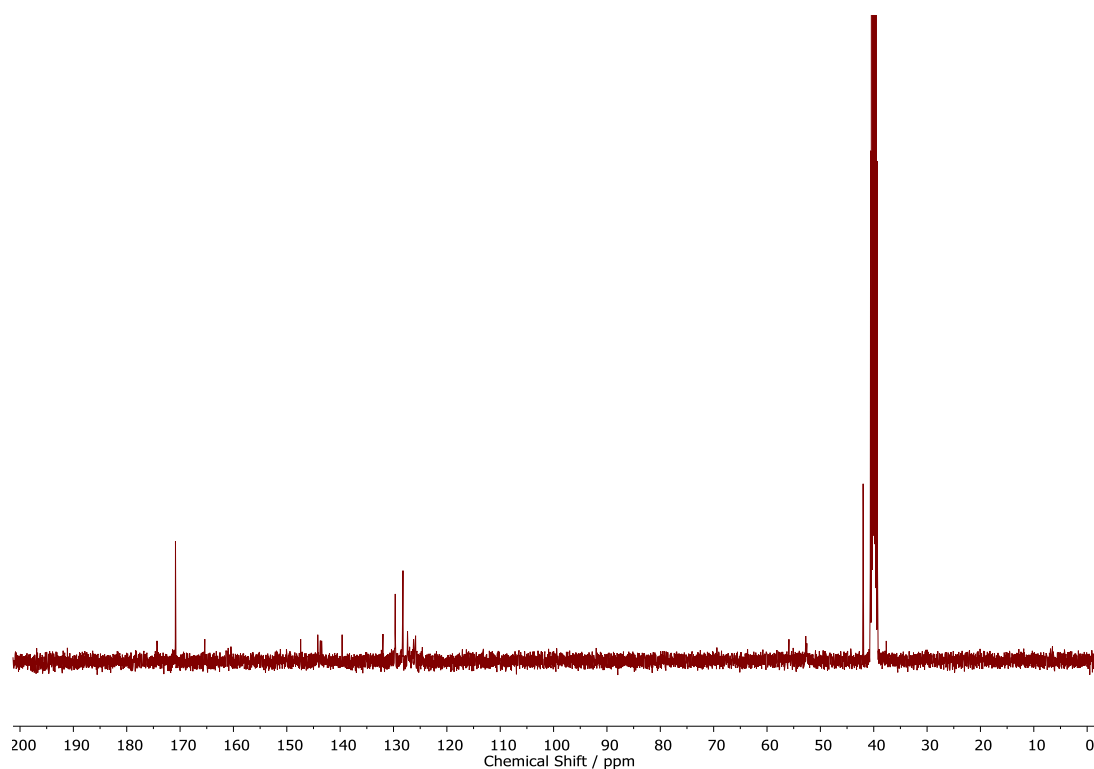


Fig S64: ^{13}C NMR spectrum of irradiated (Anth)Phe-OH in DMSO-d_6 . Sample was a self-supporting weak gel of (Anth)Phe-OH (5 mg mL^{-1}) formed by addition of $\text{GlyNH}_2\cdot\text{HCl}$ (2 equiv.), subjected to 1 h irradiation using 365 nm light then acidified using 1 M HCl prior to drying.

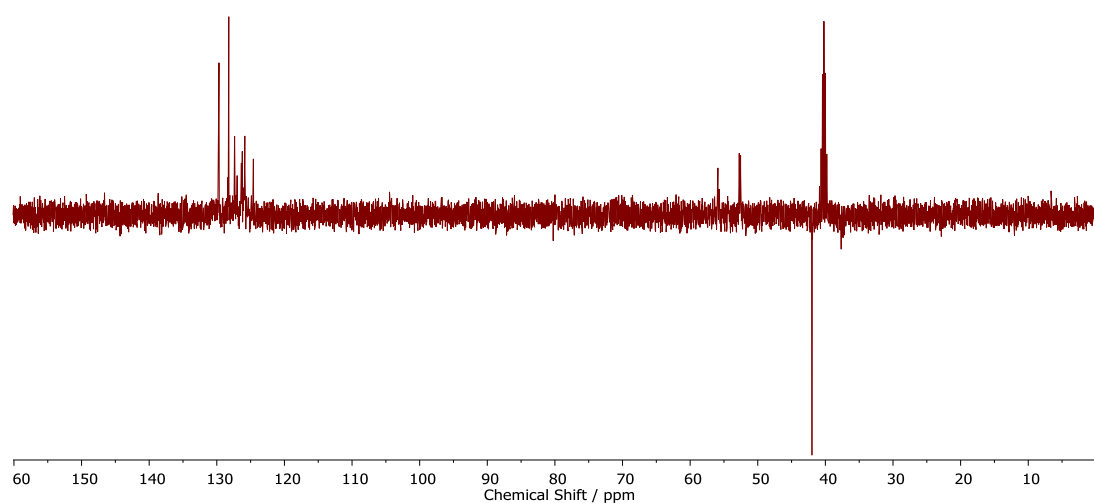


Fig S65: DEPT spectrum of irradiated (Anth)Phe-OH in DMSO-d_6 . Sample was a self-supporting weak gel of (Anth)Phe-OH (5 mg mL^{-1}) formed by addition of $\text{GlyNH}_2\cdot\text{HCl}$ (2 equiv.), subjected to 1 h irradiation using 365 nm light then acidified using 1 M HCl prior to drying.

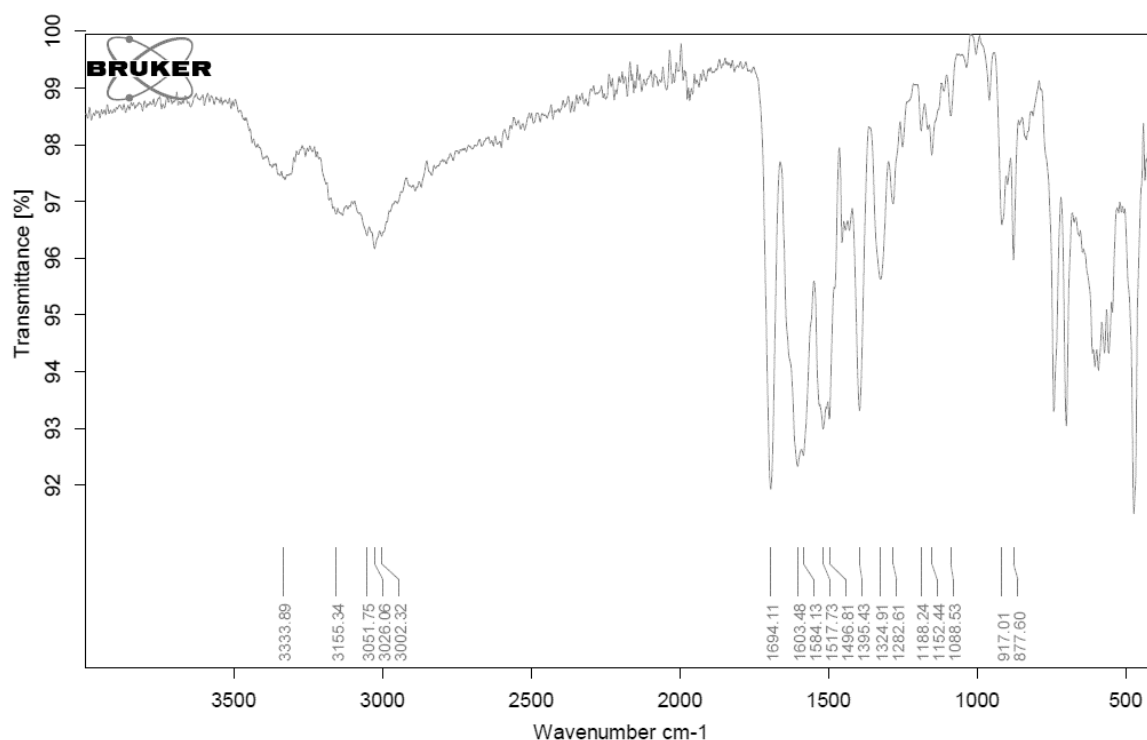


Fig S66: IR-spectrum of non-irradiated (Anth)Phe-OH in DMSO- d_6 . Sample was a hydrogel of (Anth)Phe-OH (5 mg mL⁻¹) formed by addition of GlyNH₂·HCl (2 equiv.). This region of the gel was shielded from irradiation (365 nm light) and remained in the gel phase. This gel portion was dried and acidified using 1 M HCl prior to drying.

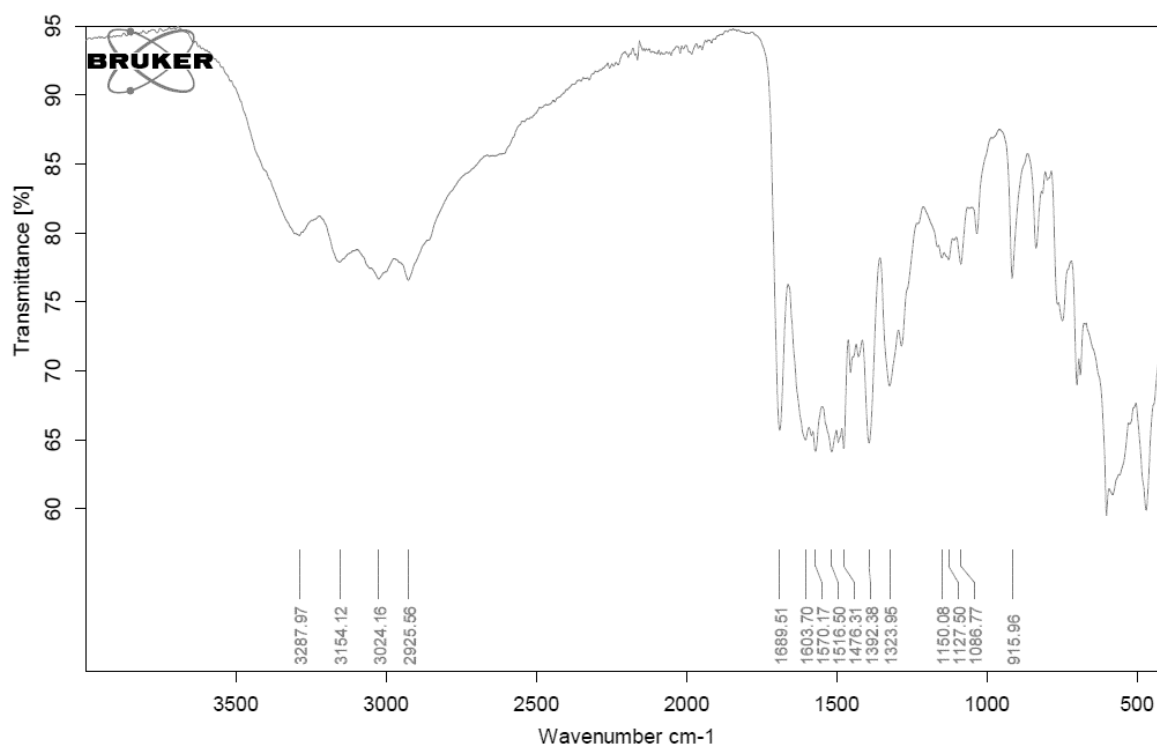


Fig S67: IR-spectrum of irradiated (Anth)Phe-OH in DMSO- d_6 . Sample was a self-supporting weak gel of (Anth)Phe-OH (5 mg mL⁻¹) formed by addition of GlyNH₂·HCl (2 equiv.), subjected to 1 h irradiation using 365 nm light then acidified using 1 M HCl prior to drying.

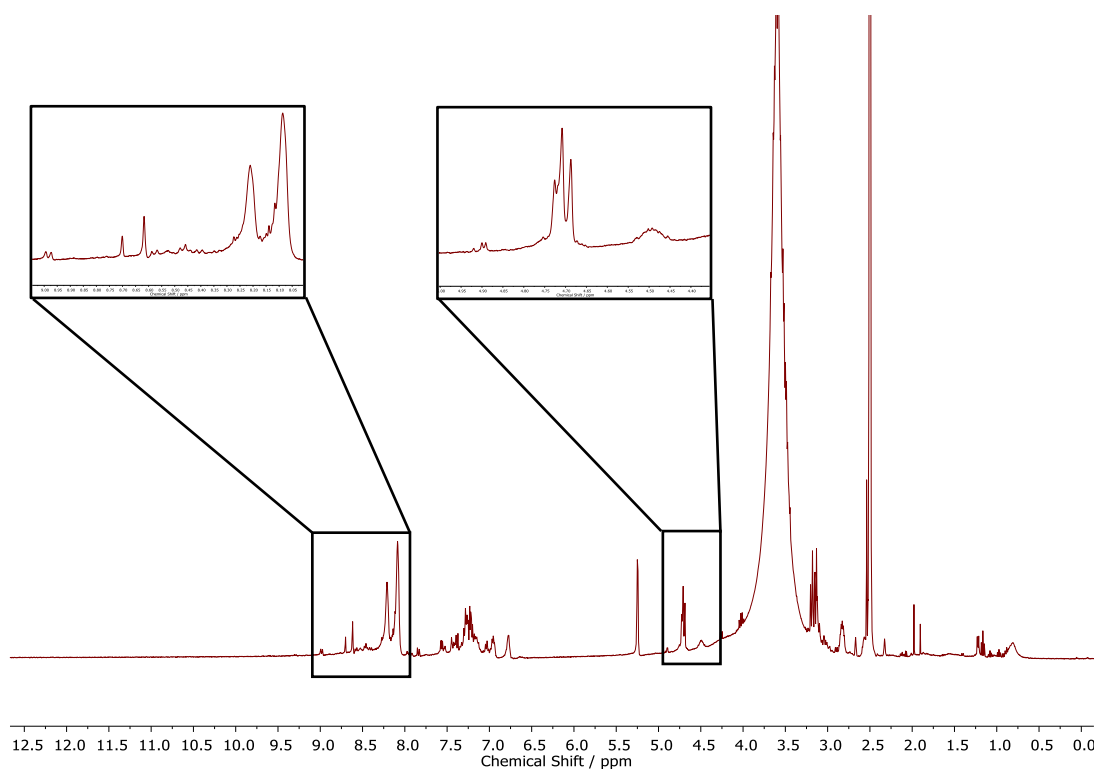


Fig S68: ^1H NMR spectrum (400 MHz) of irradiated (Anth)Phe-OH in DMSO-d_6 . Sample was a hydrogel of (Anth)Phe-OH (5 mg mL^{-1}) formed by addition of [GlcN-HCl (2 equiv.) in media], subjected to 1 h irradiation using 365 nm light then acidified using 1 M HCl prior to drying. Expansions show regions with new amide NH (9.0 - 8.0 ppm) and bridgehead CH (4.7 ppm) peaks formed after irradiation.

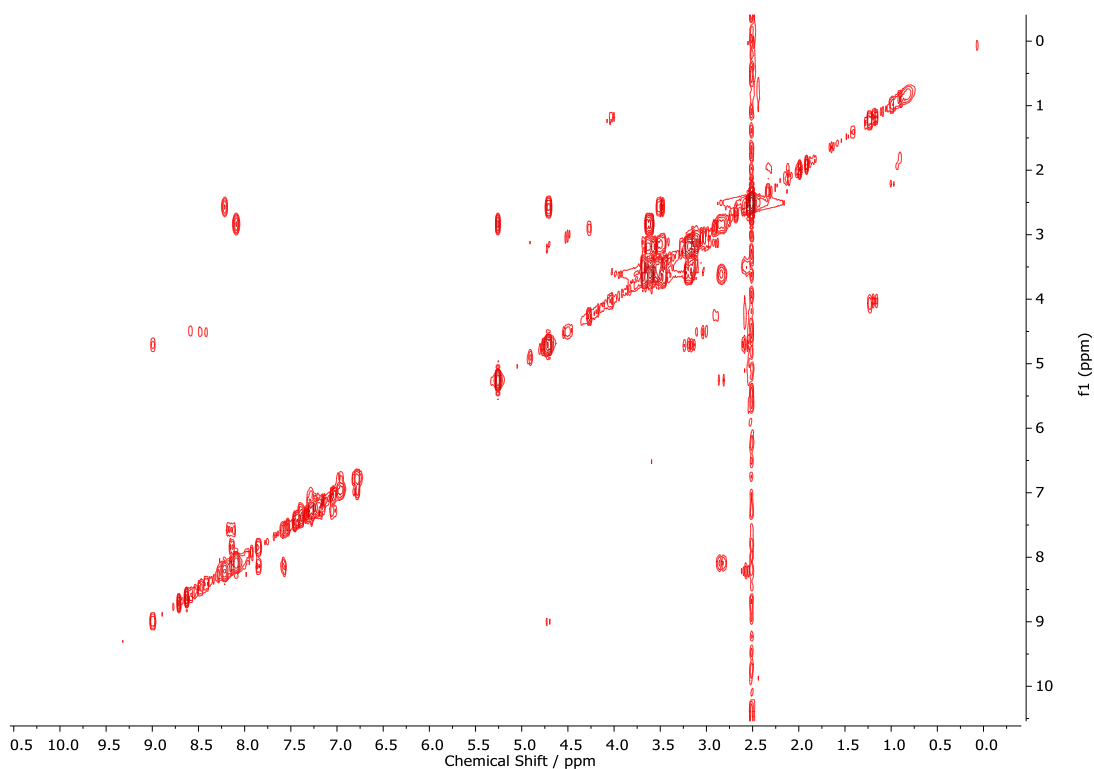


Fig S69: COSY spectrum of irradiated (Anth)Phe-OH in DMSO-d_6 . Sample was a hydrogel of (Anth)Phe-OH (5 mg mL^{-1}) formed by addition of [GlcN-HCl (2 equiv.) in media], subjected to 1 h irradiation using 365 nm light then acidified using 1 M HCl.

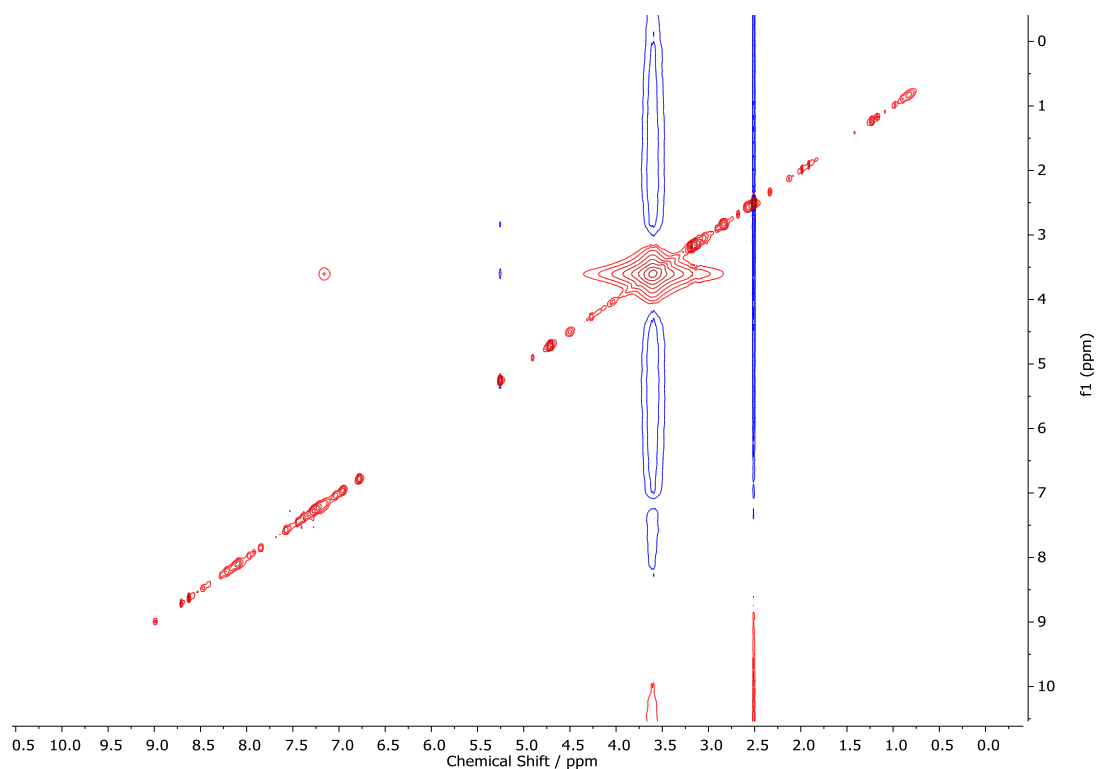


Fig S70: NOESY spectrum of irradiated (Anth)Phe-OH in DMSO- d_6 . Sample was a hydrogel of (Anth)Phe-OH (5 mg mL^{-1}) formed by addition of [GlcN·HCl (2 equiv.) in media], subjected to 1 h irradiation using 365 nm light then acidified using 1 M HCl prior to drying.

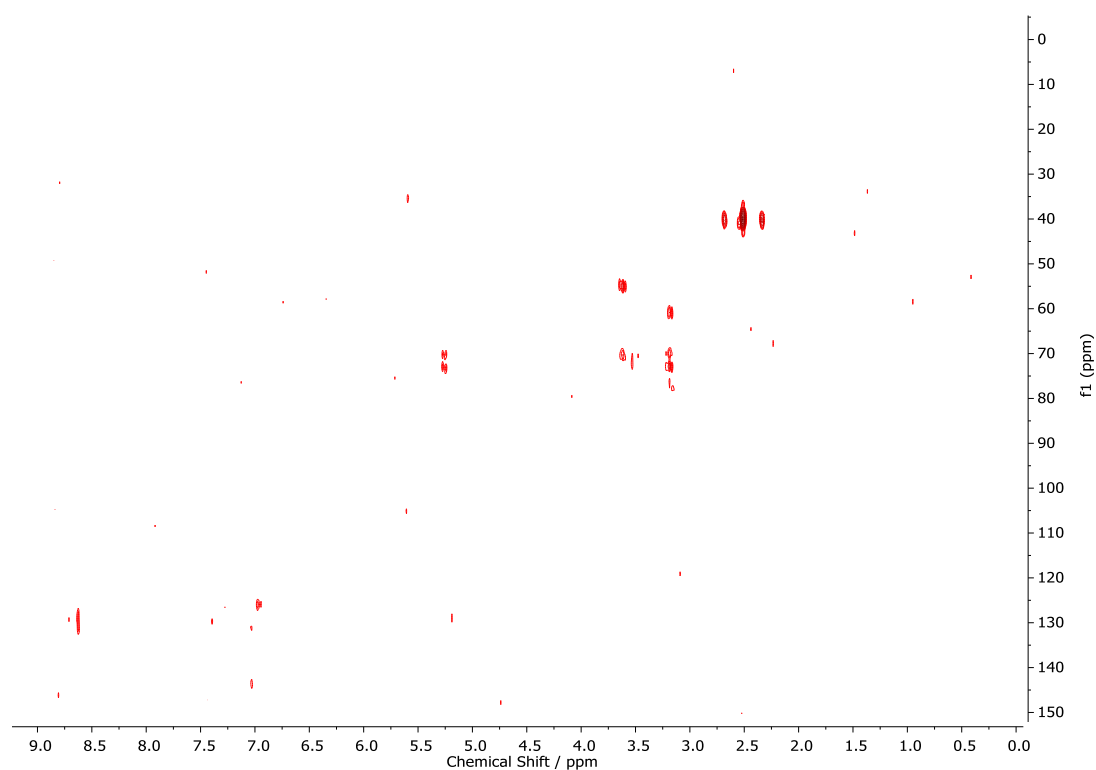


Fig S71: $^1\text{H}/^{13}\text{C}$ HMBC spectrum of irradiated (Anth)Phe-OH in DMSO- d_6 . Sample was a hydrogel of (Anth)Phe-OH (5 mg mL^{-1}) formed by addition of [GlcN·HCl (2 equiv.) in media], subjected to 1 h irradiation using 365 nm light then acidified using 1 M HCl prior to drying.

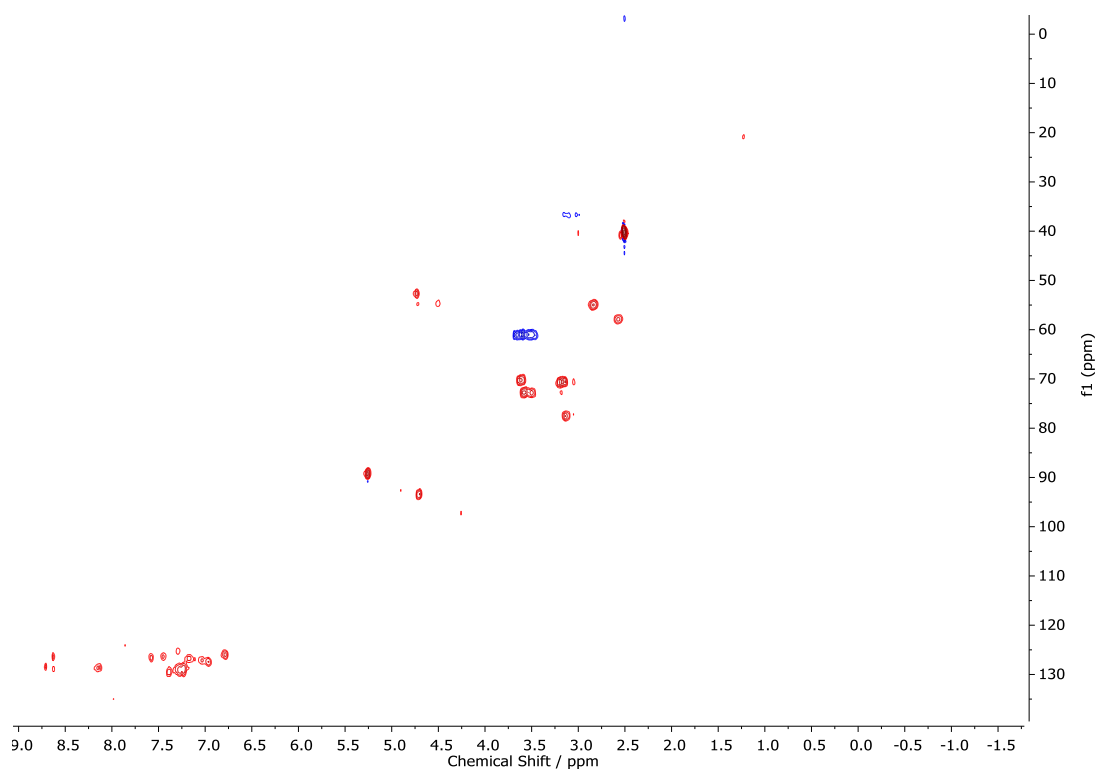


Fig S72: $^1\text{H}/^{13}\text{C}$ HSQC spectrum of irradiated (Anth)Phe-OH in DMSO-d_6 . Sample was a hydrogel of (Anth)Phe-OH (5 mg mL^{-1}) formed by addition of [GlcN-HCl (2 equiv.) in media], subjected to 1 h irradiation using 365 nm light then acidified using 1 M HCl prior to drying.

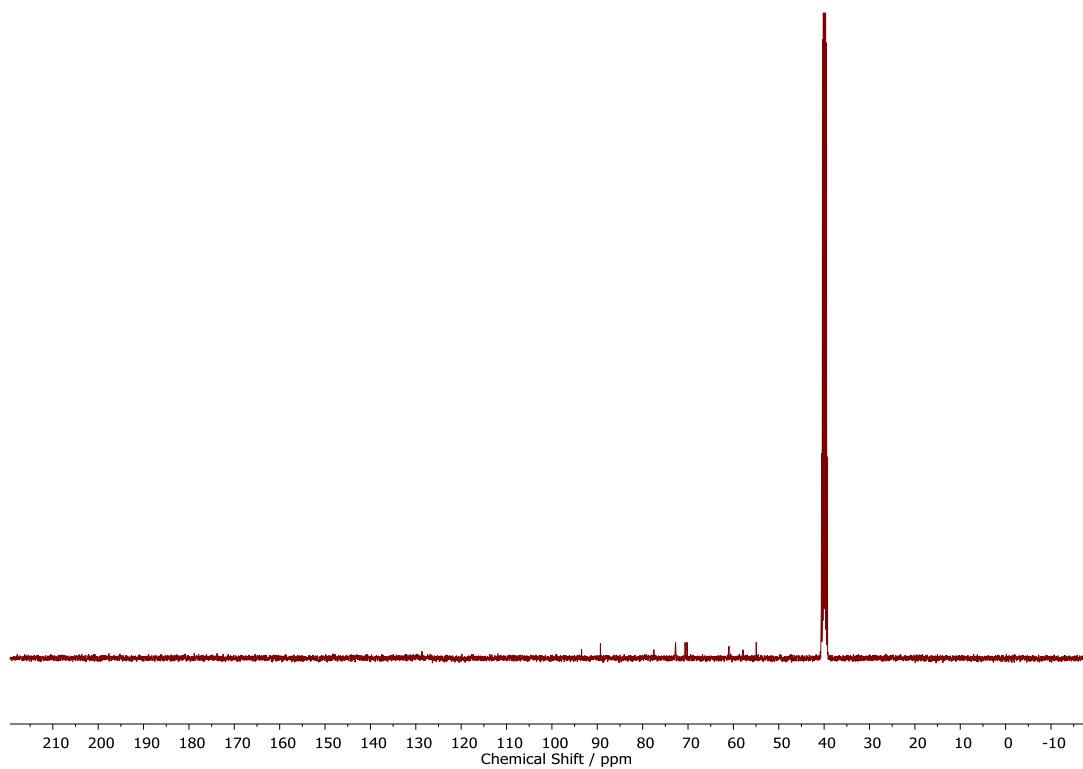


Fig S73: ^{13}C NMR spectrum (101 MHz) of irradiated (Anth)Phe-OH in DMSO-d_6 . Sample was a hydrogel of (Anth)Phe-OH (5 mg mL^{-1}) formed by addition of [GlcN-HCl (2 equiv.) in media], subjected to 1 h irradiation using 365 nm light then acidified using 1 M HCl prior to drying.

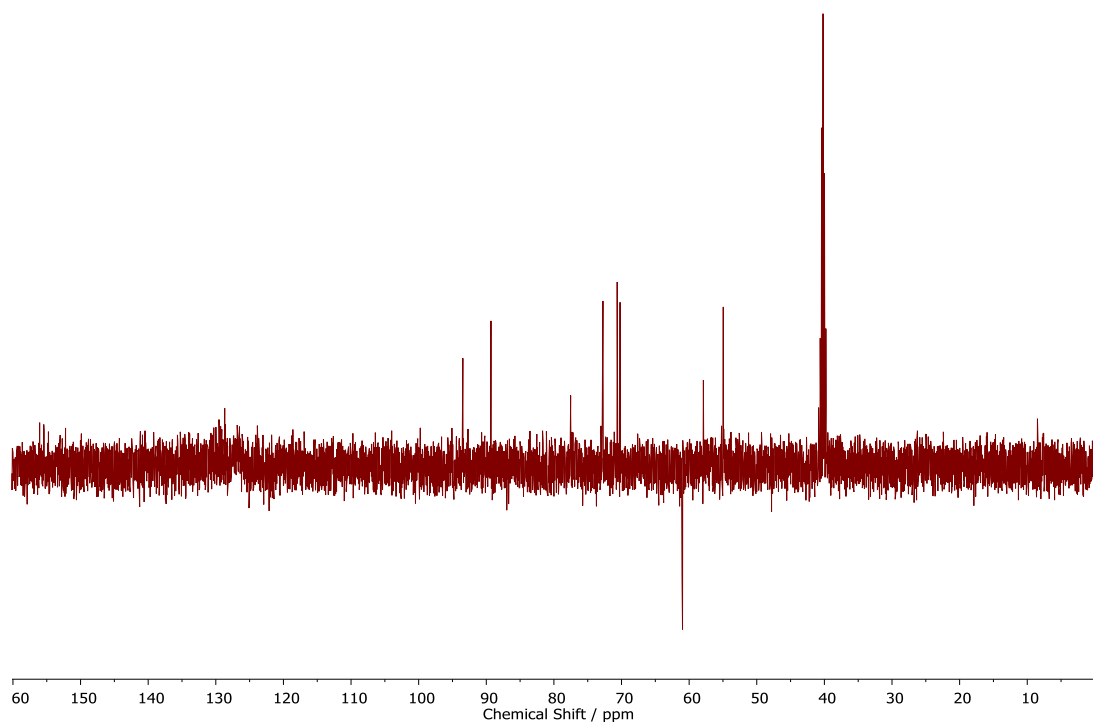


Fig S74: DEPT spectrum of irradiated (Anth)Phe-OH in DMSO- d_6 . Sample was a hydrogel of (Anth)Phe-OH (5 mg mL^{-1}) formed by addition of [GlcN·HCl (2 equiv.) in media], subjected to 1 h irradiation using 365 nm light then acidified using 1 M HCl prior to drying.



Fig S75: From left to right: empty reactor (UV on), sample in MeOH, sample in CH_2Cl_2 , and $\text{GlyNH}_2\cdot\text{HCl}$ triggered self-supporting weak gel.

Table S7: Photoreaction temperature, conversion estimated from NMR and mass spectrometry peaks corresponding to the photodimer reaction product. Calculated photodimer mass = 738.2730. Conversion was estimated by comparison of peak integrals corresponding to the photodimer (δ ca. 4.7 ppm) and monomer (δ ca. 8.7 ppm).

Experiment	Conversion / %	Mass spec found	Max reaction temperature / °C
Basic gelator solution	94	737.2624	39
CH ₂ Cl ₂	85	737.2640	34
MeOH	80	737.2680	40
GlyNH ₂ ·HCl gel – sol	81	737.2626	41
GlyNH ₂ ·HCl gel – gel	36	-	-
Media gel (+ GlcN·HCl)	63	737.3	40

S7.3. Data for dimerisation of (Anth)Phe-OH weak gels formed by addition of GlyNH₂·HCl

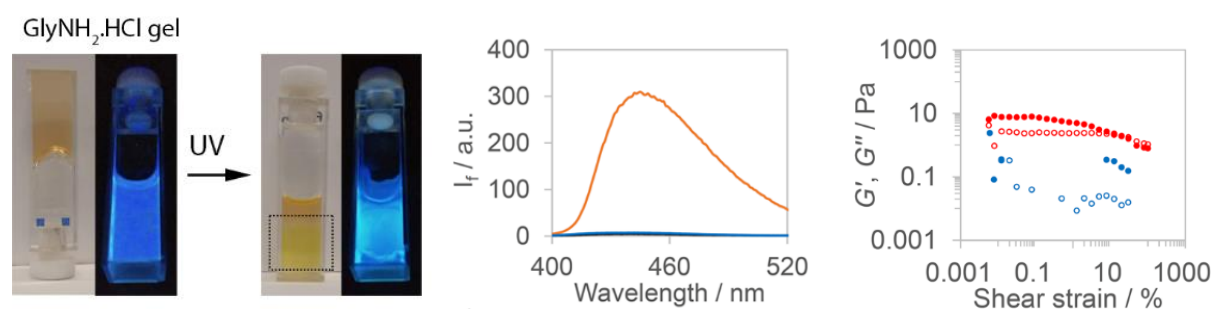


Fig S76: Data for dimerisation of (Anth)Phe-OH self-supporting gel-like materials formed by addition of GlyNH₂·HCl. Left: Optical and fluorescence images of gels prior to and after irradiation (UV); (b): Fluorescence spectra of (Anth)Phe-OH samples before gelation (blue), as a gel (red) and after irradiation (black); (c): Rheology traces of samples before (red) and after (blue) irradiation. Filled circles: Elastic modulus, (G'). Hollow circles: Loss modulus (G'').

S8. Scanning electron microscopy

S8.1. Sample preparation

SEM was carried out on lyophilised samples sputtered with gold/palladium.

S8.2. Further SEM images

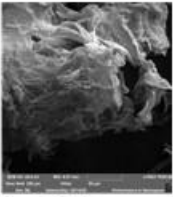
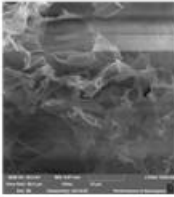

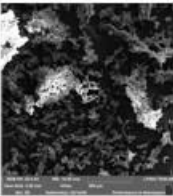
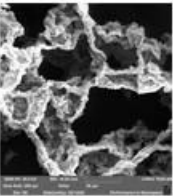
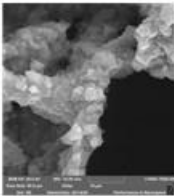
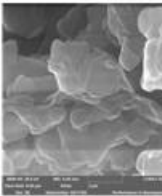
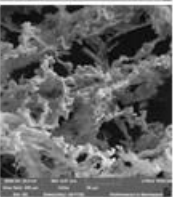
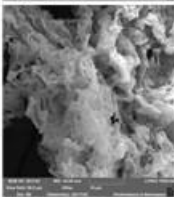
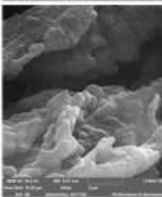
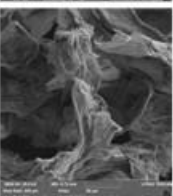
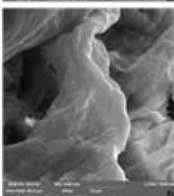
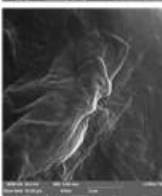
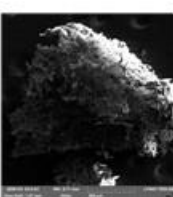
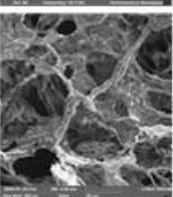
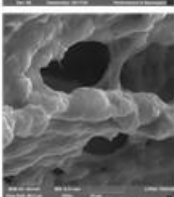
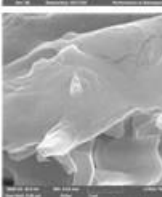
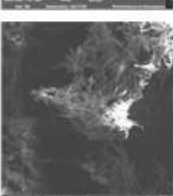
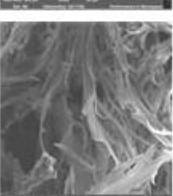


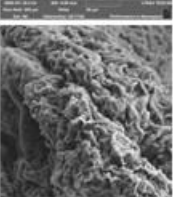
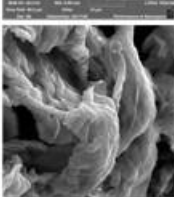
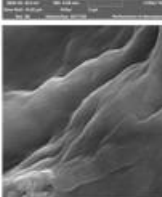
Size Sample	Image width			
	2 mm	250 μm	50 μm	10 μm
5 mg mL ⁻¹ , 2 eq. GlyNH ₂ -HCl				
5 mg mL ⁻¹ , 6 eq. GlyNH ₂ -HCl				
3 mg mL ⁻¹ , 10 eq. GlyNH ₂ -HCl				
5 mg mL ⁻¹ , 2 eq. GlcN-HCl				
3 mg mL ⁻¹ , 10 eq. GlcN-HCl				
5 mg mL ⁻¹ , Media				
5 mg mL ⁻¹ , Media + 2 eq. GlcN-HCl				

Fig. S77: SEM images of lyophilised hydrogels/gel-like materials


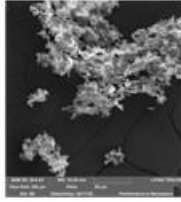
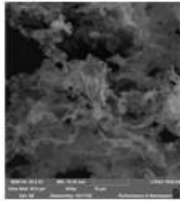
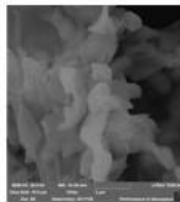
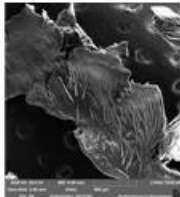
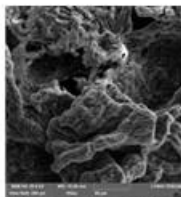
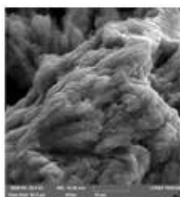
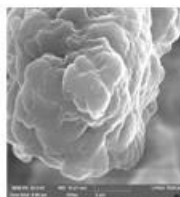
Size Sample	Image width			
	2 mm	250 μm	50 μm	10 μm
5 mg mL ⁻¹ , 2 eq. GlyNH ₂ -HCl UV irradiated				
5 mg mL ⁻¹ , Media + 2 eq. GlcN-HCl UV irradiated				

Fig. S78: SEM images of lyophilised hydrogels/gel-like materials after UV-irradiation ($\lambda = 365 \text{ nm}$) for 1 h

S9. Rheological data

S9.1. Sample preparation

Gels with a volume of 0.5 mL were formed in the wells of a 24-well cell culture plate. The gels were carefully transferred to the base plate of the rheometer for analysis.

The linear viscoelastic region (LVR) was identified using an amplitude sweep at a constant frequency of 1 Hz; each hydrogel/gel-like material was not taken out of the LVR (i.e. no significant deformation induced). A frequency sweep on each sample was then performed (Figs S79-S84, right). Frequency sweeps were performed at a constant shear strain identified from the LVR of the amplitude sweep. This value was 0.04 % for all samples with the exception of 5 mg mL⁻¹ (Anth)Phe-OH formed by addition of 2 equiv. GlcN·HCl (shear strain of 2.0%). For each sample, an amplitude sweep was then performed to the gel breakdown point (Figs S79-S84, left). All amplitude sweeps were performed at a constant frequency of 1 Hz.

Rheology error bars were calculated as the standard deviation from the mean of measurements made on three separate samples.

S9.2. Further rheological data for (Anth)Phe-OH 2 hydrogels/gel-like materials

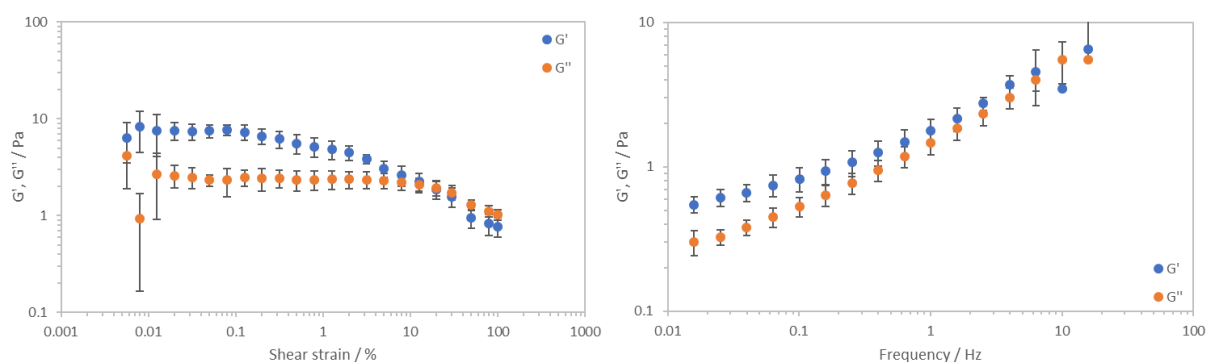


Fig. S79: Amplitude (left) and frequency (right) sweeps of (Anth)Phe-OH (5 mg mL⁻¹) gel-like materials triggered by addition of 2 equiv. GlyNH₂·HCl.

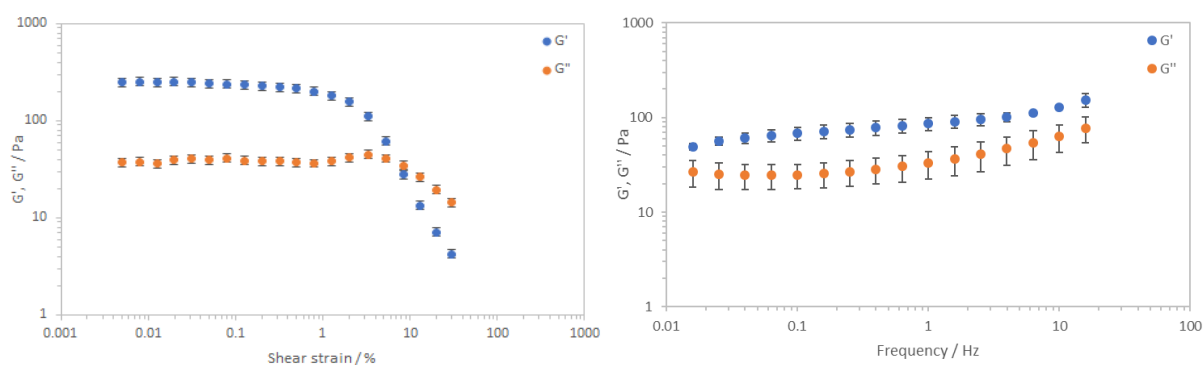


Fig. S80: Amplitude (left) and frequency (right) sweeps of (Anth)Phe-OH (5 mg mL^{-1}) hydrogels triggered by addition of 6 equiv. $\text{GlyNH}_2\cdot\text{HCl}$

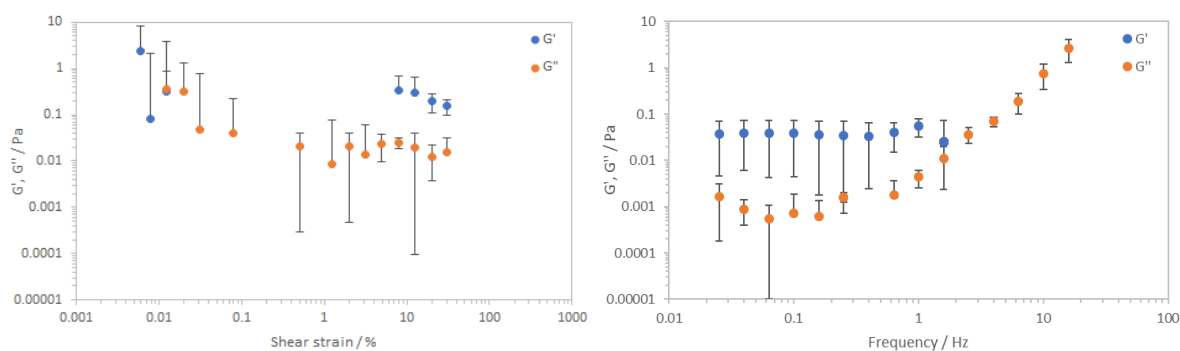


Fig. S81: Amplitude (left) and frequency (right) sweeps of $\text{GlyNH}_2\cdot\text{HCl}$ (2 equiv.) triggered (Anth)Phe-OH (5 mg mL^{-1}) gel-like materials after irradiation with 365 nm light for 1 h

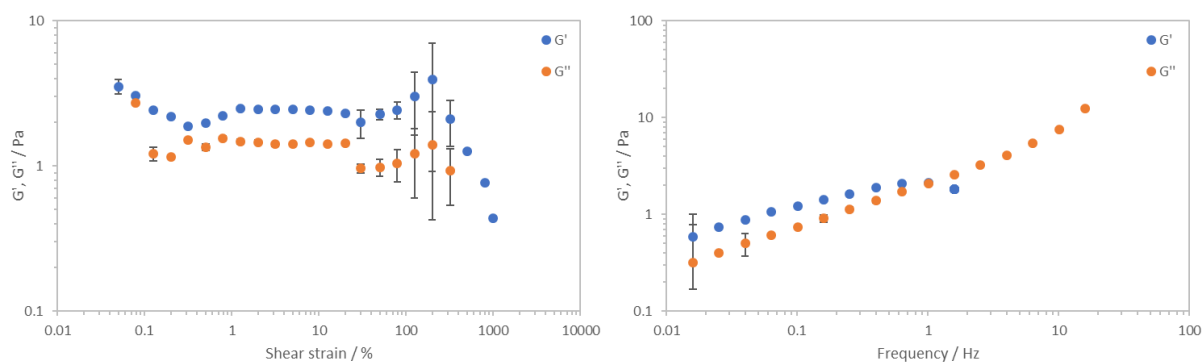


Fig. S82: Amplitude (left) and frequency (right) sweeps of (Anth)Phe-OH (5 mg mL^{-1}) gel-like materials triggered by addition of 2 equiv. $\text{GlcN}\cdot\text{HCl}$

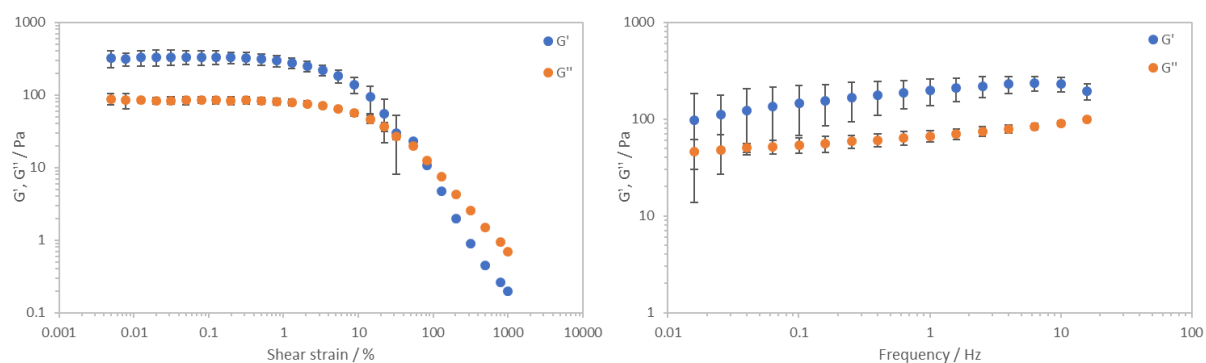


Fig. S83: Amplitude (left) and frequency (right) sweeps of (Anth)Phe-OH (5 mg mL^{-1}) hydrogels triggered by addition of cell culture media

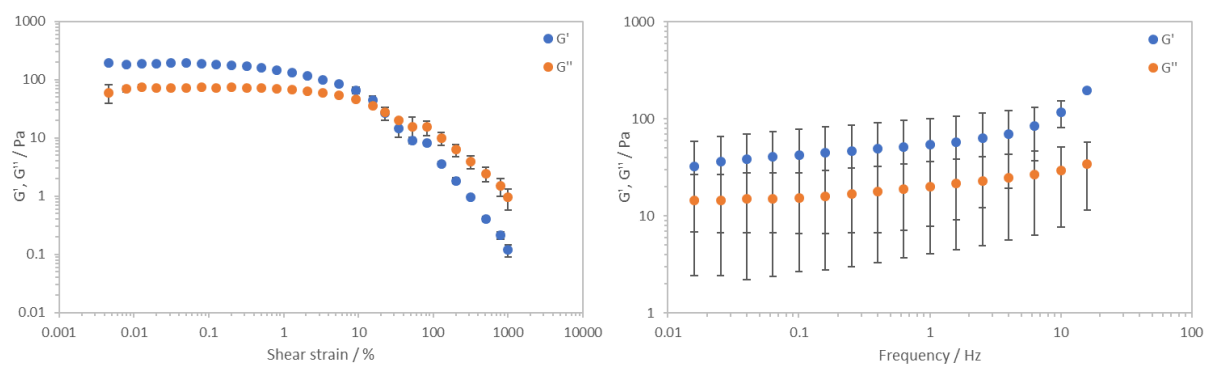


Fig. S84: Amplitude (left) and frequency (right) sweeps of (Anth)Phe-OH (5 mg mL^{-1}) hydrogels triggered by addition of cell culture media supplemented with GlcN-HCl (2 equiv.)

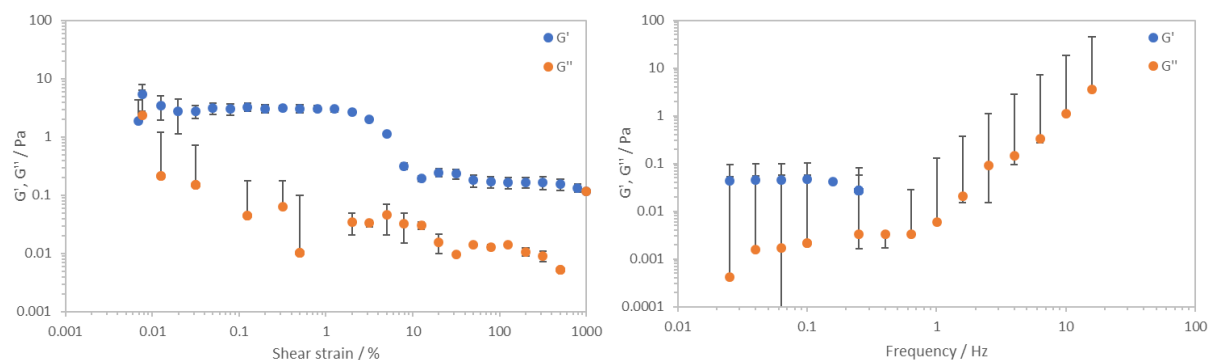


Fig. S85: Amplitude (left) and frequency (right) sweeps of GlcN-HCl (2 equiv.)-treated media triggered (Anth)Phe-OH (5 mg mL^{-1}) hydrogels after irradiation with 365 nm light for 1 h

S10. Fluorescence spectroscopy

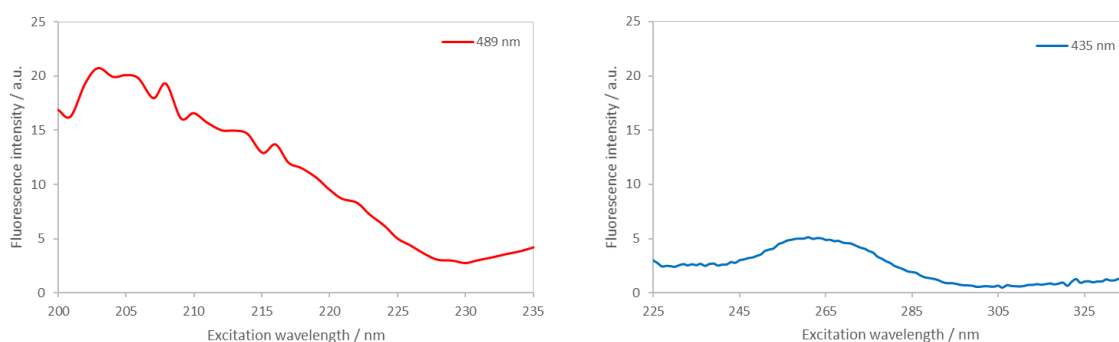
S10.1. Preparation of hydrogels/gel-like materials in cuvettes

To prepare gels of 2 mL volume in 10 mm path length cuvettes, the procedures in Section S3 were scaled up four-fold. Salt solutions were added to the cuvette prior to gelator addition.

S10.2. Fluorescence parameters

All readings were recorded using an excitation and emission slit widths of 5 nm and data points were recorded at a scan rate of 120 nm/min.

(a)



(b)

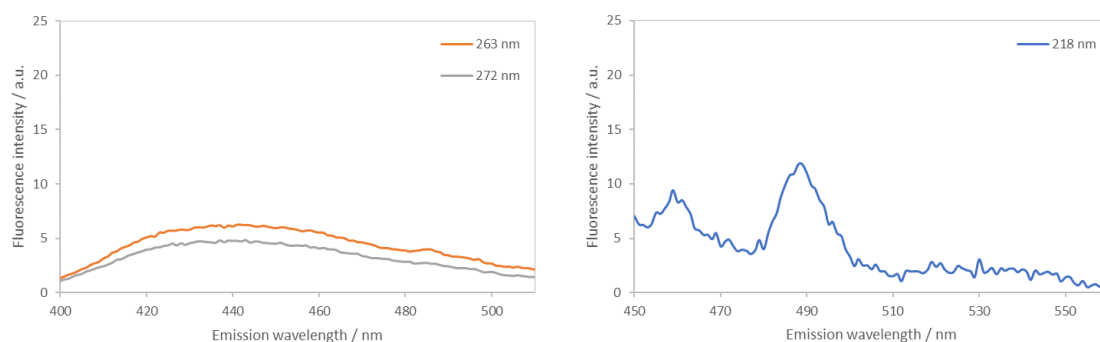


Fig. S86: Fluorescence spectra of (Anth)Phe-OH dissolved in aqueous NaOH solution (5 mg mL⁻¹). (a) Excitation (emission monitored at 489 nm (red) and 435 nm (blue)) and (b) emission (excitation at 263 nm (red), 272 nm (grey), 218 nm (blue)).

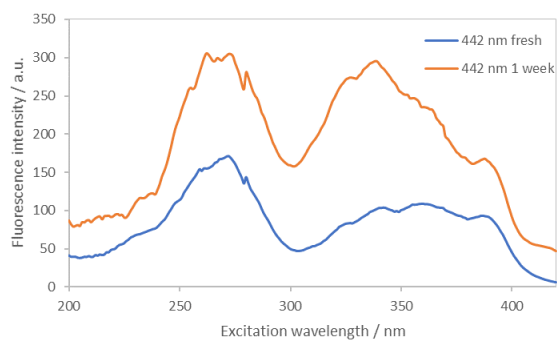


Fig. S87: Excitation spectra of GlyNH₂·HCl (2 equiv.) triggered (Anth)Phe-OH (5 mg mL⁻¹) gel-like materials, 2 h and 1 week after mixing. Monitored emission wavelength is 442 nm.

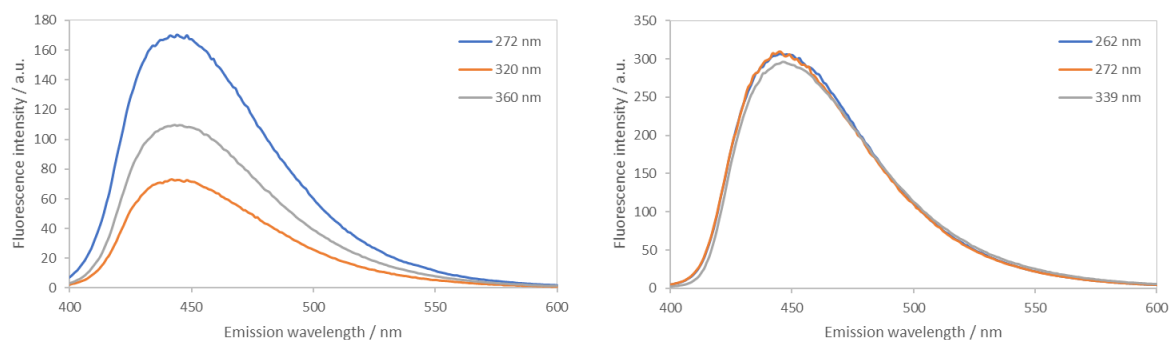


Fig. S88: Emission spectra of GlyNH₂·HCl (2 equiv.) triggered (Anth)Phe-OH (5 mg mL⁻¹) gel-like materials after 2 h (left) and 1 week (right). Excitation wavelengths are 272 nm (blue), 320 nm (orange) and 360 nm (grey).

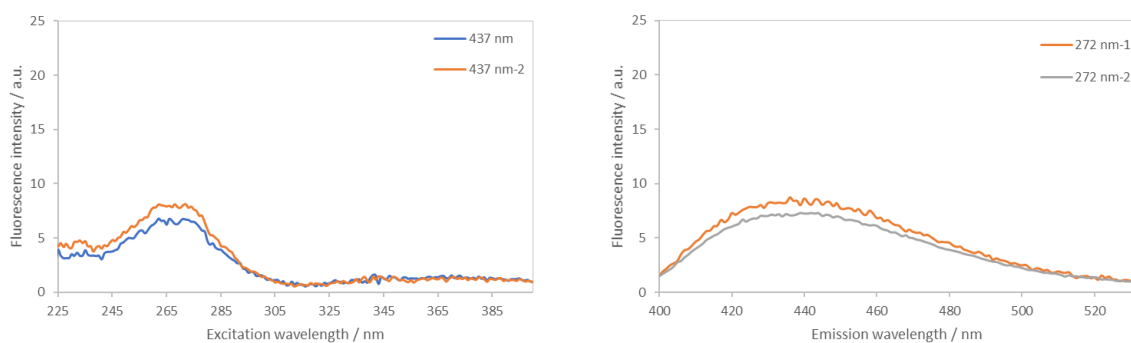


Fig. S89: Excitation (left, emission monitored at 437 nm) and emission (right, excitation at 272 nm) spectra of GlyNH₂·HCl (2 equiv.) triggered (Anth)Phe-OH gel-like materials after irradiation with 365 nm light for 1 h. Each graph represents two samples.

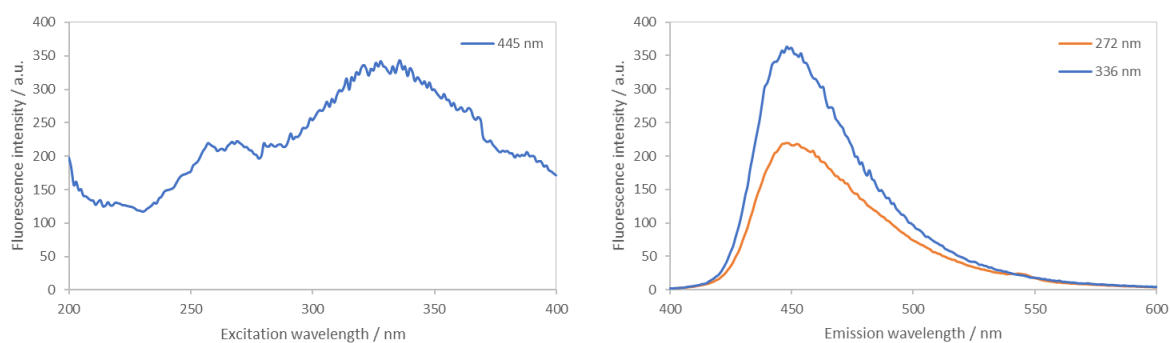


Fig. S90: Excitation (left, emission monitored at 445 nm) and emission (right, excitation at 272 nm (red) or 336 nm (blue)) spectra of (Anth)Phe-OH (5 mg mL^{-1}) hydrogels formed by addition of media supplemented with GlcN·HCl (2 equiv.)

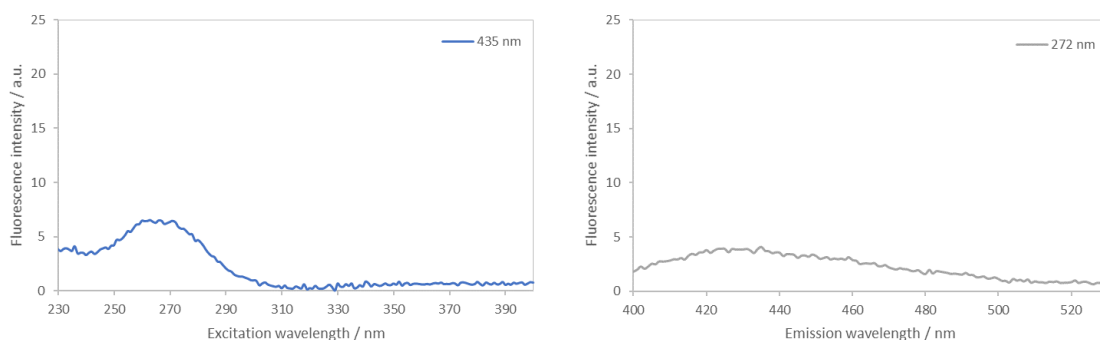


Fig. S91: Excitation (left, emission monitored at 435 nm) and emission (right, excitation at 272 nm) spectra of irradiated (Anth)Phe-OH (5 mg mL^{-1}). Samples were hydrogels formed by addition of [GlcN·HCl (2 equiv.) in media], irradiated with 365 nm light for 1 h.

We also monitored the fluorescence of (Anth)Phe-OH **2** immediately following the addition of GlyNH₂·HCl. An initial, rapid increase in the intensity – perhaps associated with some unstable structure – was followed by a reduction in fluorescence to a value similar to that recorded for freshly prepared gels in under a minute.

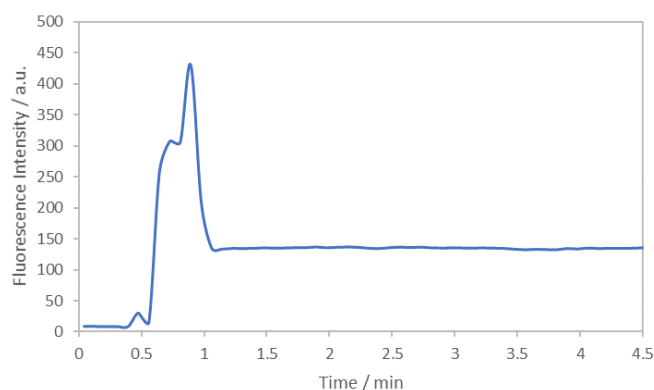


Fig. S92: Evolution of (Anth)Phe-OH emission (445 nm) after addition of GlyNH₂·HCl (2 equiv.). Salt added at after 0.5 min. Excitation wavelength = 272 nm.

S8. Cell culture studies

S11.1 *Cell culture procedure*

Chondrocytes and NIH/3T3 fibroblasts were cultured in Corning T25 cell culture flasks. All cells were cultured in high glucose Dulbecco's Modified Eagle's Medium (without sodium pyruvate) supplemented with 10% foetal bovine serum. Cell growth medium was changed every 2-3 days and cells were passaged upon reaching 80-90% confluency.

S11.2 *Preparation of gels in cell culture inserts*

Gels were prepared in Millicell Hanging Cell Culture Inserts (Merck, Millipore, PET, 8 μm pore size) which were suspended in 24-well plates. A stock solution of **2** (10 mg mL^{-1} , 0,04 M NaOH in autoclaved, deionised water) was prepared and 25 μL aliquots were pipetted into each Cell Culture Insert. To this, 25 μL media, pH adjusted with GlcN·HCl (5.8 mg mL^{-1}) was added, resulting in the instantaneous formation of a gel.

S11.3 *Cell seeding*

For 2D culture on gels of (Anth)Phe-OH **2**, cells were seeded on top of the gels within the cell culture inserts at an initial density of 20,000 cells mL^{-1} (volume 0.4 mL). A further 1 mL media (no GlcN·HCl) was added to the bottom of the well.

For 3D culture in gels of (Anth)Phe-OH **2**, cells were suspended in the GlcN·HCl-treated media at a density of 2,000,000 cells mL^{-1} prior to mixing with the gelator solution.

For control experiments, cells were seeded at a density of 20,000 cells mL^{-1} in the well plates, in either untreated or GlcN·HCl-treated media (5.8 mg mL^{-1}).

After 2 h and 72 h brightfield images of the cells were recorded on a light microscope fitted with a 4 \times objective.

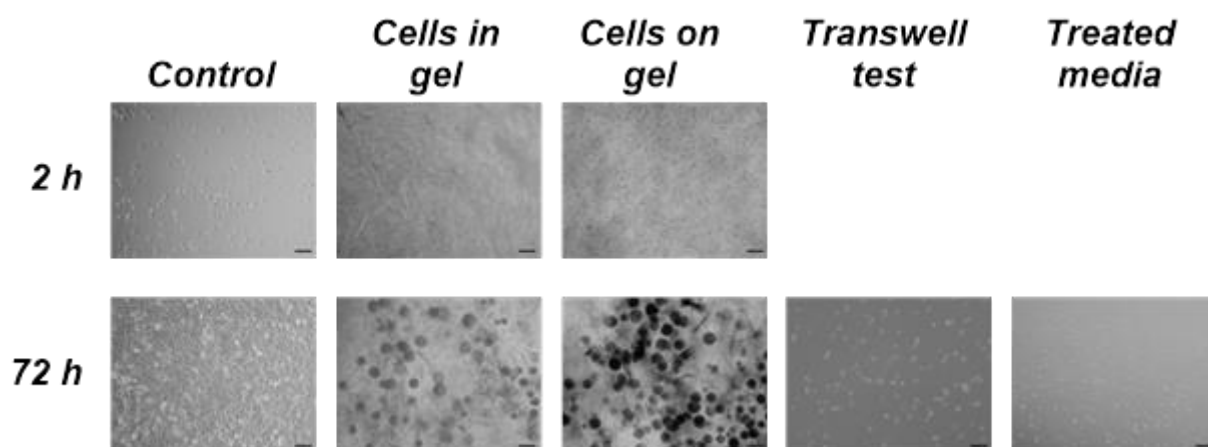


Fig. S93: Example brightfield images of NIH/3T3 cells. Scale bar = 32 μ m

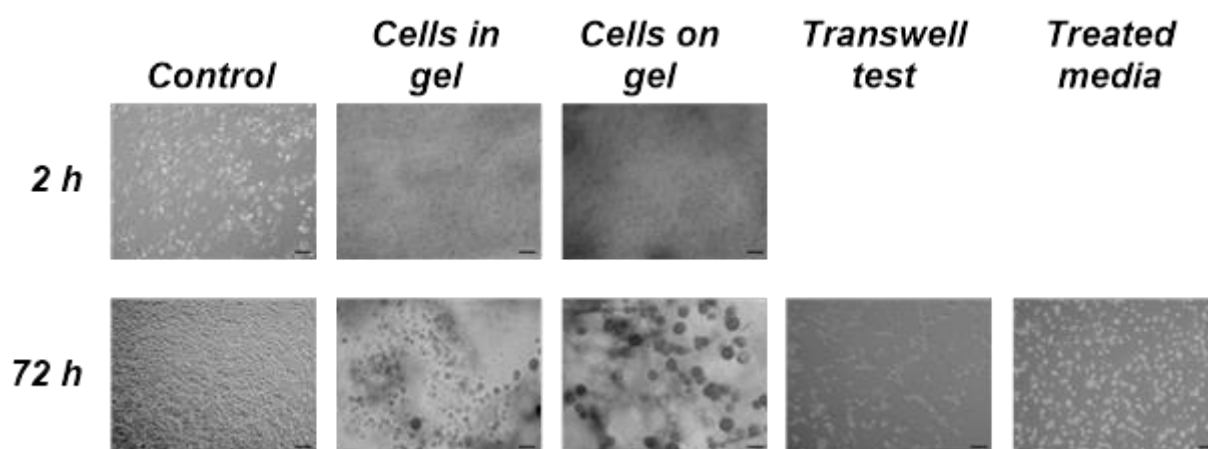


Fig. S94: Example brightfield images of chondrocytes. Scale bar = 32 μ m

S11.4 Recovery of cells for analysis by flow cytometry

After removing the media from the cell culture inserts, cells encapsulated within or seeded on top of hydrogels of (Anth)Phe-OH **2** were recovered for analysis by irradiating the samples with UV light (365 nm, 750 mAh, 5 min) to induce gel disassembly. Trypsin/EDTA was added to the cell culture insert and the sample incubated at 37°C to lift any cells which had adhered to the tissue culture plastic, and the cells suspended in fresh DMEM.

After removing the media from the wells, cells cultured on the bases of the 24-well plates were lifted with trypsin/EDTA (37°C) and the cells suspended in fresh DMEM.

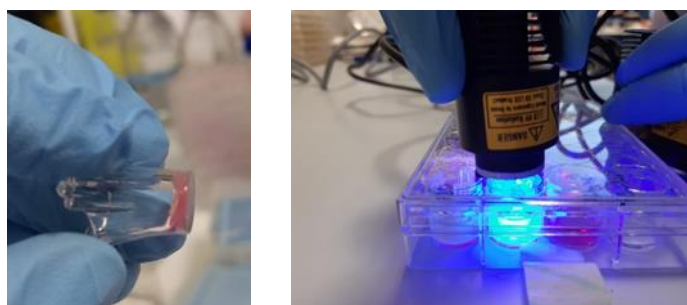


Fig. S95: Left: Image of cell-seeded (Anth)Phe-OH hydrogels formed in a transwell. Right: Image illustrating fluorescence of media under UV light after 72 h hydrogel incubation.

S11.5 Confocal microscopy

Images were collected on a Leica TCS SP8 AOBS inverted confocal microscope using a 20× objective. Images were collected using hybrid detectors with the following detection mirror settings: FITC 494-530 nm; Texas Red 602-665 nm, using the white light laser with 466 nm, 594 nm lines respectively. To eliminate cross-talk between channels, the images were collected sequentially. Data was processed using the software package Imaris (Bitplane).

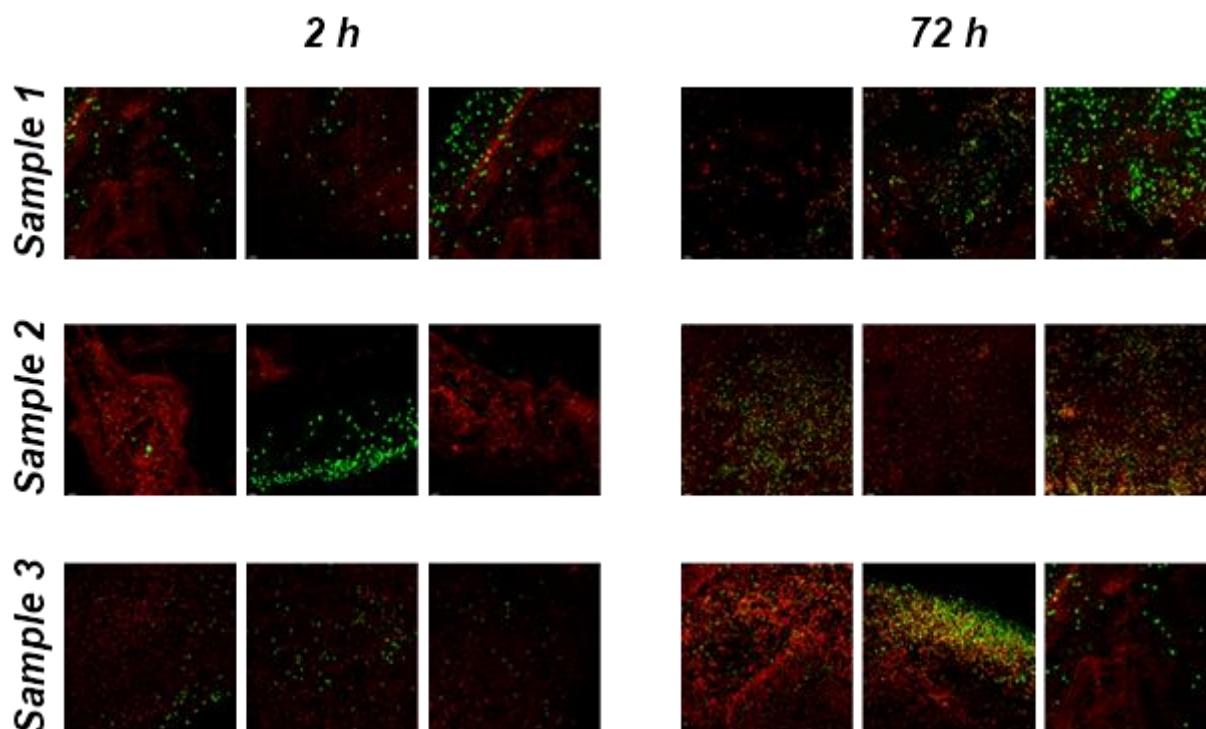


Fig. S96: Confocal microscopy images of LIVE/DEAD stained NIH/3T3 fibroblasts cultured in (Anth)Phe-OH hydrogels (LIVE = green, DEAD = red). Image dimensions = $320 \times 320 \mu\text{m}$, scale bar = $15 \mu\text{m}$.

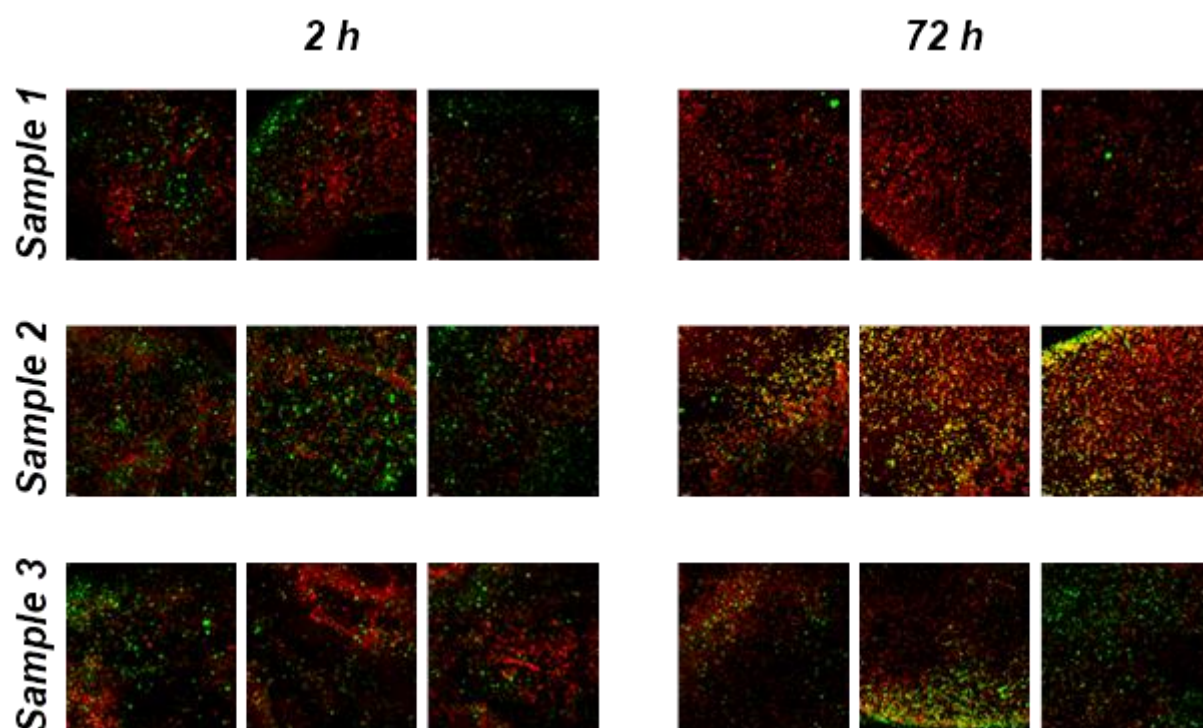


Fig. S97: Confocal microscopy images of LIVE/DEAD stained chondrocytes cultured in (Anth)Phe-OH hydrogels (LIVE = green, DEAD = red). Image dimensions = $320 \times 320 \mu\text{m}$, scale bar = $15 \mu\text{m}$.

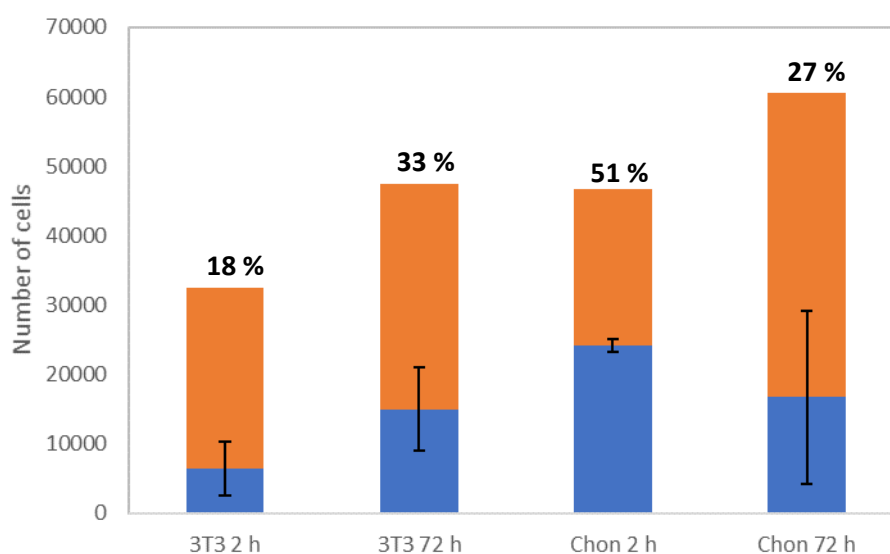


Fig. S98: Quantification of LIVE/DEAD staining from confocal microscopy images. Each column is the average of three samples, in each of which three non-overlapping images were analysed. The percentage of live cells in each sample is given above the relevant bar. It should be noted that the cell stains – particularly the ethidium bromide homodimer – are in some cases bound to gel constructs and may prevent accurate analysis. The reader is pointed to flow cytometric studies (see above) for a more accurate representation of the total cell population.

S11.6 Flow cytometry

A single cell suspension was generated prior to staining with LIVE/DEAD Fixable Blue Dead Cell Stain Kit (Life Technologies) for 15 minutes at room temperature. Cells were then washed and incubated with Annexin V (Biolegend) according to the manufacturer's instructions. Samples were acquired through the Fortessa (BD Systems, UK) and all analysis performed using FlowJo Software (Treestar, OR, USA).

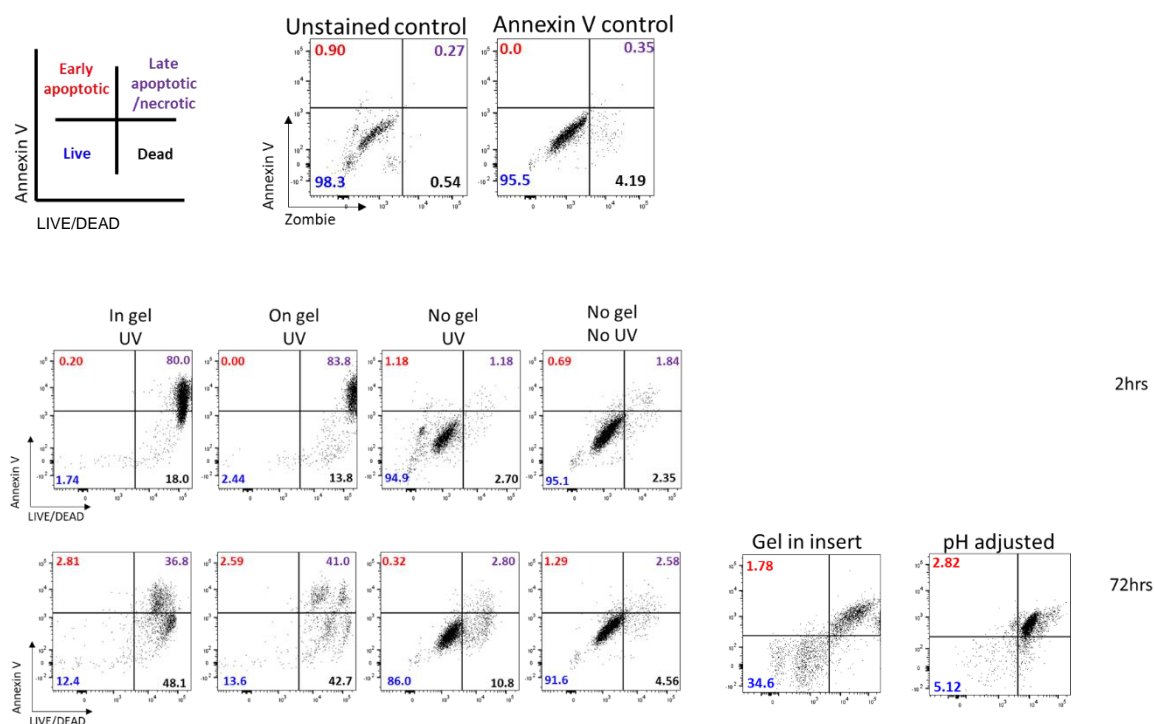


Fig. S99: Example flow cytometry data for NIH/3T3 cells

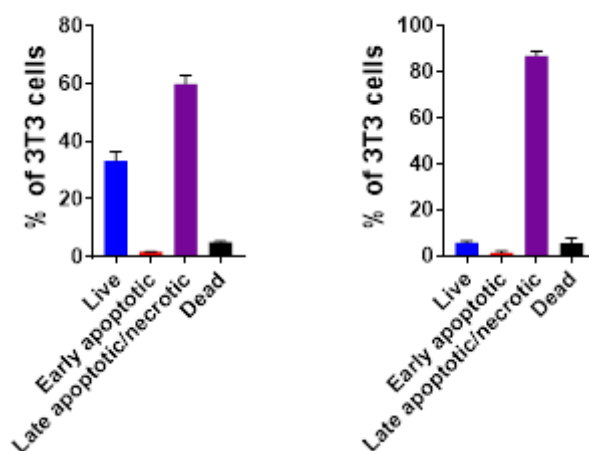


Fig. S100: Flow cytometry results for NIH/3T3 fibroblasts cultured in 24-well plates with an (Anth)Phe-OH hydrogel in transwell (left) and in GlcN-HCl treated media (right).

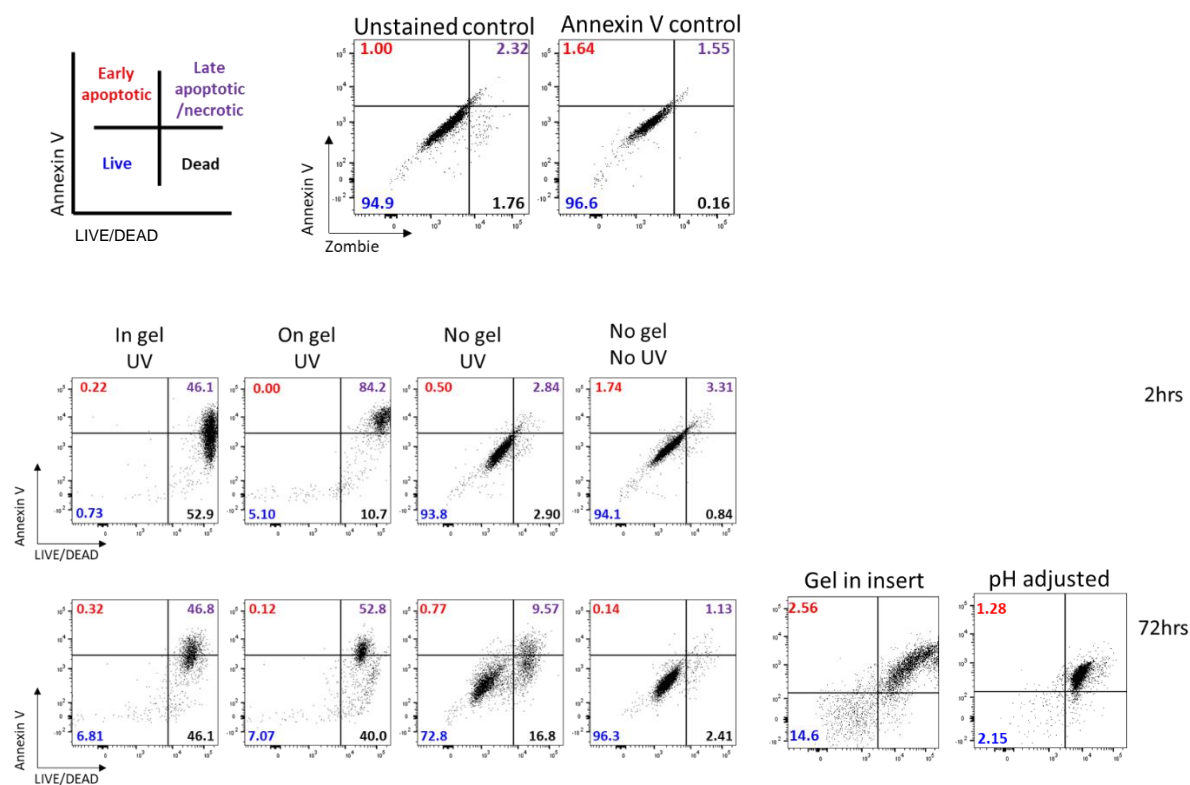


Fig. S101: Example flow cytometry data for chondrocytes

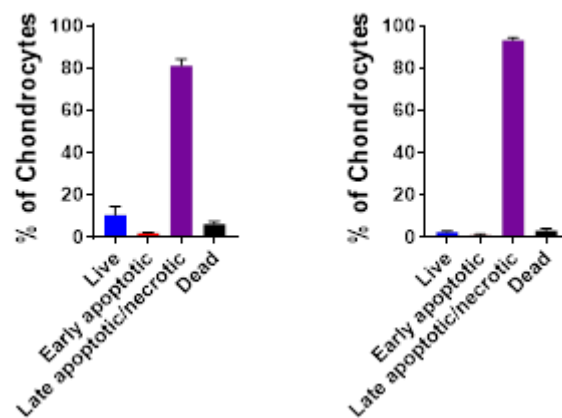


Fig. S102: Flow cytometry results for chondrocytes cultured in 24-well plates with an (Anth)Phe-OH hydrogel in transwell (left) and in GlcN-HCl treated media (right).

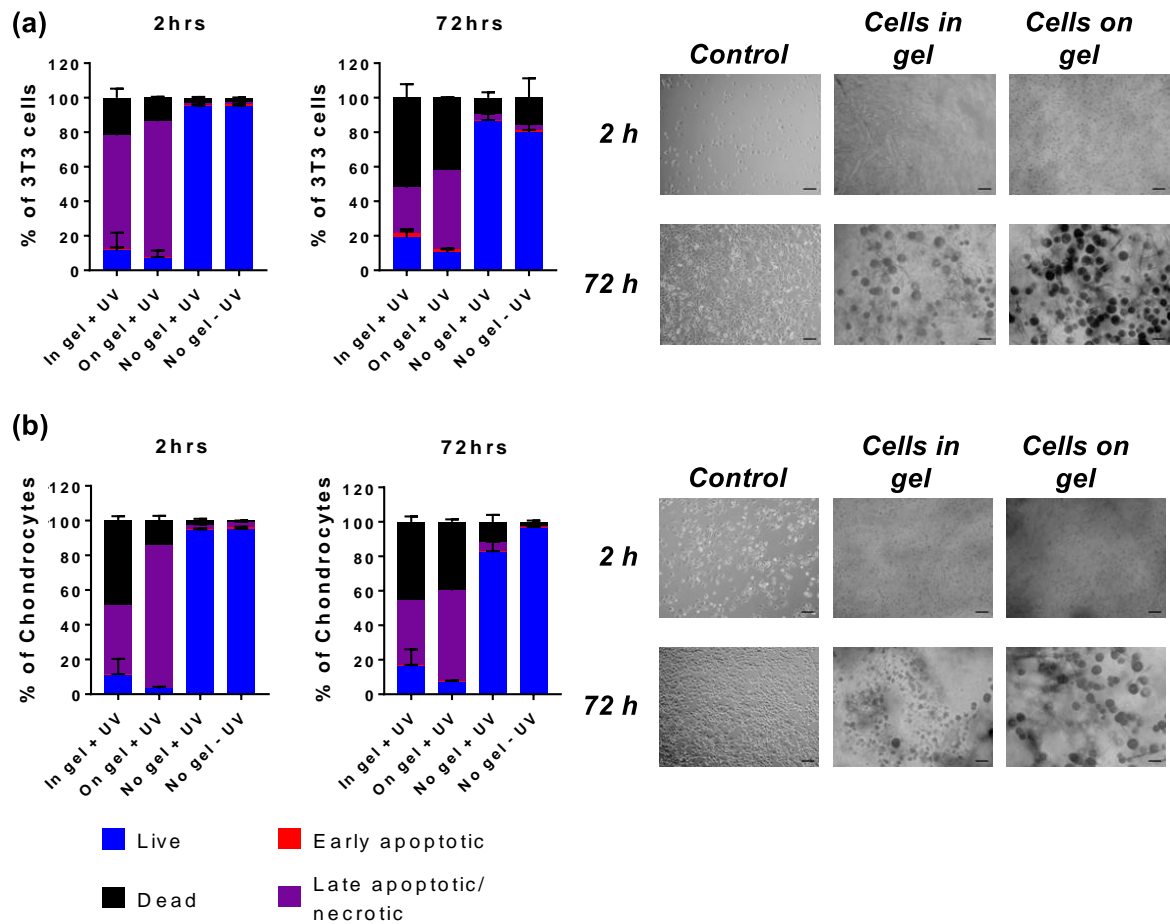


Fig. S103: Flow cytometry (left) and light microscopy (right) of NIH/3T3 fibroblasts (a) and chondrocytes (b) cultured in contact with (Anth)Phe-OH hydrogels in 2D or 3D culture. Cells grown non tissue culture plastic shown as control samples. Microscopy scale bars = 32 μ m.

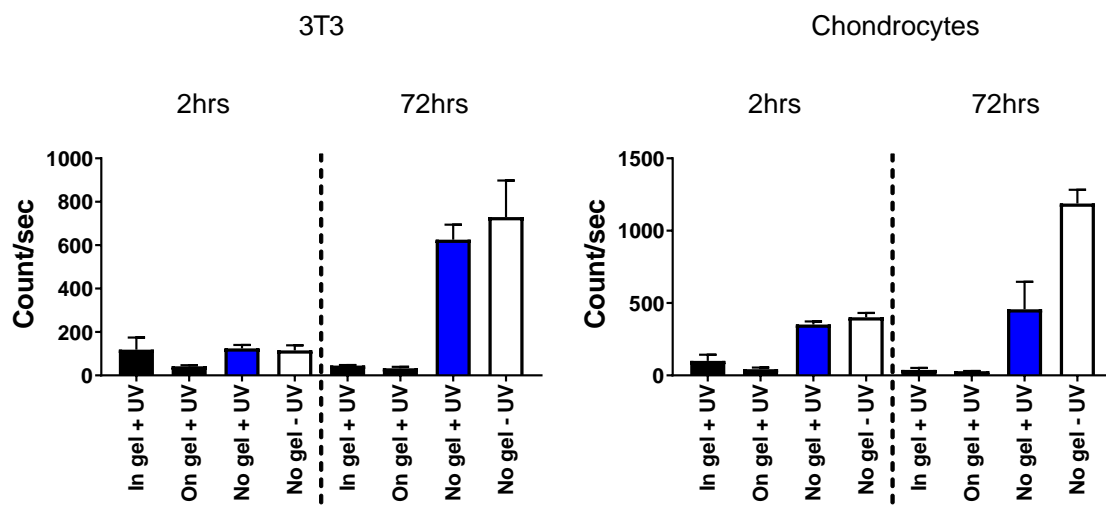


Fig. S104: Cell count/second for NIH/3T3 fibroblasts (left) and chondrocytes (right) under the different conditions. For both cell types, after 2 h the cell count/second (a proxy for cell "concentration" in the flow samples) from the 3D cultured cells and 2D on top of the gel is comparable those from the control wells. After 72 h the cell count/second remains the same for the gel cultured samples whereas cell counts are much higher for the controls because the cells have proliferated.

S9. References

-
- ¹ D. J. Adams, M. F. Butler, W. J. Frith, M. Kirkland, L. Mullen and P. Sanderson, *Soft Matter*, 2009, **5**, 1856-1862.
- ² P. R. A. Chivers and D. K. Smith, *Chem. Sci.*, 2017, **8**, 7218-7227.
- ³ D. L. Bertuzzi, T. B. Becher, N. M. R. Capreti, J. Amorim, I. D. Jurberg, J. D. Megiatto Jr. and C. Ornelas, *Global Challenges*, 2018, **2**, 1800046.
- ⁴ H. Kotani, K. Ohkubo, and S. Fukuzumi, *J. Am. Chem. Soc.* 2004, **126**, 15999-16006.
- ⁵ (a) H. Fidder, A. Lauer, W. Freyer, B. Koeppe and K. Heyne, *J. Phys. Chem. A*, 2009, **113**, 6289-6296; (b) M. Klaper, P. Wessig and T. Linker, *Chem. Commun.*, 2016, **52**, 1210-1213.
- ⁶ Y. Sako and Y. Takaguchi, *Org. Biomol. Chem.*, 2008, **6**, 3843-3847.
- ⁷ (a) Y.-C. Lin, B. Kachar and R. G. Weiss, *J. Am. Chem. Soc.*, 1989, **111**, 5542-5552; (b) H. Qiu, C. Yang, Y. Inoue and S. Che, *Org. Lett.*, 2009, **11**, 1793-1796.
- ⁸ M. Jun-ichi, W. Takehiko and I. Yoshihisa, *Chem. Lett.* 2006, **35**, 738-739.
- ⁹ (a) A. Dawn, N. Fujita, S. Haraguchi, K. Sada and S. Shinkai, *Chem. Commun.*, 2009, **16**, 2100-2102; (b) A. Dawn, N. Fujita, S. Haraguchi, K. Sada and S. Shinkai, *Org. Biomol. Chem.*, 2009, **7**, 4378-4385.